Synthesis and Antimicrobial Properties of Silver Nanoparticles Produced by Turkevich Methods and Cold Atmospheric Plasma

Ventouratou Marina

School of Chemical Engineering of the National Technical University of Athens

Supervisor:

Professor Taoukis Petros

National Technical University of Athens

Co-supervisors:

Professor Gatt Ruben & Professor Valdramidis Vasilis

University of Malta

February 2019

PROLOGUE

This diploma thesis was written to fulfill the graduation requirements of the School of Chemical Engineering of the National Technical University of Athens (NTUA). The research was conducted during the 2nd semester of 2018 at the University of Malta (UoM), within the framework of the Erasmus+ program. It was a unique and incredibly rewarding experience that offered me, not only new educational knowledge and professional skills, but also a completely new life perspective.

I would like to warmly thank my co-supervisors, Professor Vasilis Valdramidis and Professor Ruben Gatt of UoM and Professor Petros Taoukis of NTUA for their excellent guidance and support during this process. I would also like to thank Dr. Dmytro Kozak (Metamaterial Unit, UoM), Dr. Ourania Gouseti (Faculty of Engineering, University of Nottingham) and David Spiteri (Senior Professional – Laboratory, Water Services Corporation, Malta) for supplying us with valuable experimental measurements. Last, but not least, I would also like to thank Dr. Griffin Sholeem (UoM) and Dr. Maria Tsevdou (NTUA), for a great and most rewarding cooperation and for their helpful ideas on my thesis.

This work is dedicated to my family that supported me throughout my studies and especially during the time I spent abroad, and helped me to take my first steps into scientific research.

ABSTRACT

Nanoparticles have unique physiochemical properties compared to the bulk material comprising them, which make them preferable in a variety of applications including bioimaging, drug delivery and food packaging. These properties depend on the nanoparticles' morphology. Silver nanoparticles (AgNPs) have been especially distinguished for their antimicrobial efficacy against both Gram-negative and Gram-positive bacteria. However, the mechanism of their antimicrobial action has not yet been fully understood. Although their antimicrobial properties are very tempting and they are already used in a variety of consumer products, there is still worldwide concern regarding their cytotoxicity.

Bearing these unresolved issues in mind, in the present study, synthesis of AgNPs was achieved with the aim of producing different sizes and/or different shapes of nanoparticles to subsequently test their antimicrobial efficacy and their possible cytotoxicity effects. Modified Turkevich Methods and Reduction via plasma generation were used for AgNPs synthesis. *Salmonella enterica* and Normal Human Dermal Fibroblasts (NHDF) were used for the antimicrobial and cytotoxicity testing accordingly.

The results of the experiment demonstrated that all AgNPs dispersions inhibited *Salmonella enterica* at both concentrations tested (6.2 and 3.9 ppm), at 0-6 h exposure time, but the most antimicrobial one was the one produced by plasma reduction, which inhibited *Salmonella enterica* even at 0.39 ppm, followed by the one synthesized by Modified Turkevich Method at 70°C with 1:10 molar ratio of $AgNO_3$ to $Na_3C_6H_5O_7$. Nevertheless, all AgNPs also reduced Fibroblasts viability, at 3 days exposure time, at these concentrations tested on *Salmonella enterica*. The reduction of cells viability seemed to be concentration-dependent (except AgNPs synthesized by Modified Turkevich Method at room temperature with 1:10 molar ratio) and time-dependent. Most AgNPs samples did not present strong cytotoxicity effects only at low concentrations (e.g., 0.49 and 0.98 ppm), except AgNPs synthesized by plasma reduction that were found toxic on the first 2 days of exposure even at 0.39 ppm. Also, the obtained IC_{50} values of all samples were low (< 100 ppm). The smallest IC_{50} value in particular, derived from the smallest (7-15 nm) and spherical nanoparticles. Last but not least, AgNPs seem to be equally toxic and perhaps follow the same cytotoxicity action with $AgNO_3$ on the 1st day of exposure and at high concentrations (3.9 and 6.2 ppm), whereas after 24 h exposure, AgNPs of the same concentration, appear to be more toxic than $AgNO_3$. Therefore, more cytotoxicity studies are needed for their possible future use in health-related applications.

Σύνθεση νανοσωματιδίων αργύρου με μεθόδους Turkevich και ψυχρό ατμοσφαιρικό πλάσμα και μελέτη των αντιμικροβιακών τους ιδιοτήτων

Τα σωματίδια της τάξεως του νανομέτρου διαφέρουν από την πρωταρχική μορφή του υλικού επιδεικνύοντας μοναδικές ιδιότητες. Αυτή η ανακάλυψη, έστρεψε και το ενδιαφέρον της επιστημονικής κοινότητας προς τη μελέτη της παραγωγής νανοσωματιδίων και την περεταίρω χρήση τους σε μία πληθώρα εφαρμογών, όπως στην βιοαπεικόνιση, στη μεταφορά φαρμάκων και στις συσκευασίες τροφίμων (*βλ.* Εικόνα 2.1, Κεφάλαιο 2) (Zaman, Ahmad, Qadee, Rabbani, & Khan, 2014). Οι ιδιότητες των νανοσωματιδίων αλλάζουν με βάση τη μορφολογία τους, δηλαδή το μέγεθος και το σχήμα τους. Για αυτόν το λόγο, απαιτείται η παραγωγή ενός στενού εύρους μεγέθους και σχήματος νανοσωματιδίων για την χρήση τους στις διάφορες εφαρμογές, αποτελώντας το δυσκολότερο στάδιο κατά την σύνθεση τους, ακολουθούμενο από την επίτευξη υψηλής απόδοσης, χαμηλής κατανάλωσης ενέργειας και χαμηλής περιβαλλοντικής και κυτταρικής τους τοξικότητα. Το μέσο επικάλυψης που χρησιμοποιείται, όπως επίσης και η αναλογία του μέσου επικάλυψης και της % συγκέντρωσης των νανοσωματιδίων, παίζουν επίσης καθοριστικό ρόλο στις τελικές ιδιότητες των νανοσωματιδίων που συντίθενται (Inmaculada López-Lorente & Valcárcel, 2014), (Khan, Saeed, & Khan, 2017).

Τα νανοσωματίδια μετάλλων έχουν χρησιμοποιηθεί ευρέως σε ποικίλες εφαρμογές εξαιτίας της μεγάλης αναλογίας επιφάνειας-όγκου που έχουν. Αυτή η ιδιότητα τα καθιστά ιδιαίτερα δραστικά και επομένως πιο ελκυστικά στο να χρησιμοποιηθούν σε πολλές εφαρμογές (*βλ.* Εικόνα 3.1, Κεφάλαιο 3) (Christian, Von der Kammer, Baalousha, & Hofmann, 2008). Ιδιαίτερα τα νανοσωματίδια αργύρου (AgNPs) έχουν ευρέως μελετηθεί και χρησιμοποιούνται εκτεταμένα κυρίως λόγω της αποδεδειγμένης αντιμικροβιακής τους αποτελεσματικότητας έναντι των Gram θετικών και Gram αρνητικών βακτηρίων, των ιών και άλλων ευκαρυωτικών μικροοργανισμών (Rai, Yadav, & Gade, 2009) (*βλ.* Εικόνες 4.1, 4.2, Κεφάλαιο 4, για περισσότερες εφαρμογές).

Ο ακριβής μηχανισμός της αντιμικροβιακής τους δράσης δεν έχει πλήρως χαρακτηριστεί. Παρόλα αυτά, ο μηχανισμός της αντιμικροβιακής δράσης των ιόντων αργύρου έχει διασαφηνιστεί. Προηγούμενες μελέτες αναφέρουν ότι τα ιόντα αργύρου διεισδύουν στο κυτταρικό τοίχωμα των βακτηρίων μετά από αλληλεπίδραση με τις πεπτιδογλυκάνες που το αποτελούν (Mosselhy, et al., 2015) και στη συνέχεια αλληλεπιδρούν με τις βάσεις του DNA, επηρεάζοντας την ικανότητα διπλασιασμού του. Το DNA στη συνέχεια μετατρέπεται σε μια

συμπυκνωμένη μορφή, η οποία έχει παρατηρηθεί με ηλεκτρονιακή μικροσκοπία διερχομένης δέσμης (Transmission Electron Microscopy) (Mosselhy, et al., 2015), που αντιδρά με ομάδες θειόλης των πρωτεϊνών, οδηγώντας στην κυτταρική θανάτωση (Rai, Yadav, & Gade, 2009), (Radzig, et al., 2013). Πλήθος μελετών υποστηρίζουν ότι η δράση των νανοσωματιδίων οφείλεται στην απελευθέρωση ιόντων αργύρου από την οξειδωμένη τους επιφάνεια (Bondarenko, Ivask, Käkinen, Kurvet, & Kahru, 2013). Άλλες υποστηρίζουν πως οφείλεται είτε στη μηχανική διάσπαση του κυτταρικού τοιχώματος των βακτηρίων από τα ίδια τα νανοσωματίδια (Mosselhy, et al., 2015), είτε στον συνδυασμό και των δύο αυτών προαναφερθέντων μηχανισμών. Πολλές μελέτες υποστηρίζουν επίσης πως τα ιόντα αργύρου Ag^+ είναι πιο τοξικά από τα νανοσωματίδια αργύρου (Mosselhy, et al., 2015), (Seong & Lee, 2017), (Mallevre, et al., 2016). Σε κάθε περίπτωση, έχει διαπιστωθεί σε εργαστηριακό επίπεδο η καταστροφή του DNA, ο σχηματισμός δραστικών ειδών οξυγόνου (Radical Oxygen Species, ROS) που προκαλεί οξειδωτικό στρες, και η ενδοκυτταρική αύξηση των επιπέδων Ca^{2+} (Radzig, et al., 2013), (Lee, Kim, & Lee, 2014), (Seong & Lee, 2017).

Όσον αφορά στην αντιμικροβιακή δράση των νανοσωματιδίων αργύρου έναντι της *Salmonella enterica*, έχει διαπιστωθεί η αποπόλωση της εσωτερικής μεμβράνης, χωρίς διαταραχή της εξωτερικής μεμβράνης (μόνο διείσδυση), και η κυτταρική απόπτωση, κατά την έκθεση του βακτηρίου σε χαμηλές συγκεντρώσεις νανοσωματιδίων. Κατά την έκθεση σε υψηλές συγκεντρώσεις, παρατηρήθηκε και διάρρηξη της μεμβράνης (Seong & Lee, 2017). Επιπλέον, ορισμένοι ορότυποι της *Salmonella enterica*, συμπεριλαμβανομένης και της *Salmonella* Enteritidis, εμφανίζονται πιο ευαίσθητοι στα AgNPs (Berton, et al., 2014). Από προηγούμενες μελέτες, οι ελάχιστες συγκεντρώσεις αναστολής της *Salmonella enterica* από νανοσωματίδια αργύρου έχουν βρεθεί σε επίπεδα της τάξεως των 3,12-16 ppm (*βλ.* Πίνακα 4.4, Κεφάλαιο 4).

Από τις μεθόδους σύνθεσης νανοσωματιδιών που έχουν χρησιμοποιηθεί μέχρι τώρα (φυσικοχημικές και βιολογικές), προτιμώνται οι βιολογικές, κυρίως λόγω του περιορισμού της χρήσης επικίνδυνων και τοξικών διαλυτών που μερικές φορές οδηγούν και σε τοξικά υποπροϊόντα (Zhang, Liu, Shen, & Gurunathan , 2016). Παρόλα αυτά, με προσεκτική επιλογή χημικών ουσιών (που δρουν ως παράγοντες αναγωγής/σταθεροποίησης/κάλυψης), η χημική σύνθεση μπορεί να πραγματοποιηθεί με πιο «πράσινες» μεθόδους. Αυτή η μεθοδολογία περιλαμβάνει φιλικές προς το περιβάλλον χημικές ουσίες που δρουν προκαλώντας ταυτόχρονα άπωση φορτίων και στερεοχημική σταθεροποίηση των νανοσωματιδίων. Με αυτό τον τρόπο, τα νανοσωματίδια μπορούν να διατηρηθούν σε τυποποιημένο σχήμα και μέγεθος και να

αποτραπεί η συσσωμάτωσή τους (*βλ.* Εικόνα 5.2). Πολλές χημικές ουσίες έχουν χρησιμοποιηθεί στο παρελθόν, με αποτέλεσμα την παραγωγή AgNPs ποικίλων μεγεθών, συμπεριλαμβανομένων του γαλλικού οξέος ($C_7H_6O_5$) και του $NaBH_4$ (Sodium Borohydride) σε συνδυασμό με κιτρικό νάτριο (tri-sodium citrate, $Na_3C_6H_5O_7$) (*βλ.* Πίνακα 5.2, Κεφάλαιο 5).

Λαμβάνοντας υπόψιν όλα τα προαναφερθέντα ζητήματα, στόχος της παρούσας μελέτης είναι η σύνθεση νανοσωματιδίων αργύρου, διαφορετικού μεγέθους και σχήματος, με διαφορετικές μεθόδους, με σκοπό την μελέτη της αντιμικροβιακής τους ιδιότητας.

Διάφορες τροποποιήσεις της μεθόδου Turkevich χρησιμοποιήθηκαν για την χημική σύνθεση νανοσωματιδίων αργύρου. Η μέθοδος του Turkevich αρχικά περιελάμβανε την αναγωγή ενός μεταλλικού διαλύματος με κιτρικό άλας σε θερμοκρασία βρασμού, μια διαδικασία που έχει ως αποτέλεσμα την αλλαγή χρώματος του διαλύματος ανάλογα με τη μορφολογία των παραχθέντων σωματιδίων (Pacioni, Borsarelli, Rey, & Veglia, 2015), (Piñero, Camero, & Blanco, 2017), (Mazzonello, Valdramidis, Farrugia, Grima, & Gatt, 2017). Με παλαιότερες τροποποιήσεις της μεθόδου έχει επιτευχθεί σύνθεση AgNPs, όπως με προσθήκη γλυκερόλης, η οποία βρέθηκε να έχει καλή σταθεροποιητική ικανότητα (Pacioni, Borsarelli, Rey, & Veglia, 2015), με προσθήκη καυστικού νατρίου (NaOH), η οποία βρέθηκε να διευκολύνει την αναγωγή του νιτρικού αργύρου ($AgNO_3$) αλλάζοντας το pH (όσο υψηλότερο το pH τόσο μεγαλύτερη η αποπρωτονίωση του κιτρικού άλατος, καθιστώντας το πιο διαθέσιμο για κάλυψη), και τέλος με αλλαγή της θερμοκρασίας (Caswell, Bender, & Murphy, 2003).

Κατά την εφαρμογή της μεθόδου Turkevich σε θερμοκρασία δωματίου, παράχθηκαν πιο ομοιόμορφα σταθεροποιημένα σωματίδια. Η εξάρτηση του ρυθμού της αντίδρασης, με χρήση κιτρικού νατρίου ($Na_3C_6H_5O_7$) ως παράγοντα κάλυψης, βρέθηκε ότι ακολουθεί την κινητική Arrhenius, με μεγαλύτερη σύνθεση νανοσωματιδίων σε υψηλότερες θερμοκρασίες αλλά και μεγαλύτερες κατανομές μεγέθους (Mazzonello, Valdramidis, Farrugia, Grima, & Gatt, 2017). Οι τροποποιήσεις της μεθόδου Turkevich που έγιναν στην παρούσα μελέτη ήταν: η χρήση μόνο γλυκερόλης (χωρίς νερό) ως σταθεροποιητικού και αναγωγικού παράγοντα, που συντέθηκε σε θερμοκρασία δωματίου με την προσθήκη NaOH (MTM_R-1:10), και στους 70^oC (χαμηλότερη από τη θερμοκρασία βρασμού), αλλάζοντας την αναλογία του παράγοντα κάλυψης με την % συγκέντρωση νανοσωματιδίων (MTM_70-1:10 και MTM_70-1:5) (*βλ.* Κεφάλαιο 7: Πειραματική διαδικασία). Σε όλες τις περιπτώσεις, ο $AgNO_3$ χρησιμοποιήθηκε ως πρόδρομος μετάλλου και το $Na_3C_6H_5O_7$ ως παράγοντας κάλυψης.

Στην παρούσα μελέτη, η σύνθεση των AgNPs επίσης επετεύχθη με αναγωγή με πλάσμα, το οποίο παρήχθη με την δημιουργία ενός ηλεκτροχημικού κελιού και δια αλληλεπιδράσεως επιφάνειας πλάσματος-γλυκερόλης, σε ατμοσφαιρική πίεση και με διέλευση αδρανούς αερίου (Αργό) (*βλ.* κεφάλαιο 7) (plasma). Ο $AgNO_3$ χρησιμοποιήθηκε και πάλι ως πρόδρομος μετάλλου και το $Na_3C_6H_5O_7$ ως παράγοντας κάλυψης. Παραγωγή AgNPs με ψυχρό ατμοσφαιρικό πλάσμα επετεύχθη και από προηγούμενες μελέτες, χρησιμοποιώντας διαφορετικές διατάξεις (*βλ.* Πίνακα 5.3, Κεφάλαιο 5), με μικρό μέγεθος νανοσωματιδίων (στις περισσότερες περιπτώσεις λιγότερο από 10 nm) και ως επί το πλείστον σφαιρικό σχήμα. Ο κύριος μηχανισμός της αναγωγής με πλάσμα σχετίζεται με την παραγωγή επιδιαλυτωμένων ηλεκτρονίων (solvated electrons). Άλλα δραστικά είδη μπορεί επίσης να παίζουν καθοριστικό ρόλο σε ολόκληρη τη διαδικασία (ιόντα, ελεύθερες ρίζες, VUV φωτόνια) καθώς παράγονται ιόντα H και OH (Kondeti, Gangal, Yatom, & Bruggeman, 2017). Η μέθοδος παρασκευής με πλάσμα θεωρείται γενικά «πράσινη» αφού δεν δημιουργούνται επιβλαβή υποπροϊόντα. Παρόλα αυτά, υπάρχουν περιορισμοί της μεθόδου που υπόκεινται κυρίως στο κόστος και την ασφάλειά της (Kondeti, Gangal, Yatom, & Bruggeman, 2017), (Misra, Schluter, & Cullen, 2016).

Ο ποιοτικός και ποσοτικός χαρακτηρισμός των νανοσωματιδίων αργύρου που παρήχθησαν έγινε μέσω ενόργανων τεχνικών ανάλυσης, όπως η φασματοσκοπία υπερύθρου-ορατού (UV-Vis), η φασματομετρία μάζας με επαγωγικά συζευγμένο πλάσμα (ICP-Ms) και η ηλεκτρονιακή μικροσκοπία διερχομένης δέσμης (TEM). Από την ανάλυση UV-Vis, ελήφθησαν ποιοτικά στοιχεία των παραχθέντων νανοσωματιδίων, καθώς οι κορυφές απορρόφησης (peaks) εμφανίστηκαν σε όλες τις περιπτώσεις στο εύρος 350-600 nm, επιβεβαιώνοντας τη σύνθεση των AgNPs (Saeb, Alshammari, Al-Brahim, & Al-Rubeaan, 2014). Από την δευτερεύουσα ζώνη απορρόφησης (άνω των 600 nm), μπορούν να γίνουν υποθέσεις για το σχήμα των νανοσωματιδίων, αφού όταν η καμπύλη φαίνεται να αποκτά θετική κλίση, αποτελεί ένδειξη παραγωγής μη-σφαιρικών νανοσωματιδίων (Desai, Mankad, Gupta, & Jha, 2012). Σύμφωνα με αυτή την παρατήρηση, τα δείγματα MTM_R-1:10 και MTM_70-1:10 αναμένεται να είναι σφαιρικά, ενώ τα δείγματα MTM_70-1:5 και αυτό που παράχθηκε με πλάσμα αναμένονται να αποτελούνται από μη-σφαιρικά νανοσωματίδια. Επιπλέον, ανάλογα με την απορρόφηση της κορυφής, τα δείγματα ίδιων αραιώσεων με τις υψηλότερες κορυφές αναμένεται να έχουν και υψηλότερη συγκέντρωση (Desai, Mankad, Gupta, & Jha, 2012). Με βάση αυτή την παρατήρηση, το δείγμα MTM_70-1:5 αναμένεται να έχει διπλάσια συγκέντρωση από το MTM_70-1:10. Τέλος, σωματίδια μικρότερου μεγέθους αναμένονται από όσα δείγματα

εμφάνισαν την μέγιστη κορυφή απορρόφησης σε μικρότερα φάσματα (blue shift: μετατόπιση της κορυφής προς τα αριστερά) ενώ μεγαλύτερου μεγέθους αυτά που την εμφάνισαν σε μεγαλύτερα φάσματα (red shift: μετατόπιση της κορυφής στα δεξιά). Επομένως, τα μικρότερα νανοσωματίδια αναμένονται από το δείγμα MTM_R-1:10 (blue shift), ενώ τα μεγαλύτερα από το δείγμα MTM_70-1:5 (red shift) (βλ. διαγράμματα 8.13, Κεφάλαιο 8). Η σταθερότητα των νανοσωματιδίων, εξετάστηκε επίσης με ανάλυση UV-Vis, σε 4 διαφορετικούς χρόνους για διάρκεια αποθήκευσης ενός μήνα, και βρέθηκε πολύ ικανοποιητική για όλα τα δείγματα (*βλ.* δ/τα 8.8, 8.9 και 8.12, Κεφάλαιο 8). Με ανάλυση ICP-Ms έγινε ο ποσοτικός χαρακτηρισμός των νανοσωματιδίων και οι συγκεντρώσεις των δειγμάτων MTM_R-1:10, MTM_70-1:10, MTM_70-1:5 και αυτού που παράχθηκε με πλάσμα βρέθηκαν 6,2, 3,9, 8,2 και 3,9 ppm αντίστοιχα (μετά από δεκαπλάσια αραίωση με νερό, σε όλα τα δείγματα εκτός από το πλάσμα). Από τον ποιοτικό χαρακτηρισμό με TEM, το δείγμα MTM_R-1:10 βρέθηκε ότι αποτελείται από μίγμα μεγεθών, με κυρίαρχο το σφαιρικό σχήμα (σε συμφωνία με τα αποτελέσματα της ανάλυσης UV-Vis) με κατανομή μεγεθών στο εύρος 18-57 nm. Το MTM_70-1:10 βρέθηκε πως αποτελείται από σφαιρικά νανοσωματίδια (σε συμφωνία με τα αποτελέσματα της ανάλυσης UV-Vis) με κατανομή μεγεθών στο εύρος 7-15 nm. Το MTM_70-1:5 βρέθηκε πως αποτελείται από μίγμα μεγεθών, με κυρίαρχο αυτό της πυραμίδας, με μεγάλη κατανομή μεγεθών στο εύρος 6-84 nm. Τέλος, για τα νανοσωματίδια πλάσματος δεν μπόρεσαν να ληφθούν παραπάνω πληροφορίες.

Για να διερευνηθούν οι αντιμικροβιακές ιδιότητες των νανοσωματιδίων αργύρου που συντέθηκαν σε αυτή τη μελέτη, εξετάστηκε η επίδραση ενός εύρους συγκεντρώσεων AgNPs έναντι της *Salmonella enterica* σε χρόνο έκθεσης 0 (Blank-control), 2, 4 και 6 ώρες. Τα αποτελέσματα (log (CFU / mL) –time) έδειξαν ότι σε συγκέντρωση 3,9 ppm, το δείγμα πλάσματος είχε την ισχυρότερη αντιμικροβιακή δράση, ακολουθούμενο από το MTM_70-1:10. Στην ίδια συγκέντρωση, τα άλλα δύο δείγματα (MTM_R-1:10 και MTM_70-1:5) κατάφεραν να επιτύχουν ικανοποιητική αναστολή του μικροοργανισμού μετά από 26 ώρες (*βλ.* δ/τα 8.19 και 8.21, Κεφάλαιο 8). Στα 6.2 ppm, την ισχυρότερη αντιμικροβιακή δράση εμφάνισε το MTM_70-1:10 ακολουθούμενο από το MTM_R-1:10 (το πλάσμα δεν δοκιμάστηκε σε αυτή τη συγκέντρωση) (*βλ.* δ/μα 8.20, Κεφάλαιο 8). Η στατιστική ανάλυση των αποτελεσμάτων έδειξε ότι η αναστολή της *S. enterica* είναι σημαντικά εξαρτώμενη ($p<0.001$) από όλους τους πειραματικούς συντελεστές, δηλαδή από τον χρόνο, τη μέθοδο παρασκευής και τη συγκέντρωση των νανοσωματιδίων (*βλ.* Κεφάλαιο 8, Ενότητα 8.3). Οι συγκεντρώσεις που ανέστειλαν την ανάπτυξη του μελετώμενου μικροοργανισμού σε όλα τα δείγματα (μεγαλύτερη

αναστολή εμφάνισαν τα δείγματα πλάσματος και MTM_70-1:10), βρίσκονται σε συμφωνία με προηγούμενες μελέτες που διαπίστωσαν αναστολή του μικροοργανισμού από AgNPs σε εύρος συγκεντρώσεων 3,12-16 ppm. Τα σφαιρικά νανοσωματίδια φαίνεται να έχουν την μεγαλύτερη αντιμικροβιακή δράση. Δεδομένου ότι οι περιοχές των νανοσωματιδίων που έχουν άκρες και γωνίες παρουσιάζουν συσσώρευση ηλεκτρονίων και ως εκ τούτου είναι πιο δραστικές χημικά, θα ανέμενε κανείς ότι τα μη-σφαιρικά νανοσωματίδια έχουν μεγαλύτερη επίδραση στην αναστολή της Σαλμονέλας (Sau, Rogach, Jäckel, Klar, & Feldmann, 2010), (Fedlheim & Foss, 2001). Το δείγμα πλάσματος εξετάστηκε επίσης για την αντιμικροβιακή δράση έναντι της *S. enterica* σε συγκέντρωση 0,39 ppm και παρατηρήθηκε ότι εμφανίζει πολύ υψηλή αναστολή ακόμη και σε χαμηλή συγκέντρωση (*βλ.* δ/μα 8.22, Κεφάλαιο 8). Αυτό οδηγεί στην υπόθεση ότι στο δείγμα μπορεί να υπάρχουν είδη ριζών τα οποία είναι υψηλής τοξικότητας ακόμα και όταν εκτίθενται σε ανθρώπινα κύτταρα.

Σε παγκόσμιο επίπεδο, υπάρχει ένας αρκετά μεγάλος προβληματισμός ως προς την πιθανή τοξικότητα των νανοσωματιδίων, παρά το γεγονός ότι ήδη χρησιμοποιούνται σε πολλές εφαρμογές. Αυτή η ανησυχία οφείλεται στο μικρό τους μέγεθος, καθώς μπορούν να έχουν πρόσβαση σε πολύ προστατευμένα όργανα, όπως ο εγκέφαλος, μετά την είσοδό τους στον ανθρώπινο οργανισμό, και η απομάκρυνσή τους από τους ιστούς φαίνεται να είναι ένα πολύ δύσκολο έργο (Pietroiusti, Magrini, & Campagnolo, 2014). Για αυτό το λόγο, η αντιμικροβιακή τους δράση δεν είναι επαρκής παράγοντας για να μπορούν να χρησιμοποιηθούν σε εμπορικά προϊόντα ή άλλες εφαρμογές. Πρέπει πρώτα να ελεγχθεί και η τοξικότητά τους σε ανθρώπινα κύτταρα. Η κυτταρική καλλιέργεια έχει βοηθήσει στην in vitro ανάλυση των AgNPs αλλά δεν υπάρχει μια ολοκληρωμένη συγκριτική τους μελέτη λόγω των πολλών παραμέτρων που αλλάζουν σε κάθε περίπτωση (συνθήκες καλλιέργειας και μέθοδοι σύνθεσης AgNPs) (Vazquez-Muñoz, et al., 2017). Έχει αποδειχθεί όμως ότι μειώνουν την βιωσιμότητα των κυττάρων ανάλογα με τις προαναφερθείσες παραμέτρους. Ο μηχανισμός της κυτταροτοξικότητάς τους έχει αποδοθεί στην κυτταρική απόπτωση και νέκρωση κυττάρων (Ka-Ming Chan, Moriwaki, & De Rosa, 2014), στη μιτοχονδριακή δυσλειτουργία με διάρρηξη της διαπερατότητας της μεμβράνης (Galandáková, et al., 2016), στη βλάβη του DNA και το σχηματισμό ROS (Zhang, Wang, Chen, & Chen, 2014) (βλέπε επίσης Σχήμα 6.1, Κεφάλαιο 6). Ο σχηματισμός "κορώνας" των AgNPs με βιολογικά μόρια θεωρείται επίσης ένας σημαντικός παράγοντας της κυτταροτοξικότητάς τους (Pietroiusti, Magrini, & Campagnolo, 2014). Τα κύτταρα ωστόσο προσπαθούν να μειώσουν τις επιπτώσεις αυτές με μηχανισμούς άμυνας που σχηματίζουν μη επιβλαβείς ενώσεις με τα ιόντα αργύρου (σχηματισμός

σουλφιδίου αργύρου (Ag_2S) και χλωριούχου αργύρου (AgClX)) (Marchioni, Jouneau, Chevallet, Michaud-Soret, & Deniaud, 2018). Φυσικά η κυτταροτοξικότητα των AgNPs εξαρτάται από τη συγκέντρωση και από το μέγεθος τους, με τα μικρότερα σωματίδια να έχουν βρεθεί να είναι πιο τοξικά στο παρελθόν. Ο παράγοντας κάλυψης παίζει επίσης σημαντικό ρόλο, με τα κιτρικά επικαλυμμένα AgNPs να έχουν βρεθεί λιγότερο κυτταροτοξικά (Akter, et al., 2018). Πολλά AgNPs (με μεγέθη 7-100 nm και συγκεντρώσεις 0,025-400 ppm), έχουν δοκιμαστεί σε διάφορους τύπους κυττάρων από προηγούμενες μελέτες (βλέπε Πίνακα 6.1, Κεφάλαιο 6).

Στο παρελθόν, μετά από υψηλά επίπεδα έκθεσης σε ενώσεις αργύρου, είχε παρατηρηθεί το φαινόμενο «Αργύρια» (Argyria) στο δέρμα των ασθενών, όπως επίσης και προβλήματα στη διαδικασία επούλωσης των ινοβλαστών των επιθηλιακών κυττάρων. Επομένως, σε περίπτωση που τα νανοσωματίδια αργύρου χρησιμοποιηθούν για επιδερμικές εφαρμογές ή πρόκειται να εφαρμοστούν σε ανοιχτές πληγές και εγκαύματα (Galandáková, et al., 2016), (Marchioni, Jouneau, Chevallet, Michaud-Soret, & Deniaud, 2018), ο έλεγχος της τοξικότητάς τους σε φυσιολογικούς ινοβλάστες δέρματος του ανθρώπου (Normal Human Dermal Fibroblasts, NHDF) είναι ζωτικής σημασίας. Στο παρελθόν, νανοσωματίδια αργύρου με εύρος μεγεθών 1-200 nm, έχουν ελεγχθεί σε ινοβλάστες. Από την μελέτη των Paknejadi, Bayat, Salimi, & Razavi (2018), οι τιμές IC_{50} (Inhibition Concentration 50%, οι συγκεντρώσεις που μειώνουν των πληθυσμό των κυττάρων κατά 50) για AgNPs μεγέθους 6,03 nm (κυρίως σφαιρικού σχήματος), βρέθηκαν να είναι 30,64 και 14,98 ppm μετά από 24ωρη και 48ωρη έκθεση, αντίστοιχα. Από μία άλλη μελέτη, των Galandáková, et al. (2016), μη τοξικές συγκεντρώσεις για AgNPs μείγματος μεγεθών (μέσου μεγέθους 10 nm) βρέθηκαν σε εύρος συγκεντρώσεων 0,25-25 ppm, και επιπλέον, 5 nm AgNPs βρέθηκαν πιο τοξικά από το διάλυμα $AgNO_3$ που ελέγχθηκε, ενώ 20 nm και 50 nm AgNPs βρέθηκαν λιγότερο τοξικά από το $AgNO_3$. Οι Wildt, et al. (2016), επίσης διαπίστωσαν ότι τα μικρότερα νανοσωματίδια ήταν πιο τοξικά σε κύτταρα ινοβλαστών ποντικού, λόγω απελευθέρωσης ιόντων αργύρου. Τέλος, από τους Avalos, Haza, Mateo, & Morales (2014), οι συγκεντρώσεις νανοσωματιδίων 6,72 και 13,45 ppm βρέθηκαν να μειώνουν κατά πολύ την βιωσιμότητα των NHDF.

Με βάση όσα αναφέρθηκαν, συμπληρωματικά της αντιμικροβιακής δράσης των νανοσωματιδίων, κρίθηκε σημαντικό να μελετηθεί και η τοξικότητά τους σε ανθρώπινα κύτταρα. Επομένως, στην παρούσα μελέτη, ελέγχθηκε επίσης η επίδραση νανοσωματιδίων αργύρου σε φυσιολογικούς ινοβλάστες δέρματος ανθρώπου μετά από 24, 48 και 72 ώρες

έκθεσης σε ένα εύρος συγκεντρώσεων. Η βιωσιμότητα των κυττάρων μετρήθηκε με την μέθοδο MTT (3-(4,5-dimethylthiazol-2-yl)-2,5-diphenyltetrazolium bromide) και ερμηνεύτηκε σαν ποσοστό ως προς τα επιζώντα κύτταρα την ημέρα 0 (αυτά που επεξεργάστηκαν μόνο με το θρεπτικό υλικό αύξησης). Σαν δείγματα αναφοράς, εκτός από τα κύτταρα επεξεργασμένα μόνο με θρεπτικό υλικό DMEM (Dulbecco's Modified Eagle Medium**,** με 10% εμβρυακό ορό βόειου), χρησιμοποιήθηκαν το διμεθυλοσουλφοξείδιο (DMSO) 1,6%, που είναι τοξικό για τα κύτταρα (αρνητικός μάρτυρας), και το $AgNO_3$ 250 μM, που βρέθηκε από προηγούμενη μελέτη (Kaplan, Ciftci, & Kutlu, 2016), πως είναι τοξικό σε μετασχηματισμένα κύτταρα ινοβλαστών εμβρύου αρουραίου (H-ras transformed 5RP7) (θετικός μάρτυρας). Γενικά, τόσο ο χρόνος όσο και η μέθοδος επεξεργασίας των κυττάρων είχαν σημαντική επίδραση στην επί τοις εκατό (%) βιωσιμότητα ως προς τα κύτταρα αναφοράς (κύτταρα εκτεθειμένα μόνο στο θρεπτικό μέσο – DMEM) της ημέρας 0 ($p<0,001$). Συγκρίνοντας με την % βιωσιμότητα των κυττάρων αναφοράς, σε κάθε ημέρα έκθεσης, το MTM_R-1:10 έδειξε σημαντική μείωση της βιωσιμότητας σε όλες τις συγκεντρώσεις, εκτός από τη συγκέντρωση 0,49 ppm, στην οποία δεν εμφανίστηκε τοξική συμπεριφορά μόνο την 1η ημέρα. Παρόλα αυτά, δεν εμφάνισε σε καμία συγκέντρωση παραπάνω από 35% μείωση της βιωσιμότητας των κυττάρων και η μείωση της βιωσιμότητας φαίνεται να μην εξαρτάται σημαντικά από την συγκέντρωση αλλά από το χρόνο (*βλ.* Σχήμα 8.23, Κεφάλαιο 8, για στατιστική σημαντικότητα). Το MTM_70-1:10 σε συγκέντρωση 0,49 ppm, εμφάνισε σημαντική κυτταροτοξική επίδραση μόνο την 1η ημέρα (μικρής στατιστικής σημαντικότητας: $p<0,05$). Αυτή η συγκέντρωση και η συγκέντρωση των 0,98 ppm, ήταν και οι μόνες που δεν εμφάνισαν σημαντική επίδραση στη βιωσιμότητα των κυττάρων με την πάροδο του χρόνου. Με αύξηση της συγκέντρωσης παρόλα αυτά, εμφανίζεται και αντίστοιχη μείωση της βιωσιμότητας των κυττάρων, η οποία στην μεγαλύτερη συγκέντρωση (6,2 ppm), την τελευταία ημέρα έκθεσης (3η), ανέρχεται μέχρι και στο 60% (*βλ.* Σχήμα 8.24, Κεφάλαιο 8). Το MTM_70-1:5, επίσης δεν έδειξε τοξική επίδραση στους ινοβλάστες σε συγκέντρωση 0,49 ppm, καθ' όλη τη διάρκεια της έκθεσης, ενώ σε συγκεντρώσεις 0,98 και 1,95 ppm, βρέθηκε τοξικό μόνο την τελευταία ημέρα έκθεσης. Η μείωση της βιωσιμότητας φαίνεται και σε αυτή την περίπτωση να εξαρτάται σημαντικά από τη συγκέντρωση, με την υψηλότερη χρησιμοποιούμενη συγκέντρωση (6,2 ppm) να προκαλεί μείωση της τάξεως του 56%. Επιπλέον, όλες οι συγκεντρώσεις μείωσαν σημαντικά τη βιωσιμότητα με την πάροδο του χρόνου (*βλ.* Σχήμα 8.25, Κεφάλαιο 8, για σημαντικότητα), εκτός από την συγκέντρωση 0,49 ppm που δεν έδειξε καμία επίδραση. Το δείγμα πλάσματος σε συγκέντρωση 0,39 ppm, βρέθηκε μη τοξικό μόνο την 3η ημέρα, ενώ τις άλλες 2 ημέρες βρέθηκε τοξικό, με χαμηλή στατιστική σημαντικότητα

($p<0,05$), και παρατηρήθηκε επίσης σημαντική μείωση της βιωσιμότητας σε σχέση με το χρόνο (*βλ.* Εικόνα 8.25, Κεφάλαιο 8, για σημαντικότητα). Όταν συγκρίθηκαν όλα τα δείγματα AgNPs σε συγκέντρωση 3,9 ppm (*βλ.* δ/μα 8.27, Κεφάλαιο 8), όλα εμφάνισαν σημαντική μείωση της βιωσιμότητας σε σύγκριση με τα κύτταρα αναφοράς (Untreated). Όταν συγκρίθηκαν όλα τα δείγματα AgNPs σε όλες τις συγκεντρώσεις την 3η ημέρα έκθεσης (*βλ.* δ/μα 8.28, Κεφάλαιο 8), μόνο το δείγματα MTM_70-1:10 και MTM_70-1:5 σε συγκέντρωση 0,49 ppm βρέθηκαν μη τοξικά. Ειδικότερα, το MTM_70-1:10 σε συγκέντρωση 0,49 ppm παρουσίασε σημαντικά υψηλότερη % βιωσιμότητα σε σχέση με τα κύτταρα αναφοράς ($p<0,001$). Αυτή η αύξηση θα μπορούσε να αποδοθεί στις φυσιολογικές μεταβολές του κυτταρικού μεταβολισμού. Όσον αφορά στα υπόλοιπα δείγματα αναφοράς (θετικοί και αρνητικοί μάρτυρες), το DMSO φάνηκε να έχει αδρανοποιήσει αποτελεσματικά το ήμισυ του πληθυσμού των κυττάρων καθ' όλη τη διάρκεια της μελέτης και το $AgNO_3$ εμφάνισε σημαντικά χαμηλότερη βιωσιμότητα σε σχέση με τον αρνητικό μάρτυρα (Untreated) όλες τις ημέρες έκθεσης (*βλ.* δ/τα 8.23-8.28, Κεφάλαιο 8, για σημαντικότητα), ενώ παρέμεινε σταθερό με την πάροδο του χρόνου. Η σημαντικότητα της διαφοράς του $AgNO_3$ με τα δείγματα AgNPs αλλάζει ανάλογα με τον χρόνο έκθεσης και τη συγκέντρωση των AgNPs, και επομένως κάποιο συμπέρασμα ως προς την σχετική τους τοξικότητα δεν μπορεί να εξασφαλιστεί (*βλ.* Κεφάλαιο 8.4). Ωστόσο, παρατηρήθηκε ότι σε μεγάλες συγκεντρώσεις (3,9 και 6,2 ppm), όλα τα δείγματα AgNPs εμφάνισαν ίδια τοξικότητα με το $AgNO_3$ την 1η ημέρα έκθεσης (εξαιρείται το δείγμα πλάσματος), ενώ στις ίδιες συγκεντρώσεις, γίνονται πιο τοξικά από το $AgNO_3$ μετά την 1η ημέρα έκθεσης.

Τέλος, υπολογίστηκαν οι συγκεντρώσεις που μειώνουν κατά 50% την βιωσιμότητα των ινοβλαστών (IC_{50}) για όλα τα δείγματα νανοσωματιδίων (εκτός του πλάσματος) και σε όλες τις ημέρες έκθεσης (24, 48, 72 h) (*βλ.* Πίνακα 8.5, Κεφάλαιο 8). Αυτές βρέθηκαν σε εύρος μεταξύ 4,40-13,54 ppm για τα δείγματα MTM_70-1:10 και MTM_70-1:5. Για το δείγμα MTM_R-1:10, η τιμή IC_{50} δεν μπόρεσε να υπολογιστεί, καθώς η γραμμική παλινδρόμηση που χρησιμοποιήθηκε στις προηγούμενες περιπτώσεις, δεν είχε καλή προσαρμογή στα πειραματικά δεδομένα αυτού του δείγματος, δεδομένου και του μικρού εύρους των συγκεντρώσεων που ελέγχθηκε. Στις χαμηλότερες συγκεντρώσεις (0-0,98 ppm) του MTM_R-1:10, η βιωσιμότητα των κυττάρων τείνει να μειώνεται γραμμικά και έπειτα σταθεροποιείται, χωρίς να μπορεί να εκτιμηθεί η πιθανή συμπεριφορά του δείγματος σε υψηλότερες συγκεντρώσεις. Η τιμή του παρόλα αυτά, εκτιμάται πως βρίσκεται στο εύρος 6,2-100 ppm. Σε κάθε περίπτωση, την χαμηλότερη συγκέντρωση IC_{50} εμφανίζει το MTM_70-1:10. Δυστυχώς, παρά τις πολλές προσπάθειες του επιστημονικού κλάδου, δεν έχει καταστεί δυνατόν να παραχθεί μια

τυποποιημένη μέθοδος για την εκτίμηση της τοξικότητας των νανοσωματιδίων και αυτό γιατί οι παράμετροι που αλλάζουν σε κάθε μελέτη είναι πολλοί. Το μέσο διασποράς των νανοσωματιδίων είναι η σημαντικότερη παράμετρος που αλλάζει μεταξύ των εργαστηριακών μελετών και μεταξύ in vitro και in vivo συνθηκών. Ανάλογα με το μέσο διασποράς, αλλάζει και η συμπεριφορά τους (για παράδειγμα η συσσωμάτωσή τους και ο σχηματισμός «κορώνας» με τα βιολογικά μόρια) (*βλ.* Κεφάλαιο 6). Επομένως, υπάρχει ανάγκη εκτίμησης της πραγματικής έκθεσης του ανθρώπου σε νανοσωματίδια μέσω των διαφορετικών οδών χορήγησης (δερματική, στοματική και αναπνευστική οδός), και το ανώτερο και κατώτερο όριο της συγκέντρωσης των νανοσωματιδίων δεν είναι συγκεκριμένο (Drasler, Sayre, Steinhäuser, Petri-Fink, & Rothen-Rutishauser, 2017). Το χαμηλότερο όριο σύμφωνα με το Παγκόσμια Εναρμονισμένο Σύστημα Ταξινόμησης και Επισήμανσης Χημικών Προϊόντων των Ηνωμένων Εθνών, μπορεί να εκληφθεί στα 100 ppm (στοματική και δερματική χορήγηση) (Lee, et al., 2017). Από την μελέτη των Farcal, et al. (2015), φαίνεται επίσης πως τιμές IC_{50} μικρότερες των 100 ppm, και ιδίως αυτές που είναι μικρότερες των 30 ppm, μπορούν να θεωρηθούν υψηλής τοξικότητας. Επομένως, τα νανοσωματίδια που παρήχθησαν σε αυτή τη μελέτη μπορούν να θεωρηθούν κυτταροτοξικά.

Εν κατακλείδι, το δείγμα των νανοσωματιδίων αργύρου που συντέθηκε με αναγωγή με πλάσμα, βρέθηκε να έχει την υψηλότερη αντιμικροβιακή δράση σε συγκεντρώσεις 3,9 και 0,39 ppm. Παρά την πολύ χαμηλή συγκέντρωσή του, το ίδιο δείγμα των 0,39 ppm βρέθηκε να είναι κυτταροτοξικό τις 2 πρώτες ημέρες της έκθεσής του σε κύτταρα NHDF. Αυτό ενισχύει την αρχική υπόθεση που έγινε, πως πιθανές δραστικές ενώσεις που υπάρχουν στο δείγμα βλάπτουν τόσο την *S. enterica* αλλά και τα ανθρώπινα κύτταρα. Επιπλέον, η παραγωγή τους ήταν πολύ χαμηλής απόδοσης. Περισσότερες μελέτες θα χρειαστούν για να χαρακτηριστεί η μορφολογία τους και η κυτταροτοξικότητά τους σε μεγαλύτερες συγκεντρώσεις. Το δείγμα MTM_70-1:10 των AgNPs, με νανοσωματίδια σφαιρικού σχήματος και μεγέθους 7-15 nm, βρέθηκε επίσης να έχει πολύ ικανοποιητική αντιμικροβιακή δράση έναντι του μελετώμενου μικροοργανισμού αλλά παρουσίασε επίσης την χαμηλότερη τιμή IC_{50}. Μόνο η χαμηλότερη συγκέντρωση αυτού του δείγματος (0,49 ppm) δεν εμφάνισε σημαντικά κυτταροτοξικά αποτελέσματα. Το MTM_70-1:5 (6-84 nm) δεν ήταν επίσης κυτταροτοξικό μόνο σε συγκέντρωση 0,49 ppm. Σε συγκεντρώσεις 0,98 και 1,95 ppm, έδειξε κυτταροτοξική δράση την τελευταία ημέρα έκθεσης. Όσον αφορά την κυτταροτοξική συμπεριφορά των AgNPs σε σχέση με τον $AgNO_3$, AgNPs με μεγαλύτερες συγκεντρώσεις (3.9 και 6.2 ppm), σε μεγαλύτερη της 24ωρης έκθεση, εμφανίζονται πιο τοξικά. Αυτό έρχεται σε αντιπαράθεση με προαναφερθείσα μελέτη που

αναφέρει ότι τα μεγαλύτερα νανοσωματίδια είναι και λιγότερο τοξικά από το $AgNO_3$, καθώς στην παρούσα εργασία, φαίνεται πως ακόμα και τα μεγαλύτερα νανοσωματίδια, μετά τις 24 ώρες και μέχρι τις 72 ώρες έκθεση, γίνονται εξίσου τοξικά (Galandáková, et al., 2016). Παρόλα αυτά, το εύρος μη τοξικών συγκεντρώσεων που βρέθηκε από την ίδια μελέτη (0,25-25 ppm) μετά από 24ωρη έκθεση, έρχεται σε συμφωνία με τα δείγματα MTM_R-1:10 και MTM_70-1:5, καθώς περιλαμβάνει την συγκέντρωση 0,49 ppm που βρέθηκε μη τοξική την $1^η$ ημέρα έκθεσης. Τέλος, σε αυτή τη μελέτη παρατηρήθηκαν τιμές IC_{50} στο ίδιο εύρος (< 30 ppm) με αυτές που βρέθηκαν από τη μελέτη των Paknejadi, Bayat, Salimi, & Razavi (2018). Επειδή οι τιμές IC_{50} που υπολογίστηκαν ήταν πολύ μικρότερες από 100 ppm, τα νανοσωματίδια είναι πιθανόν να είναι τοξικά όταν εισέρχονται στον ανθρώπινο οργανισμό (π.χ. μέσω της στοματικής ή δερματικής οδού). Ειδικότερα, η μικρότερη τιμή IC_{50}, εμφανίστηκε για τα μικρότερα νανοσωματίδια, κυρίως σφαιρικού σχήματος, κάτι που επιβεβαιώνεται από προηγούμενες μελέτες που υποστηρίζουν ότι όσο μικρότερα είναι τα νανοσωματίδια τόσο πιο ευαίσθητα είναι τα ανθρώπινα κύτταρα όταν εκτεθούν σε αυτά ((Souza, Franchi, Rosa, da Veiga, & Takahashi, 2016), (Zapór, 2016)). Το συμπέρασμα έρχεται επίσης σε συμφωνία με τους Avalos, Haza, Mateo, & Morales (2014), που υποστήριξαν ότι σφαιρικά νανοσωματίδια σε συγκεντρώσεις κοντά στα 6,2 ppm, εμφάνισαν υψηλή κυτταροτοξική δράση. Φυσικά, όσο μεγαλύτερο το εύρος μεγεθών των νανοσωματιδίων, τόσες περισσότερες επαναλήψεις είναι απαραίτητες για την βεβαιότητα του αποτελέσματος και επομένως, τα δείγματα MTM_R-1:10 και MTM_70-1:5, με εύρος μεγεθών 18-57 και 6-84 nm αντίστοιχα, απαιτούν πολλές ακόμα επαναλήψεις.

Είναι επίσης σημαντικό να αναφερθεί ότι τα AgNPs μπορούν να αλληλεπιδράσουν με το MTT και τα αποτελέσματα να επηρεαστούν. Η μέθοδος MTT ελέγχει την ικανότητα των κυττάρων να μετατρέπουν το MTT σε φορμαζάνη μέσω αναγωγών NADP(H) από μιτοχονδριακά ένζυμα (αλλαγή χρώματος από κίτρινο σε μωβ). Αυτή η δράση διεξάγεται μόνο όταν τα κύτταρα είναι ζωντανά. Το μιτοχονδριακό στρες που μπορεί να προκληθεί από έκθεση των κυττάρων σε νανοσωματίδια, μπορεί να προκαλέσει χαμηλότερη ανίχνευση κατά την ανάλυση με φασματομετρικές μεθόδους, ακόμη και όταν υπάρχουν ζωντανά κύτταρα (Kaplan, Ciftci, & Kutlu, 2016). Επιπλέον, μια άλλη πιθανή αλληλεπίδραση των AgNPs που μπορεί να παρεμβαίνει στα πειραματικά αποτελέσματα, είναι η αλληλεπίδρασή τους με τα αντιβιοτικά, αφού έχει αναφερθεί σε πολλές μελέτες πως έχουν συνεργιστική δράση (π.χ. (Katva, Das, Moti, Jyoti, & Kaushik, 2017), (Deng, et al., 2016), (Jamaran & Rahimian Zarif, 2016)), δεδομένου ότι το θρεπτικό υλικό που χρησιμοποιήθηκε περιείχε αντιβιοτικά.

Για τους παραπάνω λόγους, συμπεραίνεται πως η χρήση των νανοσωματιδίων αργύρου που παρήχθησαν σε αυτή τη μελέτη σε εφαρμογές που επιτρέπουν την πρόσβασή τους στον ανθρώπινο οργανισμό, έχει υψηλό ρίσκο για την ανθρώπινη υγεία. Ωστόσο, τα αποτελέσματα της κυτταροτοξικότητας σε αυτή την μελέτη, λήφθηκαν μόνο με τη μέθοδο MTT. Απαιτείται λοιπόν περαιτέρω έρευνα για την επαλήθευση αυτών των πειραματικών αποτελεσμάτων και με διαφορετικές μεθόδους «ανάγνωσης» της βιωσιμότητας των κυττάρων. Το μέσο διασποράς που χρησιμοποιήθηκε είχε επίσης αντίκτυπο στα πειραματικά αποτελέσματα, όπως το νερό, που ήταν το αρχικό μέσο διασποράς των AgNPs μετά την σύνθεσή τους. Έπειτα, το θρεπτικό μέσο καλλιέργειας περιείχε επίσης FBS (Fetal Bovine Serum -ορό εμβρύων βοοειδών) και αντιβιοτικά που επίσης επιδρούν στην τελική συμπεριφορά των νανοσωματιδίων. Οι in vitro με τις in vivo μελέτες διαφέρουν επίσης για τον ίδιο λόγο. Επομένως, χρειάζεται διεξοδική μελέτη όλων των παραπάνω παραγόντων που μπορεί να επηρεάζουν τα κυτταροτοξικά αποτελέσματα που προέκυψαν από αυτή την μελέτη πριν απορριφθεί η μελλοντική τους χρήση σε ιατρικές και φαρμακευτικές εφαρμογές.

Περισσότερες μελέτες επίσης θα χρειαστούν για να ελεγχθεί η αντιμικροβιακή δράση αυτών των AgNPs κατά της *S. entetica* σε συγκεντρώσεις μικρότερες των 3.9 ppm, και συγκεκριμένα στις πολύ χαμηλές συγκεντρώσεις όπου δεν εμφάνισαν σημαντικά κυτταροτοξικά αποτελέσματα (0,49 και 0,98 ppm). Μεγαλύτερο εύρος συγκεντρώσεων πρέπει επίσης να ελεγχθεί σε κύτταρα NHDF, για την εύρεση της καταλληλότερης καμπύλης βιωσιμότητας συναρτήσει της συγκέντρωσης και τον υπολογισμό της τιμής IC_{50} του δείγματος MTM_R-1:10. Τέλος, απαιτούνται μελέτες για τον χαρακτηρισμό των μορφολογικών χαρακτηριστικών των νανοσωματιδίων του δείγματος του πλάσματος, προκειμένου να ληφθούν περισσότερες πληροφορίες σχετικά με τον μηχανισμό της αντιμικροβιακής και κυτταροτοξικής τους δράσης. Με αλλαγή κάποιων παραμέτρων της σύνθεσής τους, η μέθοδος σύνθεσης μέσω πλάσματος θα μπορούσε να οδηγήσει σε νανοσωματίδια που δρουν ως πολύ καλοί αντιμικροβιακοί παράγοντες με χαμηλή κυτταροτοξικότητα.

CONTENTS

1. History of Nanotechnology

The term "nanometer" was introduced by Richard Zsigmondy, who won the 1925 Nobel Prize in chemistry after measuring the size of particles, such as gold colloids, using a microscope. However, the father of Nanotechnology is considered to be Richard P. Feynman, the 1965 Nobel Prize winner in Physics, after his inspiring 1959's seminal lecture titled "There's plenty of room at the bottom", in which he proposed the manipulation of the matter in atomic scale. In 1974 Norio Taniguchi, a Japanese scientist of Tokyo Science University, coined the term *Nanotechnology* to describe semiconductor processes in the nanoscale (Hulla, Sahu, & Hayes, 2015). The most important steps in the history of Nanotechnology from 1981 to 2016 are shown in Figure 1.1.

Year	Items
1981	Scanning tunneling electron microscope that could process single atoms.
1985	Discovery of fullerene, 60 carbon atoms in a circle (C60).
1992	Discovery of carbon nanotubes that are stronger than steel; can be used in drug delivery, energy storage, and power transmission.
1993	Discovery of quantum dots.
2000	Construction of passive nanoparticles for applications as nano fuel cells and in products of daily use, including cosmetics.
2005	Construction of active nanoparticles for target-directed drugs and other adaptive structures.
Future	Nanosystems, hierarchical nanoarchitectures, atomic devices, nano DNA-based computers, diagnostic robots, etc.

Figure 1.1. *The most important steps in the history of Nanotechnology (Singh, 2016).*

2. Nanoparticles

Nanoparticles (NPs) is a combined name. At the International System of Units (SI), the term "nano" is used to describe a reduction by 10^9 times. Therefore, the nanosized world is typically measured in nanometers. According to IUPAC glossary, nanoparticles are ultrafine particles having an aerodynamic diameter less than 100 nm but larger than molecular ones (> 1 nm) (Konwar & Baquee, 2013).

Some authors classify the nanostructures according to the number of dimensions that exceed 100 nm, i.e. the number of dimensions that exceed the nanoscale. Thus, these materials can be 0D, 1D, 2D or 3D. A 0D material has all its dimensions comprised in the nanometric scale, such as metallic NPs or quantum dots. A 1D nanostructure has one dimension above nanoscale (e.g., carbon nanotubes). 2D nanostructures have two dimensions above nanoscale (e.g., surface nanocoatings, thin films of molecular monolayers) and lastly, a 3D nanostructure escapes nanoscale but the material is comprised by a set of nanoparticles forming a block of micro/macrometric size (e.g., nanoporous materials, powders) (Inmaculada López-Lorente & Valcárcel, 2014).

The importance of nanoparticles production and use was recognised when researchers found that size can influence the physiochemical properties of a substance (e.g., the optical properties). Nanoparticles of the same material and same dimensions are considered identical (homogeneous), whereas those of different materials, in the same size, present different colours, for example 20-nm gold (Au), platinum (Pt), silver (Ag), and palladium (Pd) NPs have characteristic wine red, yellowish gray, black and dark black colours, respectively. Nanoparticles of the same material present characteristic colours and different properties in accordance to the variation of size and shape, something that has been widely utilized in bioimaging applications. The ratio between the capping agent (molecules sometimes used to prevent the further growth of nanoparticles and their agglomeration by attaching to their surface, as further elaborated below[1]) and % nanoparticle concentration, also affect the colour of the solution. Any alterations of the above factors influence the absorption properties of NPs and hence different absorption colours are observed (Inmaculada López-Lorente & Valcárcel, 2014), (Khan, Saeed, & Khan, 2017). The reason of these changes in nanoparticles properties

[1] *See* pages: 2 (THE SURFACE LAYER), 15 and 17 (Physicochemical synthesis of AgNPs)

due to morphological changes is further explained below[2].

Except from bioimaging, nanoparticles find many more applications in many scientific fields like chemistry, engineering, physics, biology, and medicine, as presented in the figure below (Figure 2.1).

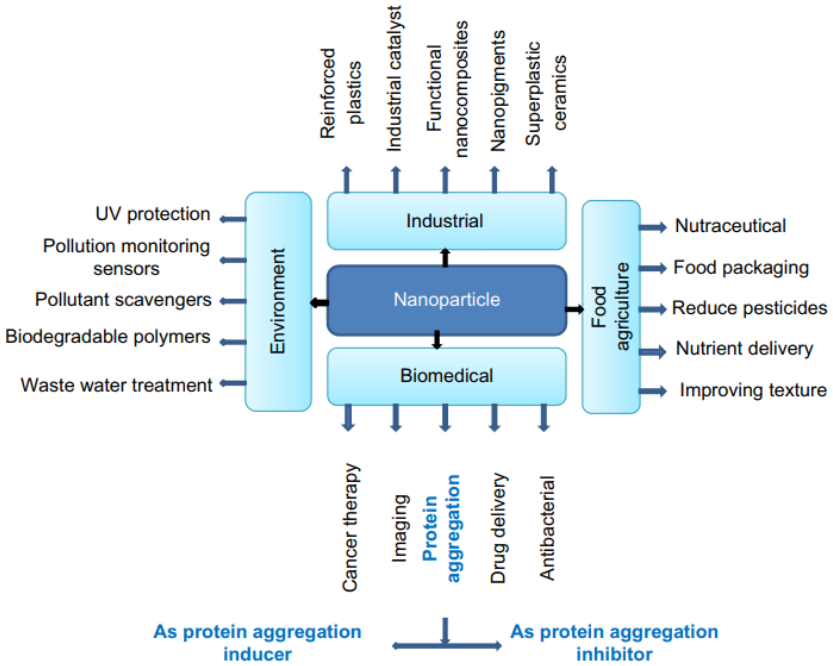

Figure 2.1. *Application of nanoparticles in various fields such as in the biomedical, environmental, industrial, and food agriculture industries* (Zaman, Ahmad, Qadee, Rabbani, & Khan, 2014).

Since the physical and chemical properties of nanoparticles differ to a high extent from the same properties of the bulk material, nanoparticles are considered as complex materials rather than just smaller divisions of the same element. A basic example of the importance of the careful examination of their complexity, especially their characteristics related to their structure, is the ability of nanoparticles to interact with other molecules. Thus, nanoparticles can be split into three layers for better examination (Christian, Von der Kammer, Baalousha, & Hofmann, 2008).

1. *THE SURFACE LAYER:* Nanoparticles with charged surface are easily disperse in aqueous media. Nevertheless, many materials do not have convenient surfaces for the stabilization of localized charges. In those cases, the surface may be

[2] *See* 2.1 Features and Characteristics of nanoparticles

functionalized with a variety of small molecules, metal ions, surfactants and polymers (otherwise called capping agents) that can cling to it with a covalent-like bond and also contain charged groups (e.g., the use of citrate for the stabilization of gold and silver sols).

2. *THE SHELL:* This layer is chemically different from the core in all aspects, and it basically constitutes the second layer of the nanoparticle, that covers the core and has a different structure (e.g., quantum dots, which contain a core of one material, such as cadmium selenide, and a shell of another, such as zinc sulfide). Although, this layer is made intentionally most of the times, does not mean that it cannot occur through other processes too (e.g., iron oxide is rapidly formed on the surface of iron nanoparticles after preparation).

3. *THE CORE:* This is essentially the central portion of the nanoparticle and usually refers to the NP itself. In general, the properties that are of great interest for physics and chemistry communities are dominated by the properties of the core, whilst ecotoxicology does not focus there (Khan, Saeed, & Khan, 2017), (Christian, Von der Kammer, Baalousha, & Hofmann, 2008).

Nanoparticles are generally classified in many categories according to their morphology, size and chemical properties. Based on their physical and chemical composition, some general well-known classes are:

1. Inorganic nanoparticles (e.g., noble metal NPs, quantum dots, etc.)

2. Organic nanoparticles (e.g., fullerenes, carbon nanotubes, dendrimers, etc.)

3. Mixed nanoparticles (e.g., gold nanoparticles modified with calixarenes, carbon nanotubes functionalized with ferrocene, etc.)

(Inmaculada López-Lorente & Valcárcel, 2014)

2.1 Features and characteristics of nanoparticles

In this section, the most important physical and chemical properties, depending on the morphology, that make nanoparticles differ from the bulk material and more tempting to be used in various applications, are discussed.

SELF ASSEMBLY

Self-assembly is the process by which nanoparticles spontaneously organize into ordered, macroscopic structures, with non-covalent interactions (e.g., van der Waals interactions, electrostatic interactions, hydrophobic/hydrophilic interactions, hydrogen bonds), so that the system minimizes its free energy and reaches thermodynamic equilibrium state. To form long-range superlattices, narrow size distribution and uniform shape of the particles are required. Therefore, particles morphology is an important factor in determining the geometrical packing in organized structures (Grzelczak, Vermant, Furst, & Liz-Marzán, 2010) (Sau, Rogach, Jäckel, Klar, & Feldmann, 2010).

CHEMICAL REACTIVITIES

Nanoparticles have different chemical features compared to their bulk counterparts or constituent atoms and molecules. This is due to the fact that absorption and reactivity highly depend on their surface structure. The surface structure of nanoparticles may differ due to surface relaxation and reconstruction, the presence of adsorbed layers of reaction by-products and stabilizing molecules, etc. Furthermore, the surface structure changes in accordance to size, shape, and number of components of a particle. It is obvious that the larger the surface area the more the reactions with the environment and subsequently, the more radical the alterations in chemical reactivity (Sau, Rogach, Jäckel, Klar, & Feldmann, 2010).

SURFACE PLASMON RESONANCE (SPR)

Localized surface plasmons are charge density oscillations confined to metallic nanoparticles. This oscillation of electrons that enhances scattering and absorption, is the main reason why metal nanoparticles have received great attention nowadays. The surface plasmon resonance wavelength and the extent of the subsequent enhancement, also highly depends on the size, shape and composition (core-shell) of nanoparticles. Plasmon resonant nanoparticles' biocompatibility makes them also suitable to be used in therapeutic applications (Ammari, Deng, & Millien, 2016), (Jain, Seok Lee, El-Sayed, & El-Sayed, 2006).

3. Metal Nanoparticles

Historically, it was the discovery of Raman scattering effect (SERS), therefore the discovery of the connection between electromagnetic enhancements and plasmon resonance, that initiated the concentrated interest on metal nanoparticles. This led to experimental and theoretical investigations on the different shapes of nanoparticles (Fedlheim & Foss, 2001).

The most interesting property of metal nanoparticles is their large surface-area-to-volume ratio. More specifically, this property means that nanoparticles may be unstable due to their large curved surface and the concentrated energy on it, especially in the edge-like and corner-like regions of the surface where electrons are confined. This affects the nanoparticles' chemical reactivity and surface bonding properties. Also, this electron confinement effect modifies nanoparticles' spectral properties via shifting of quantum levels and change in transition probabilities. Therefore, changes in the shape of nanoparticles are accompanied with changes in their chemical and physical properties since their surface characteristics, and therefore their orientation of electron confinement change, as mentioned before (Chapter 2) (Christian, Von der Kammer, Baalousha, & Hofmann, 2008). Studies have shown that nonspherical nanoparticles have more localized energy and therefore can be used in even more favorable applications, since corners induce more surface plasmons. That makes them ideal for chemical, catalytic, and local field related applications (Sau, Rogach, Jäckel, Klar, & Feldmann, 2010), (Fedlheim & Foss, 2001).

The observation that their optical, electronic, and chemical properties are also size-dependent, sparked an even greater research activity on the synthesis and organic functionalization of different size and shape of metal nanoparticles (Kamat, 2002). This is something to be expected since nanoparticles of different sizes show different structural motifs (e.g., icosahedra, octahedra, cuboctahedra, decahedra, etc.), composition and energetic conditions (Noguez, 2007).

Different types of metal nanoparticles and their main applications in different fields are presented in Figure 3.1.Many different metal nanoparticles like copper, zinc, titanium, magnesium, gold, and silver were studied by several researchers, with silver nanoparticles being extensively investigated due to their high antimicrobial efficacy against bacteria, viruses and other eukaryotic micro-organisms (Rai, Yadav, & Gade, 2009).

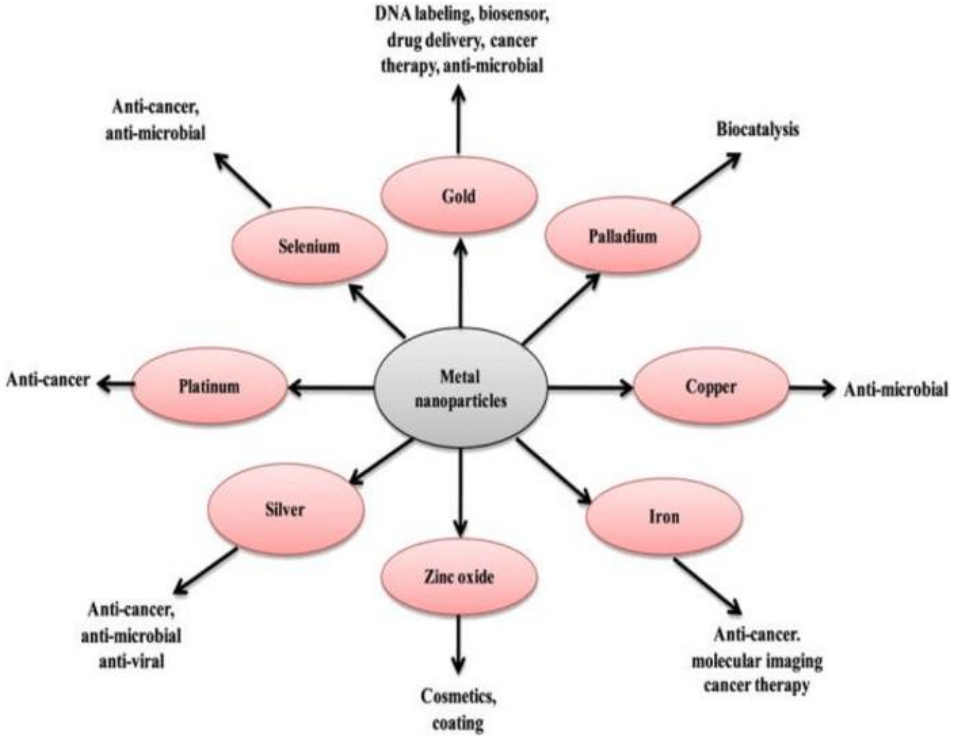

Figure 3.1. *Different types of metal nanoparticles and their applications (Khandel & Kumar Shahi, 2016)*

4. Silver nanoparticles (AgNPs)

4.1 Antimicrobial activity of silver and silver nanoparticles

Silver started being used as an element for treatment centuries ago. In 1700, silver nitrate was used to cure many diseases such as venereal diseases, fistulae from salivary glands, bone and perianal abscesses. In the 19th century, wounds, burns and even opthalmia were cured with the use of silver nitrate solutions. In the 20th century, silver's use as wound healing was even greater due to the Second World War (Rai, Yadav, & Gade, 2009). Silver was in fact the main component in creams for wounds. However, with the discovery of antibiotics, in 1928 by Alexander Fleming, the use of silver and its compounds was stopped (Ebrahiminezhad, Taghizadeh, Taghizadeh, & Ghasemi, 2017). This was due to the fact that silver ions had the disadvantage of forming complexes and thus their action remained only for a short time (Deepak, Kalishwaralal, Pandian, & Gurunathan, 2011). Also, they caused side effects like chemical conjunctivitis, pain and visual impairment that were contributing factors to the disappearance of silver from medicine. It was after decades of applying antibiotics that the use of silver started coming in the limelight again, since bacteria started developing antimicrobial resistance. In fact, the World Health Organization (WHO) declared this issue as the main theme for the World Health Day 2011. Therefore, since silver ions act in a different way than antibiotics, oxidizing and affecting all physiological points in a microbial cell, it was once again a new hope (Ebrahiminezhad, Taghizadeh, Taghizadeh, & Ghasemi, 2017).

In 1960, Moyer introduced the use of 0.5% silver nitrate for the treatment of burns, supporting that this solution doesn't have an impact on epidermal proliferation and it also possesses antibacterial property against *Staphylococcus aureus*, *Pseudomonas aeruginosa* and *Escherichia coli*. In 1968, the first silver sulfadazine cream (silver nitrate combined with sulfonamide) was available as an antimicrobial agent to treat burns (Rai, Yadav, & Gade, 2009). In modern sciences, silver appeared in a novel form, as silver nanoparticles (AgNPs) (Deepak, Kalishwaralal, Pandian, & Gurunathan, 2011).

Silver nanoparticles, like all nanoparticles and especially metal, are studied nowadays due to their unique physiochemical properties including optical, electrical, thermal and biological. Their antibacterial properties though remain the main reason of their extent use (Zhang, Liu, Shen, & Gurunathan , 2016). In fact, the number of their applications has increased intensively in only a decade. In 2005, the Nanotechnology Consumer Product Inventory (CPI) was created,

making a first list of consumer products using nanoparticles. The number of those products was 54 at that time. Until 2016, the number was increased to no less than 2000 products, with 622 companies in 32 countries involved in their production (Vance, et al., 2015). From all nanoparticles, silver nanoparticles are the most popularly advertised and maintain the leadership in all these products by being present in a very big amount of them (25%) (Pourzahedi, Vance, & Eckelman, 2017). These products find a variety of applications, as it is shown in the image below (fig. 4.1).

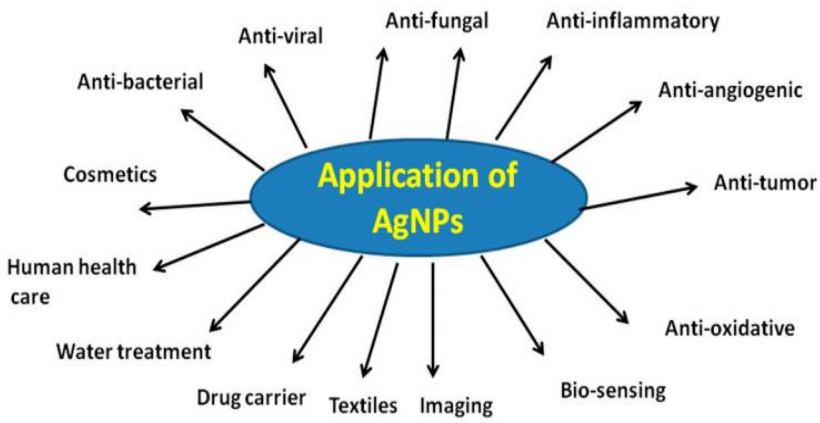

Figure 4.1. *Various applications of AgNPs (Zhang, Liu, Shen, & Gurunathan , 2016).*

The sectors of AgNPs applications that hold the leadership and how AgNPs use is distributed among all these applications, has been statistically examined by a study made back in 2012 (fig.4.2).

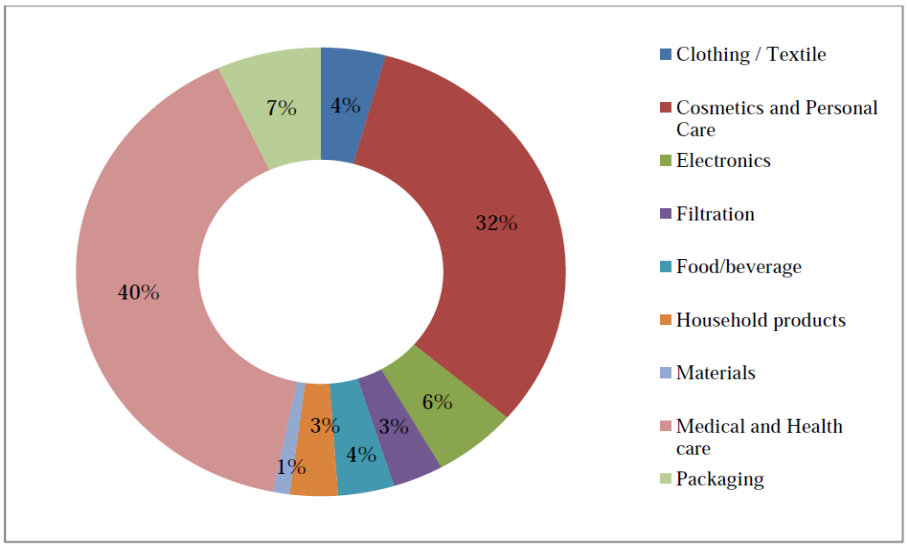

Figure 4.2. *Nanosilver use in various applications of consumer products (Lem, et al., 2012).*

Some examples of consumer products are: food containers (e.g., A-DO Global Co., South Korea), fabric softeners (e.g., IRIN, Aekyung, South Korea), cotton sheet sets (e.g., AgActive, United Kingdom), socks (e.g., AgActive, United Kingdom), wound pads (e.g., Hansaplast®, Germany), refrigerators (Daewoo Electronics, Germany) etc. More examples have been listed in detail by the Project on Emerging Nanotechnologies (Pourzahedi, Vance, & Eckelman, 2017).

To enhance AgNPs' antimicrobial capacity, manufacturers incorporate AgNPs particles within the matrix of their products or applying them in novel coatings so as to control their release and antimicrobial action (Pourzahedi, Vance, & Eckelman, 2017).

4.2 Mechanism of AgNPs Antibacterial action

The effect of size and shape on the antimicrobial action of AgNPs has been widely studied in the literature. The smaller the particle size the greater the antimicrobial action (Guzman, Dille, & Godet, 2012), due to the larger surface-to-volume ratio (Zhang, Liu, Shen, & Gurunathan , 2016). Different shapes inhibit bacterial growth at different concentrations. For example, truncated triangular nanoparticles intercept further bacterial growth in lower concentrations than spherical nanoparticles (Rai, Yadav, & Gade, 2009). Of course, except from the size and shape of AgNPs, the treatment time plays an important role. Furthermore, many studies have proven the positive action of AgNPs to the reduction of both Gram-positive (e.g., *Bacillus*, *Enterococcus*, *Listeria*, *Staphylococcus* spp.) and Gram-negative (e.g., *Escherichia*, *Pseudomonas*, *Salmonella* spp.) bacteria cells (refer for examples to Guzman, Dille, & Godet (2012), Radzig, et al. (2013), (Mosselhy, et al., 2015) and (Bondarenko, Ivask, Käkinen, Kurvet, & Kahru, 2013)). The exact mechanism of this antibacterial action is yet not fully understood.

Nevertheless, the action of silver ions has been previously discussed. It has been reported that their cations penetrate the bacteria cell wall after interacting with its peptide and glycan ports (Mosselhy, et al., 2015) and then interact with the bases of DNA, affecting its ability to replicate. DNA subsequently turns into a condense form that reacts with the thiol group proteins, resulting in cell death (Rai, Yadav, & Gade, 2009), (Radzig, et al., 2013). This conglomeration of DNA can be observed by Transmission Electron Microscopy (TEM) (Mosselhy, et al., 2015).

Previous researchers have argued that nanoparticles' mechanism of antimicrobial action is the release of silver-ions from their oxidized monolayer on their surface area. Consequently, NPs with no oxidized surface are no toxic to bacteria cells. On the other hand, the antimicrobial effect of NPs has been reported even without any ion release (Bondarenko, Ivask, Käkinen, Kurvet, & Kahru, 2013), (Radzig, et al., 2013). A recent study by Mosselhy, et al., (2015), claims that the mechanism of AgNPs action is different from that of Ag^+ in the form of $AgNO_3$, since AgNPs desrupt the bacterial cell wall and lead to the leakage of the intracellular content. Therefore, the toxicity induced by AgNPs is different from that of Ag^+ in the form of $AgNO_3$. Another study though by Bondarenko, Ivask, Käkinen, Kurvet, & Kahru, (2013), claims that Ag^+ it is the only reason of AgNPs antimicrobial action, since except Ag^+ dissolution (long-distance mechanism of action of AgNPs), even the cell-nanoparticle interaction (short-distance mechanism of action of AgNPs) is happening again due to the gathering of ions, e.g., Ag^+ and H^+ cations, at the surface of nanoparticles. This is because when nanoparticles are dispersed in an aquous environment they become electrically charged and mainly with negative charge. Lastly, oxidative stress caused by AgNPs itself and by released silver ions, is also proposed by Radzig, et al., 2013, as a mechanism of bacterial DNA damage since they inhibit respiratory enzymes and forming reactive oxygen species (ROS). Increase of Ca^{2+} levels inside the bacterial membrane is also known to lead in bacterial death (Lee, Kim, & Lee, 2014), (Seong & Lee, 2017). From the literature, many studies have proven that Ag^+, on each own as a solution (e.g., $AgNO_3$), has higher cytoxicity (Mosselhy, et al., 2015), (Seong & Lee, 2017), (Mallevre, et al., 2016).

In most of the studies till now, *Escherichia coli* was used as a model for Gram-negative bacteria. Gram-positive and Gram-negative bacteria react differently in AgNPs exposure, since they have differences in the membrane structure. Gram positive bacteria have a thicker peptidoglycan cell wall, thus the penetration of Ag^+ in the cytoplasma is much more difficult (Rai, Yadav, & Gade, 2009). In the literature, many different synthesized nanoparticles have been tested on *E. coli* cells, with different shapes, sizes and concentrations. At Table 3.1, the Minimum Inhibitory Concentration (MIC[3]) of AgNPs synthesized with different sizes, is presented.

[3] the lowest concentration that inhibits the growth of a microorganism, *Andrews, 2001*

Table 4.1. Selected studies on the antibacterial activity of AgNPs on *E. coli* (Wolny-Koładka & Malina, 2017).

Size (nm)	MIC of AgNPs (ppm)
Not declared	100
10-15	25
21	75
23	10
30	5-10
75	9.843
55	0.25
1-100	12.43
10	3.12
48	18-21

Table 4.2 summarizes other extensively studied bacteria and the MICs of AgNPs and $AgNO_3$. In this case, AgNPs were synthesized by using aqueous Chamaemelum nobile extract as a green alternative method.

Table 4.2. Minimum Inhibition Concentrations (MICs) of AgNPs and $AgNO_3$ (Erjaee, Rajaian, & Nazif, 2017).

Bacteria	MIC (ppm)	
	AgNPs	$AgNO_3$
E. coli	7.8	15.6
*S.*Typhimurium	7.8	15.6
S. aureus	31.2	62.5
B. subtilis	15.6	31.2

The greatest challenge nowadays and the focus of most studies is the parallel action of AgNPs with antibiotics. Preliminary observations have shown that AgNPs can increase the antibacterial effects of antibiotics they are mixed with, including penicillin, amoxicillin, vancomycin, clindamycin and especially erythromycin against multiresistant strains. Some applications are referring to multiresistant isolates of *P. aeruginosa, E. aerogenes*, and against methicillin-resistant *S. aureus*. This will lead to overcome the challenge of the multidrug-resistant bacterial strains (Berton, et al., 2014). The combinations of AgNPs with antibiotics could lead to a synergistic effect, as it has been reported by many studies (e.g., (Katva, Das, Moti, Jyoti, & Kaushik, 2017), (Deng, et al., 2016), (Jamaran & Rahimian Zarif, 2016)). Panáček, et al., 2016 have even reported that sub-inhibitory and very low concentrations of AgNPs combined with antibiotics, were effective at a number of tested strains, except from KPC-*positive Klebsiella pneumoniae*. Evidently, less studies have focused on *Salmonella* spieces.

Table 4.3. MICs (mg/L) of AgNPs, antibiotics alone and antibiotics in combination with AgNPs, at different silver concentrations below MICs of AgNPs against ESBL-*positive Escherichia coli* strains (COX – cefotaxime, CZD – ceftazidime, MER – meropenem, CIP – ciprofloxacin, GEN – gentamicin) (Panáček, et al., 2016).

Antibiotic/AgNPs	**MIC (mg/L)**				
AgNPs alone	0.8				
	COX	**CZD**	**MER**	**CIP**	**GEN**
Antibiotic alone	4	16	0.06	>32	0.5
Antibiotic+AgNPs 0.4 mg/L	0.03	0.125	0.06	0.125	0.125
Antibiotic+AgNPs 0.2 mg/L	0.125	0.125	0.06	0.125	0.125
Antibiotic+AgNPs 0.1 mg/L	1	2	0.06	0.5	0.125
Antibiotic+AgNPs 0.05 mg/L	1	16	0.06	2	0.125

4.2.1 Nanoparticles action on *Salmonella* cells

Salmonella spp., also known as enteric bacteria, are gram-negative, rod-shaped bacteria that belong to the Enterobacteriaceae family. Its strains can be classified into two species: *S. enterica* and *S. bongori* that are then subdivided to many others, as it is shown in the figure below. Salmonella strains are almost always pathogenic, either to humans or to other warm-blooded animals, but *Salmonella enterica subsp. Enterica* is the most important since it's responsible for 99% of clinical infections. The most common diseases caused by Salmonella are typhoid fever (mostly by *S.* Typhi and *S.* Paratyphi A, B and C) and gastroenteritis (Madigan, Martinko, Bender, Buckley, & Stahl, 2015), (Jenkins, Rentenaar, Landraud, & Brisse, 2017).

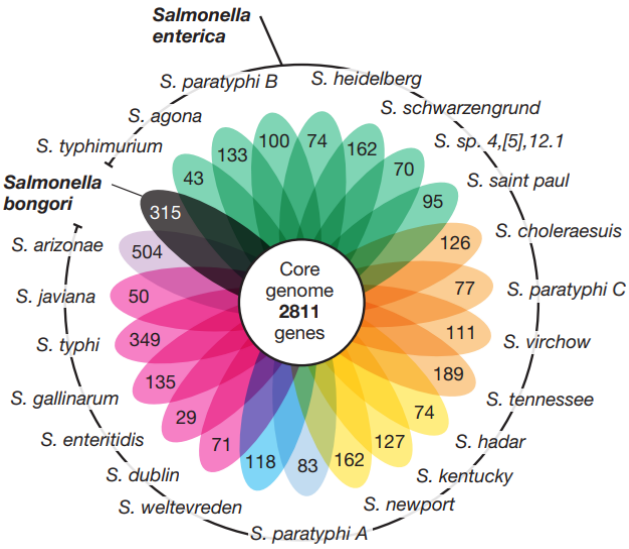

Figure 4.3. *Flowerplot of the Salmonella enterica pan genome. The average number of gene families found in each genome is represented, as being unique to each serovar (strain) (Jenkins, Rentenaar, Landraud, & Brisse, 2017).*

There is limited information about the inhibitory capacity of AgNPs against different *Salmonella* serovars. Although *Salmonella* and *Escherichia coli* (on which many studies are available[4]) are closely related bacteria, when exposed to AgNPs, the mechanism of action of AgNPs may present differences. For example, Chand Dakal, Kumar, Majumdar, & Yadav, 2016, mention cell lysis as a mechanism of action for *Salmonella* Typhi, as it was found in

[4] *See* pages 9 and 10

their research from previous studies, whereas AgNPs on *Escherichia coli* do not seem to express such mechanism of antibacterial action. A possible reason for that differentiation of AgNPs action between these two bacteria is, as examined in the past by Heinrichs, Yethon, & Whitfield, 1998, and Winfield & Groisman, 2004, the structural variations in the outer core oligosaccharides and their differential regulation of homologous genes. Therefore, there are differences in their bacterial lipopolysaccharides (LPS: they provide characteristic components of the outer membranes of Gram-negative bacteria that protect their integrity (Chand Dakal, Kumar, Majumdar, & Yadav, 2016), (Heinrichs, Yethon, & Whitfield, 1998)). LPS plays an important role to nanoparticles mechanism of action since its negative charge promotes their adhesion (Chand Dakal, Kumar, Majumdar, & Yadav, 2016), (Wang, Hu, & Shao, 2017).

Pathogenic gram-negative bacteria have an outer and inner membrane, something that makes them highly toxic since they have a stronger defense mechanism. A study by Seong & Lee, 2017, showed that the structure of the outer membrane of *Salmonella enterica* serotype Typhimurium was not disrupted (no structure damage was observed) when treated with AgNPs, while the inner membrane's depolarizartion increased. When high concentrations of AgNPs were investigated, they even observed membrane disruption. Therefore, it was assumed that AgNPs smaller than the pore size, can penetrate the outer membrane, causing a destruction of ion homeostasis that leads to an overload of intracellular ions like Ca^{2+}. This deregulation of Ca^{2+} leads to a number of phenomena, from alterations in cellular structure to alterations in gene expression, that all contribute to cell death. ROS accumulation was not recognized as a decisive factor of AgNPs to *Salmonella enterica* cells growth inhibition at this particular study. Another study, by Berton, et al., 2014, showed that different serotypes of *Salmonella enterica* have different reaction with AgNPs. In fact, silver nanoparticles seem to destroy the cell membrane of *S.* Enteritidis, entering into the cell and damaging the cytoplasma which results in the cell lysis, whereas they do not seem to cause any morphological damage in *S.* Senftenberg cells. That means that some *Salmonella enterica s*erovars are more sensitive to AgNPs, but their interaction is certain since AgNPs attach to the cell membrane.

Some minimum inhibitory concentrations (MICs) of AgNPs of *Salmonella enterica* and its serovars can be found at Table 4.4 below.

Table 4.4. Minimum Inhibitory Concentrations (MICs) of AgNPs, synthesized by different methods and with different sizes, of *Salmonella enterica* and its serovars.

Size (nm)	Method of synthesis	Salmonella strains	MIC (ppm)	Reference
~ 10	Chemical (nanosilver colloid product)	*Salmonella* Typhimurium	3.12	(Zarei, Jamnejad, & Khajehali, 2014)
15	Chemical (colloid nanosilver 10 w/w%, Polyoxyethylene Glycerol Trioleate and Tween 20)	*Salmonella* Enteritidis	10	(Klein, et al., 2011), (Mallevre, et al., 2016)
-	Green synthesis (AgNO3-plant extracts-Hyaluronic acid)	*Salmonella* Typhi	30 µg	(Enemaduku Abalaka, Benjamin Akpor, & Osemwegie, 2017)
10-25	Chemical reduction (Silver nitrate, sodium borohydride, tri-sodium citrate, hydrogen peroxide, polyvinylpyrrolidone)	*Salmonella* Typhimurium	8	(Omara, Zawrah, & Samy, 2017)
		Salmonella Enteritidis	16	

5. Methods of silver nanoparticles synthesis

Due to their multiple applications that keep expanding, various methods of silver nanoparticles synthesis are being developed. Generally, the methods of nanoparticles synthesis can be separated in two main categories:

1. Top-down methods

The top-down methods use techniques that allow to fabricate particles with external manipulation of the bulk material with controlled tools that cut, mill and shaped materials, in the desired shape and size (Singh, 2016). Some examples of these methods are:

- the grinding of the bulk material followed by a stabilizing and protecting agent (Beyenea, Werknehb, Bezabha, & Ambaye, 2017),
- nano-imprint, soft and step and flash lithography, embossing, particle replication in non-wetting templates, solvent molding-based fabrication, ultraviolet (UV) embossing and focused ion beam and nano-dispension methods (Singh, 2016).

2. Bottom-up methods

The bottom-up methods use molecular components as starting material and include chemical reduction, electrochemical methods, and sono-decomposition (Inmaculada López-Lorente & Valcárcel, 2014), (Zhang, Liu, Shen, & Gurunathan , 2016), (Beyenea, Werknehb, Bezabha, & Ambaye, 2017). This is the most convenient method of producing nanoparticles in large scale.

A representative graph of these two categories of nanoparticles synthesis is shown in Figure 5.1.

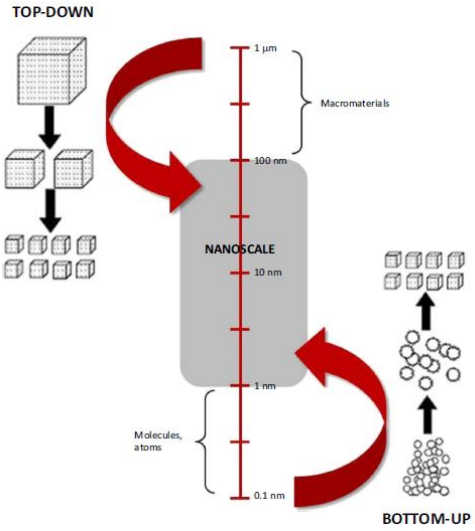

Figure 5.1. *Scheme of the two approaches employed in the fabrication of nanomaterials: "top-down" and "bottom-up" (Inmaculada López-Lorente & Valcárcel, 2014).*

AgNPs methods of synthesis can be furthered categorized in physicochemical and biological methods. Most AgNPs production is based on physicochemical techniques, such as chemical reduction, electrochemical methods, and photochemical reduction. However, these methods seem to have limitations since they are expensive (high operational cost and energy needs) and most of the times hazardous (toxic solvents and byproducts) (Tripathi, Kumar, & Kumar, 2017), (Zhang, Liu, Shen, & Gurunathan , 2016). On the contrary, bionanotechnology, seems to promote greener synthesis of nanoparticles, since biological methods show high yield, solubility, and high stability. These methods are rapid and non-toxic and the produced nanoparticles have well-defined size and morphology under optimized conditions (Zhang, Liu, Shen, & Gurunathan , 2016).

5.1 Physicochemical Synthesis of AgNPs

As far as physical methods are concerned, the most important ones are the evaporation – condensation, using a tube furnace at atmospheric pressure, and laser ablation. Specifically, for the synthesis of AgNPs, other physical methods that have also been used include spark discharging and pyrolysis. In contrast to the chemical methods, the physical ones are more rapid, non hazardous (since no hazardous chemicals are being used) and most of the times they offer a more homogeneous distribution of AgNPs. Laser ablation especially, offers pure and

clean metallic nanoparticles. On the other hand though, the yield is lower and the energy consumption is higher (Zhang, Liu, Shen, & Gurunathan , 2016), (Beyenea, Werknehb, Bezabha, & Ambaye, 2017). Some of these methods are mentioned in Table 5.1 along with the average shape and size of AgNPs produced. More specific references to these methods can be found in the study of Syafiuddin and co-workers (Syafiuddin, et al., 2017).

Table 5.1. Synthesis of silver nanoparticles by means of physical approach (the average shape and the wider range of sizes produced until now) (Syafiuddin, et al., 2017).

Method	Shape	Silver size (nm)
Laser ablation	Spherical	2.5-120
Small ceramic heater	Spherical	6-21.5
Thermal decomposition	Spherical	3.1 ± 0.7 - 50

As far as chemical methods are concerned, the preparation of nanoparticles is usually performed with the use of water and organic solvents. For metal nanoparticles, this process usually involves three main components (Zhang, Liu, Shen, & Gurunathan , 2016):

i. metal precursors,
ii. reducing agents, and
iii. stabilizing /capping agents.

In contrast to physical methods, chemical methods have high yield, but they are also expensive, and most of the chemicals used are toxic and hazardous (e.g. borohydride, thio-glycerol, 2-mercaptoethanol), as well as the byproducts. Furthermore, the manufactured particles are not of expected purity, as their surfaces are covered by chemicals, and a well-defined size is also difficult to be achieved (Zhang, Liu, Shen, & Gurunathan , 2016).

5.1.1 Chemical reduction

The chemical reduction method is based on the dissolution of a metal salt in a suitable solvent, followed by the reduction of metal ions to zero-oxidation state, using organic and inorganic reducing agents (Banach & Pulit-Prociak, 2016), (Beyenea, Werknehb, Bezabha, & Ambaye, 2017). The completion of this process is easily recognized by the change in colour of the

solution, due to the free of charge electrons in the conduction band and the positively charged nuclei at the surface of nanoparticles (Beyenea, Werknehb, Bezabha, & Ambaye, 2017). The most common obstacle encountered in this method is the agglomeration of nanoparticles. The grouping that is a result from the nanoparticles tendency to stick with each other, exceeding the nanoscale (self-assembly[5]). Therefore, the biggest challenge is the prevention of the agglomeration so that the particles remain in their nanosize. For this reason, other large particles (usually referred to as capping agents[6]) are introduced to the system to prevent their further growth due to their strong interaction with the surface of the metal nanoparticles (Banach & Pulit-Prociak, 2016). The capping agents provide a barrier to nanoparticles interaction with each other, based on charge or steric stabilization of the colloid. The former, involves a surface with counter ions and some solvent molecules that bind to the surface of nanoparticles (the Stern layer). Therefore, same charged nanoparticles repulse each other, according to Coulomb's law. Steric stabilization involves the adhesion of a relatively long molecule at the surface of the nanoparticle, which has high affinity for the solvent. Therefore, the barrier to aggregation is related to the interactions of the polymer chain with itself and with the solvent (Christian, Von der Kammer, Baalousha, & Hofmann, 2008).

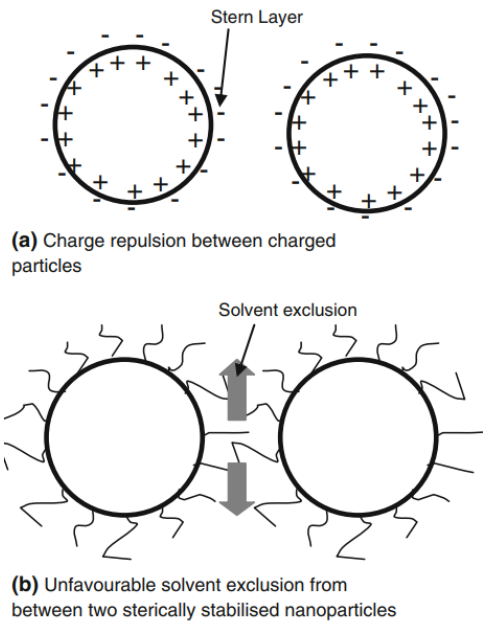

Figure 5.2. *A diagrammatic representation of (a) a charged stabilised nanoparticle and (b) a stetically stabilised nanoparticle* (Christian, Von der Kammer, Baalousha, & Hofmann, 2008)

The mechanism of formation of silver nanoparticles by the reduction of silver in a colloidal solution involves two steps: nucleation and growth, according to Ostwald ripening. Small

[5] *See* page 3

[6] *See* page 2 (The Surface layer)

particles first are dissolved in the solution and then grow into larger particles in two stages (Cheng, et al., 2014), as it is shown in Figure 5.3.

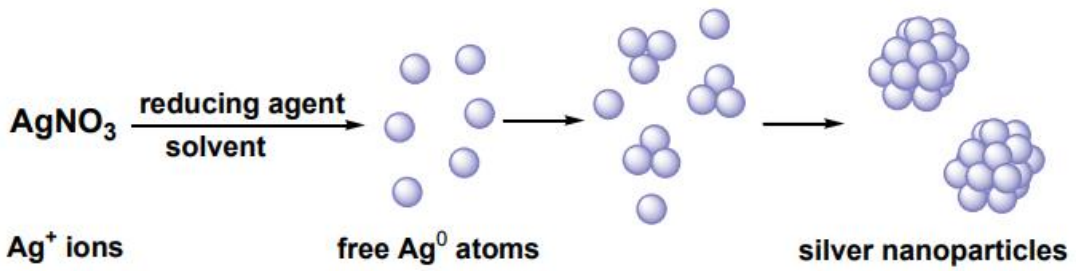

Figure 5.3. Mechanism of formation of silver nanoparticles from the chemical reduction in solution of the $AgNO_3$ salt (García-Barrasa, López-de-Luzuriaga, & Monge, 2011).

AgNPs sizes synthesized by previous studies with different reduction and stabilizer/capping agents, are summarized in Table 5.2.

The selection of the medium is the most important factor that defines the final properties and surface chemistry of particles (Christian, Von der Kammer, Baalousha, & Hofmann, 2008). Furthermore, for this process to be more ecofriendly, a careful selection of solvents and reducing and capping agent has to be made too. Most of the chemical compounds used in the past as reducing agents had a negative impact to the environment as well as the human health, since many of those were toxic, carcinogenic and unfriendly to the skin (e.g. Hydrazine hydrate, Formaldehyde, Sodium borohydride, Aniline, Sodium dodecyl, Polyvinylpyrrolidone, Ethylene glycol) (Banach & Pulit-Prociak, 2016).

An example of an environmentally benign solvent is glycerol ($C_3H_8O_3$), and its use in nanotechnology has been neglected. In a previous study, by Kouz & Varma, 2013, it was found to be used for production of Ag nanowires, replacing the much more commonly used Ethylene Glycol in the polyol process (the polyol serves two roles: reductant and surfactant), under microwave.

Plant extracts has also been extensively used as stabilizing and reducing agents to make the chemical method for the production of nanoparticles eco-friendly. Examples of plants used for this purpose are (Banach & Pulit-Prociak, 2016):

- Aloe vera
- Camelia sinensis

- Eucalyptus macrocarpa
- Dog rose

This concept represents the beginning of the biological method of synthesis of metal nanoparticles.

Table 5.2. Synthesis of silver nanoparticles using chemical reduction (Syafiuddin, et al., 2017).

Silver salt	Reduction agent	Stabilizer/Capping agent	Silver size (nm)
$AgNO_3$	Hydrazine hydrate and sodium citrate	Sodium dodecyl sulfate	10–20
$AgNO_3$	Gallic acid	Gallic acid	7–89
$AgNO_3$	Hydrazine hydrate and citrate of sodium	Sodium dodecyl sulfate	10–20
$AgNO_3$	Sodium borohydride	Tri-sodium citrate	~5
$AgNO_3$	Aniline	Etyltrimethlyammonium bromide	10–30
$AgNO_3$	Ethylene glycol	Poly(vinyl pyrrolidone)	50–175
$AgNO_3$	Ethylene glycol	Poly(vinyl pyrrolidone)	8–10
$AgNO_3$	NaOH	Polyanionic Na + poly(γ-glutamic acid)	17.2 ± 3.4 to 37.3 ± 5.5
$AgNO_3$	Trisodium citrate dehydrate (TSC) and potassium tartrate	Poly(vinyl pyrrolidone), sodium dodecyl sulfate (SDS)	20–100
$AgNO_3$	Glucose	Poly(vinyl pyrrolidone)	20–80
$AgNO_3$	Poly(vinyl pyrrolidone) and gelatin	Glucose, fructose, lactose, and sucrose	35
$AgNO_3$	D-Glucose	carboxy methyl cellulose, NaOH	5–15
$AgNO_3$	Poly(ethylene glycol)	Poly(ethylene glycol)	15–30
$AgNO_3$	NaOH and Sodium borohydride	Oleic acid (OA) and poly(acrylic acid) (PAA)	13–478
$AgNO_3$	Ethylene glycol	Poly(vinyl pyrrolidone)	17 ± 2
$AgNO_3$	Alkali lignin (low sulfonate)	Alkali lignin (low sulfonate)	7.3 (±2.2) and 14.3 (±1.8)
$AgNO_3$	NaOH	Alkali lignin (low sulfonate)	5–100

5.1.1.1 Turkevich' s method

In 1951, Turkevich reported the synthesis of gold nanoparticles in aqueous solution at boiling temperature using sodium citrate to reduce $AuCl4^{-}$. This method is now known as the Turkevich' s method and is used for other metals too. Lee and Meisel first prepared AgNPs in water, using this method. Today, it is known that citrate acts as a reducing and as a stabilizing agent for silver nanoparticles (Pacioni, Borsarelli, Rey, & Veglia, 2015). The reduction taking place between citrate ions and silver ions is as follows:

$$4Ag^{+} + C_6H_5O_7Na_3 + 2H_2O \rightarrow 4Ag^{0} + C_6H_5O_7H_3 + 3Na^{+} + H^{+} + O_2 \uparrow$$

During this reaction the colourless silver nitrate solution changes colour upon addition of sodium citrate. This colour change depends on the size of silver nanoparticles that are produced (Piñero, Camero, & Blanco, 2017), (Mazzonello, Valdramidis, Farrugia, Grima, & Gatt, 2017).

A study by Pacioni, Borsarelli, Rey, & Veglia, 2015, showed that following this method, the plasmon maximum absorbance was at 420 nm. Nevertheless, this reduction method has a slow rate, so it needs more time to be completed, and larger nanoparticles are produced (50–100 nm). After the first particles are produced by the reduction of Ag^{+}, the remaining anion can complex to the metal surface and thus decrease the total amount of citrate available in the bulk to further reduce more Ag^{+}. Interestingly, it seems that the addition of glycerol to the solution can reduce polydispersity and more controlled-size nanoparticles can be obtained, around 30 nm, without affecting the shape (spherical). Since this solvent has high viscosity ($\eta \approx 1{,}400$ cp) the reduction is slower and the characteristic color appears later. A theory of this action is that glycerol protects AgNPs from further ripening.

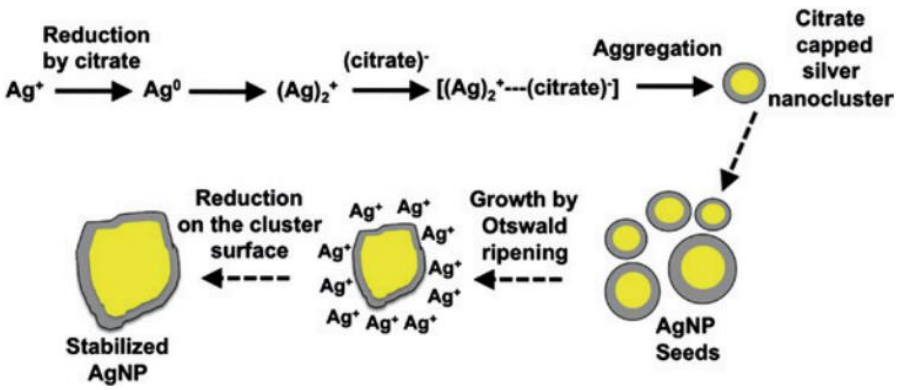

Figure 5.4. *Representation of the nucleation and growth mechanisms for AgNP obtained by the citrate method (Pacioni, Borsarelli, Rey, & Veglia, 2015).*

The addition of NaOH is proven to have an effect to the whole reaction since it changes the association and capping ability of citrate with silver (Pacioni, Borsarelli, Rey, & Veglia, 2015). A change in concentration of NaOH results in different morphology for nanoparticles. A study by Caswell, Bender, & Murphy, 2003, showed that the reaction of silver salt ($AgNO_3$) with sodium citrate in the presence of NaOH, led to the formation of silver nanowires. In fact, by changing the amount of NaOH added to the solution, different shapes of nanoparticles appeared. This is due to the fact that the higher the pH (the higher the amount of NaOH), the more deprotonated the citrate (pK_{a3}=6.4) and the more available for capping the silver (appearance of rods among the nanowires). But also, there is the theory that hydroxide ion might be in competition with the citrate for capping the silver ion. That's why there is a difference in morphology.

From the same study, by Caswell, Bender, & Murphy, 2003, it also seems that the action of sodium citrate as capping agent changes with the temperature. At room temperature, more uniformly stabilized nanoparticles are produced, whereas at boiling temperature, the equilibrium constant for citrate binding to certain crystal faces of silver, begin to differ. There are crystal faces not covered by citrate which leads to the growth of nanoparticles on only one axis. From another study by Mazzonello, Valdramidis, Farrugia, Grima, & Gatt, 2017, where trisodium citrrate was used as a capping agent and its ratio with silver nitrate as well as the temperature were tested, the reaction rate was also found to have an Arrhenius-like exponential relation to the temperature, and was independent of the trisodium citrate concentration. Moreover, with the increase of temperature, the size of AgNPs produced also increased. At higher temperatures the shape of AgNPs produced had a bigger distribution but mostly spherical and rod shaped nanoparticles were produced. A change in the growing mechanism of nanoparticles with the change of the temperature was also observed in a study by Piñero, Camero, & Blanco, 2017, where ascorbic acid, sodium borohydride and trisodium citrate were used as capping agents, and they suggested that at 5 and 20°C the aggregation mechanisms was conducted by aggregation of atoms and at higher temperatures by aggregation of clusters.

5.1.2 Reduction by atmospheric plasma generation

Plasma is considered as the fourth state of matter, after solid, liquids and gases. It is the intermediate state, before phase transition, where structures are becoming looser, and then break down. More specifically, at higher energies, the molecules and single atoms that are

included in gases, start losing their structure, liberating free electrons and ions. This exact state of ionized gas, consisting of neutral molecules, electrons, and positive and negative ions, is plasma (Niemira, 2012).

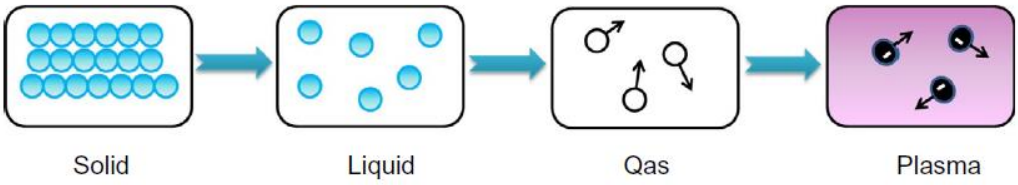

Figure 5.5. *Pictorial representations of the four states of matter (Misra, Schluter, & Cullen, 2016).*

The needed energy required, can be given to the system by different sources, such as (Misra, Schluter, & Cullen, 2016):

- ✓ Heat
- ✓ Electricity
- ✓ Laser light
- ✓ Radiation
- ✓ Extremely rapid compression.

This energy acquired from plasma, can be retained for a certain period of time and then, when particles recombine with each other, it's released as visible and UV light. Not all atoms in the gas are ionized when plasma is generated. Within hot plasmas (typically when heated in the order of 20000 K), also called equilibrium plasmas or thermal plasmas, all species are extremely reactive, but within cooler plasmas, also called NTP (nonequilibrium plasmas) or cold plasmas, some of the chemical species are more reactive than others. The chemical composition of the feed gas is a determining factor in the types of reactions that the plasma can initiate (Misra, Schluter, & Cullen, 2016).

Cold plasma is obtained at atmospheric or reduced pressures (vacuum) and therefore, it requires less power input. It can be generated by an electric discharge in a gas at lower pressure or by using microwaves. Typical set-ups for plasma generation at atmospheric pressure include (Misra, Schluter, & Cullen, 2016):

- ✓ Corona discharge,
- ✓ Glow discharge,

- ✓ Dielectric Barrier Discharge (DBD),
- ✓ Radio-Frequency (RF) and microwave (MW) radiation, and
- ✓ Gliding Arc Discharge.

Three of the above methods (radio-frequency, glow discharge and dielectric barrier discharge) of generation of plasma, which are the most commonly used, are represented diagrammatically in Figure 5.6.

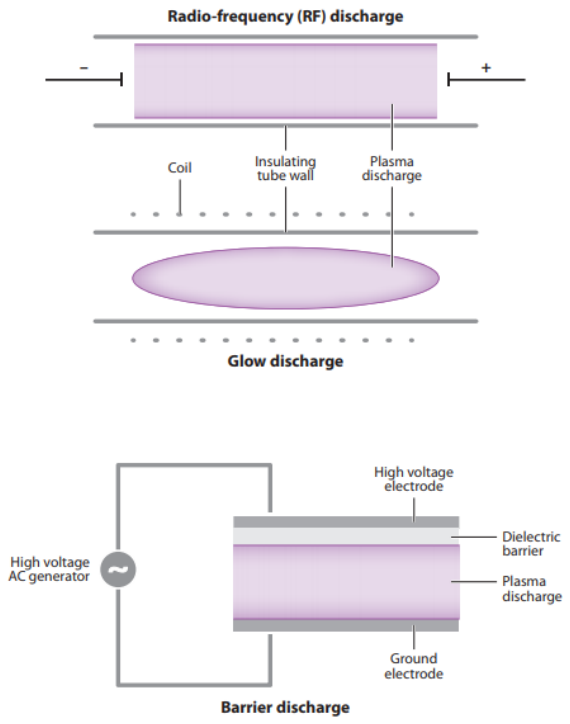

Figure 5.6. *Diagrammatic representation of three basic types of discharges: radio frequency discharge (top), glow discharge (middle), barrier diascharge (bottom). The physical conformations of the various elements can be varied according to need and design requirements. Cold plasma discharges are indicated by the purplecolored zones* (Niemira, 2012).

As far as plasma generation in liquid is concerned, this can be subdivided into four main categories:

i. Gas discharge between an electrode and the electrolyte surface

ii. Direct discharge between two electrodes (in forms such as solution plasma, discharge plasma in liquid, electric spark discharge, arc discharge, capillary discharge, and streamer discharge)

iii. Contact discharge between an electrode and the surface of surrounding electrolyte

iv. Radio frequency (RF) and microwave (MW) generation (Saito & Akiyama, 2015).

Cold plasma has a variety of applications, from medicine to Electronics and Food Sciences, while its use in nanotechnology is constantly increasing (Misra, Schluter, & Cullen, 2016). Many studies have shown the successful synthesis of silver nanoparticles using a plasma generated method, with the above-mentioned methods. Most of them are using the Plasma-Liquid Interaction (PLI) technique. Based on literature, Table 5.3 summarizes all plasma techniques used for AgNPs synthesis, changing the raw material and the liquid.

Table 5.3. Silver nanoparticles (AgNPs) synthesis via techniques for plasma generation in liquid taken from (Saito & Akiyama, 2015) (references omitted).

	Raw materials	Liquid	Configuration
AgNPs	Ag rod or wire	Solution	ii: arc discharge, submerged arc , electric spark discharge, wire explosion, plasma electrolysis (DC), iv: RF plasma in water (20 kPa), MW plasma, and MW-induced plasma
		Molten Salt	i: discharge electrolysis (DC 200~400 V)
	Ag Metal Foil	Solution	i: microplasma
	$AgNO_3$	Solution	i: microplasma, DC glow discharge, ii: liquid phase plasma reduction (25–30 kHz), and Arc discharge
		Ionic Liquid (IL)	i: plasma electrochemistry in ILs

Specific examples of AgNPs synthesis with the above techniques, in chronological order, are the following studies by:

- Richmonds & Mohan Sankaran, 2008, where silver and gold nanoparticles were synthesized by microplasma reduction of aqueous cations using a solid metal anode (spherical Ag nanoparticles ≤ 10 nm in diameter),
- Zhang, Guo, & Ma, 2011, where spherical silver nanoparticles with a mean diameter ~3.5 nm, were synthesized at plasma-liquid interface after silver ions reduction by an

atmospheric argon dielectric barrier discharge jet, using $AgNO_3$, Ethanol as solvend and reducing agent, PVP as surfactant,

- Sato, Mori, Ariyada, Atsushi, & Yonezawa, 2011, where silver nanoparticles were produced by plasma induced by radiated microwave from tungsten electrodes il $AgNO_3$/water/PVP liquid at atmospheric pressure (spherical nanoparticles with mean diameter ~4.5 nm)
- Huang, et al., 2013, where silver nanoparticles were synthesized by the formation of an electrochemical cell with an atmospheric-pressure He microplasma cathode and a Pt foil anode immersed in a $AgNO_3$/fructose/de-ionized water solution, at temperature 25ºC and 70ºC (mostly spherical with diameters 15-40 nm depending on the ratio between $AgNO_3$ and Fructose and the temperature), and
- Kondeti, Gangal, Yatom, & Bruggeman, 2017, where silver nanoparticles were produced at plasma-liquid interface after silver ions reduction by an RF-driven atmospheric pressure plasma jet, in touching (mostly spherical with diameter ≤ 5 nm) and non-touching conditions (mostly spherical with diameter ≥ 5 nm), in presence and in absence of Fructose as stabilizer, with only Ar and a mixture of Ar and H_2 as feed gas.

It appears that in most cases, spherical NPs with diameter less than 10 nm are synthesized and in only some cases, nanorods and polygonal NPs are generated (Saito & Akiyama, 2015).

Exploring the way of silver ions reduction via plasma, in the research by Kondeti, Gangal, Yatom, & Bruggeman, 2017, many possible mechanisms are proposed by changing the conditions (RF generated plasma touching and no-touching the liquid, with fructose as surfactant and without etc.). The main mechanism of action of plasma, for reducing the silver ions, is considered to be the solvated electrons that it generates with the simple reaction below.

$$Ag^+ + e^- \rightarrow Ag^0$$

These electrons appear only in a very small surface, a layer of about 10 nm, at the plasma-liquid interface. But plasma also transfers ions, reactive species, radicals and UV/vacuum ultraviolet (VUV) photons to the liquid. Therefore, H and OH are also produced by VUV photons, and through different mechanisms, they also take part to the reduction of silver ions:

- H atoms can reduce silver ions according to the reaction below.

- OH does not reduce Ag+ reduction on its own but it reacts with hydrocarbon molecules and therefore affects the concentrations of H and e_{aq}^{-}. It can also react with alcohols, through hydrogen abstraction, which leads to radicals.

AgNPs production via plasma, is considered a green method of synthesis, since no harmful byproducts are generated, especially if the surfactant/stabilizer is also an environmentally friendly substance (e.g., glycerol) (Kondeti, Gangal, Yatom, & Bruggeman, 2017).

Nevertheless, there are limitations of the method and the biggest one is related to the expense and safety. The cost of plasma processing may be high, depending on the gas or gas mixture expenses, and the additional safety measures which are required for the high voltages (Misra, Schluter, & Cullen, 2016).

5.2 Biological / Green methods of synthesis

The biological methods of synthesis of nanoparticles is a major scientific priority due to the many obtained advantages. They are simple, cost effective, dependable, and environmentally friendly approaches. The basic idea of green synthesis lies on the utilization of biological systems including bacteria, fungi, plant extracts, and small biomolecules like vitamins and amino acids, as an alternative method to chemical methods (Zhang, Liu, Shen, & Gurunathan , 2016). That way, synthesized nanoparticles can be biologically and cytologically compatible (Akter, et al., 2018). Bacteria like *Pseudomonas stutzeri*, *Lactobacillus* strains, *Bacillus licheniformis*, *Escherichia coli*, *Brevibacterium casei*, fungi including *Fusarium oxysporum*, *Ganoderma neo-japonicum* Imazeki, and plant extracts such as *Allophylus cobbe*, *Artemisia princeps* and *Typha angustifolia*, are only some examples of those used for the synthesis of environmentally friendly AgNPs (Tripathi, Kumar, & Kumar, 2017).

The raising question is how these prokaryotic and eukaryotic organisms can help producing metal nanoparticles. The answer lies on the defense mechanisms of these organisms after exposure to high levels of metals. These mechanisms may involve the alteration of the chemical nature of the toxic metal into a non-toxic form that results to nanoparticles of the metal concerned. Evidently, the type of metal plays an important role since most of the organisms have developed resistance to some metals and therefore the choice of the organism is limited (Pantidos & Horsfall, 2014).

Biological synthesis can be subdivided into two categories:

- Bio-reduction, where metal ions are chemically reduced into metal nanoparticles which are a more stable form that can be more easily removed, by an enzyme in need for oxidation.
- Bio-sorption, where metal ions bind to the cell wall of the organism, which in many organisms is able to form stable complexes in the form of nanoparticles (Pantidos & Horsfall, 2014).

Microbial synthesis of metal nanoparticles can be done either intracellularly or extracellularly. The intracellular synthesis requires biomass of culture. On the other hand, when only the culture supernatant is treated with aqueous solution of silver nitrate, then it forms silver nanoparticles extracellularly without the need for a cell lysis step. The extracellular formation is therefore cheaper and has a simpler downstream processing, but the intracellular one can help in the removal of heavy metals from contaminated environments (Tripathi, Kumar, & Kumar, 2017), (Pantidos & Horsfall, 2014).

The average size of AgNPs synthesized with this method is at the range 50-100 nm. Generally, AgNPs synthesized using biological reducing and capping agents have shown wide variations in shape and in size but most of the NPs produced were reported to have a predominantly spherical shape. Past studies have also shown that green-synthesized nanoparticles are much less toxic compared to the chemically-synthesized ones (Akter, et al., 2018), (Sabri, Umer, Awan, Hassan, & Hasnain, 2016).

Despite the many advantages, the exact mechanism of the reduction process is yet to be fully understood and controlled and therefore there is still a barrier that needs to be overcome for these methods. Moreover, the maintenance of the culture medium and the stabilization of all the conditions like the optimum pH, the temperature feasibility, or the salinity of the culture, are very difficult (Sabri, Umer, Awan, Hassan, & Hasnain, 2016).

6. Toxicity concerns on silver nanoparticles

Despite the many advantages of nanoparticles due to their applications, there is a growing concern about their potential toxicity. Although the bulk materials may be harmless, little is known about their nanoscale toxic characteristics. Due to their small size, when a nanoparticle enters the human body, it can take almost every possible direction and reach biological pathways by crossing biological barriers. Therefore, it has access to highly protected organs such as the brain and the testes. Furthermore, the removal of nanomaterials from tissues seems to be much slower and more difficult compared to that of the bulk form, because nanomaterials are poorly taken over by macrophages. That means that nanoparticles may actually injure biological structures and may reside longer in these compartments (Pietroiusti, Magrini, & Campagnolo, 2014).

The effects of silver nanoparticles on mammalian cells have been examined in vitro on cell cultures or in vivo on animals (with oral administration). As far as cell culture is concerned, this is a technique in which cells are removed from an organism and placed in a fluid medium, making it easier to be studied. Keeping the appropriate conditions, cells can live and grow with cell division (mitosis) or differentiation (change into specific types with functions analogous to tissues or organs of the organism). This technique finds its origins in a Yale University laboratory in 1907 when Ross Harrison removed nerves of a frog and maintained them in a simple salt solution for several days (Lynn, 2009).

However, the few available studies that exist on the toxicity of silver nanoparticles cannot offer a complete comparative analysis. Firstly, they contrast the effect of silver nanoparticles in on only a few different biological groups (two or three). Secondly, the culture media, the culture conditions and methodologies are different. Last but not least, the sizes, the shapes, the capping agent etc. also vary. Therefore, due to the absence of an accurate comparative analysis, the toxicity of AgNPs has not been determined yet at a full extent (Vazquez-Muñoz, et al., 2017).

It is proven that AgNPs exposure could induce the changes of cell shape, reduce cell viability, increase lactate dehydrogenase (LDH: an enzyme indicator of permeabilization of plasma membrane) release and finally result in cell apoptosis and necrosis (Ka-Ming Chan, Moriwaki, & De Rosa, 2014). Mitochondrial dysfunction via interruption of mitochondrial membrane permeability has also been observed in vitro (usually via TEM analysis) (Galandáková, et al., 2016). As it is mentioned before, AgNPs cytotoxicity is also an outcome of oxidation stress

caused by AgNPs and the release of silver ions. The very active surface of AgNPs results in the generation of original free radicals and silver ions release initiates the production of hydroxyl radicals in acidic endo/lysosomes. AgNPs are associated with genotoxicity as a result of DNA damage and chromosomes from oxidation stress and may also induce mutagenicity (Zhang, Wang, Chen, & Chen, 2014). Nanoparticles have the tendency to bind with molecules present to biological fluids, such as proteins (in the blood) and lipids (in the pulmonary environment). This formation, otherwise called "corona", can be an additional aspect to increase toxicity (Pietroiusti, Magrini, & Campagnolo, 2014). The last phenomenon is the only one that occurs for all types of NPs.

The above possible mechanisms of toxicity action of AgNPs are presented in Figure 6.1.

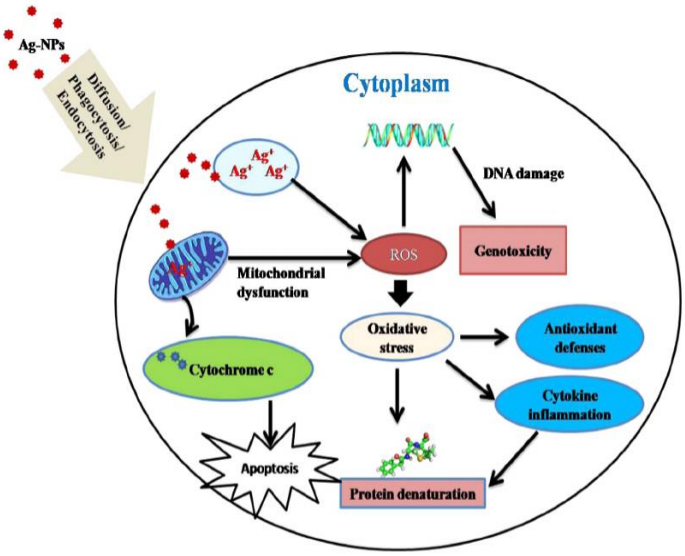

Figure 6.1. *Possible uptake process and mechanism of cytotoxicity induced by AgNPs in different cell lines based on the metadata of several studies (Akter, et al., 2018).*

There are processes though, taking place in biological environments, that limit toxicity since they limit silver ions bioavailability. These processes involve the formation of silver sulfide (Ag_2S) and silver chloride ($AgCl_X$) as a result of the presence of sulfide and chloride and their very low solubility constants. Ag_2S is non-toxic and acts as a scavenger in Ag(I) bioavailability (Marchioni, Jouneau, Chevallet, Michaud-Soret, & Deniaud, 2018). The above forms of transformation of AgNPs after entering a biological system are represented in Figure 6.2.

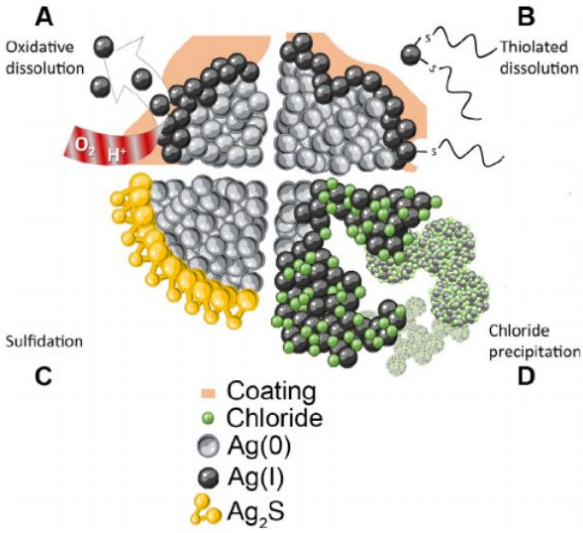

Figure 6.2. *Scheme of the main AgNP transformations occuring in biological media. (A) Oxidative dissolution process enabling Ag(I) release in solution, (B) thiol-assisted AgNP dissolution, (C) AgNP passivation due to Ag sulfidation, (D) Chloride-induced AgNP transformation* (Marchioni, Jouneau, Chevallet, Michaud-Soret, & Deniaud, 2018).

From previous studies it can be reported that a change in the physiochemical characteristics of AgNPs (e.g., particle size, dose, agglomeration) can result in a subsequent change in their toxicity level. It also appears that AgNPs toxicity is size and concentration dependent, i.e., the smaller the particle, the greater the cytotoxicity, since they generate more reactive oxygen species (ROS) while the minimum concentration level that induces toxicity varies according to the cell type. The type of coating also plays an important role since it defines the final shape of nanoparticles and it prevents aggregation and silver ions dissolution. Modification of the coating, with different capping agents, can affect bioactivity. Citrate- and polyvinylpyrrolidone (PVP)- coated AgNPs that were tested on cell lines to compare their toxicity with uncoated AgNPs, were proven to be less cytotoxic than the uncoated ones. In fact, citrate coatings can improve the stability of colloidal AgNPs and decrease their toxicity (Akter, et al., 2018).

Different sizes and shapes of silver nanoparticles with different exposure doses that were tested from previous studies on various types of cell lines are presented in Table 6.1. More studies can be found at the review by Zhang, Shen, & Gurunathan, Silver Nanoparticle-Mediated Cellular Responses in Various Cell Lines: An in Vitro Model, 2016.

Table 6.1. Effects of silver nanoparticles on various cell lines according to exposure dose, exposure time and size.

Exposure dose of AgNPs	Exposure time	Size (nm)	Type of cell line used	Major outcomes	Reference
93.5 (ppm) and 0.73 (ppm)	24 h	7-25 nm	RTL-W1 (a rainbow trout liver cell line) RTG-2 (a fibroblast-like gonadal cell line) RTH-149 rainbow trout hepatoma cell line	1.concentration dependent reduction in viability 2.IC_{50} values in vitro: 10.7 to 75.9 µg/mL 3.lysosomal damage as an important indicator for detecting nanoparticle specific effects	(Connolly, et al., 2015)
0.025–5.0 ppm	24 and 72 h	10 and 100 nm	Chinese hamster ovary (CHO) types: CHO-XRS and CHO-K1	1.concentration- and size-dependent reduction in viability 2.greater long-term toxicity of bigger particles due to higher DNA fragmentation 3.greater induction of ROS from smaller particles 4.cells apoptosis from smaller particles 5.CHO-XRS5 line is more susceptible to damage caused by AgNPs	**(Souza, Franchi, Rosa, da Veiga, & Takahashi, 2016)**

1-400 ppm 1-10 ppm	24 h	20-40 nm	Liver primary cells of mice Human liver HepG2 cell	1.Cytotoxic effect of AgNPs on both cell lines (IC50 value of HepG2: 2.764 ppm, IC_{50} value of liver primary cells of mice: 121.7 ppm) 2. stronger inhibitory effect (44 times) on the growth of cancerous cells (HepG2 cell line) compared to the normal cells (primary liver cells of mice)	(Faedmaleki, Shirazi, Salarian, Ahmadi Ashtiani, & Rastegar, 2014)
0.5-15 ppm	24 h	10, 40 and 100 nm	Chinese hamster ovary cells (CHO-9) Sertoli cells (15P-1) Murine lung macrophages (RAW264.7)	1.strong cytotoxic activity at low concentrations (2÷13 ppm) 2.overproduction of ROS even at lower concentrations than the cytotoxic ones 3.oxidative damage of DNA 4.smaller nanoparticles more toxic	**(Zapór, 2016)**

6.1 AgNPs toxicity on Fibroblast cells

Fibroblasts are the most abundant cell type within all the body's connective tissues. These cells are extensively used in cell cultures, both for transient primary cell culture or permanent as transformed cell lines. They are mesenchymal-derived cell types that play an important role in physiological processes like the synthesis of extracellular matrix (ECM), epithelial differentiation, regulation of inflammation and wound healing. Moreover, fibroblasts are also responsible for secretion of growth factors and work as scaffolds for several other cell types, acting as the main mediator cell for tissue fibrosis and scar formation. Fibroblasts are easy to

culture and maintain in vitro and they are now well established (Fernandes, et al., 2016). The way Fibroblasts act for wound repair starts with the disruption of the skin barriers. When this occurs, pro-inflammatory factors are produced and macrophages begin to form granulation tissue and release cytokines (IL-1 and IL-6) and growth factors (i.e., fibroblast growth factor [FGF], transforming growth factor [TGF] and epidermal growth factor [EGF]). Tissue remodeling involves collagen formation by Fibroblasts, leaving a scar. Generally, prolongation of the inflammatory phase of this wound healing procedure, results in the formation of non-healing wounds. Silver nanoparticles have been found to support the wound-healing process something that is confirmed by their ability to decrease the production of proinflammatory cytokines and epidermal growth factors (Franková, Pivodová, Vágnerová, Juráňová, & Ulrichová, 2016).

It has been observed that topical application of Ag compounds, specifically silver nitrate ($AgNO_3$) and silver sulfadiazine, may cause Argyria (blue grey colouration rooted to skin sulfidation) after high exposure levels or cease the healing process of fibroblast and epithelial cells because of their toxicity (Galandáková, et al., 2016), (Marchioni, Jouneau, Chevallet, Michaud-Soret, & Deniaud, 2018). Abnormal elevation of blood silver level and argyria-like symptoms following the use of AgNPs (15 nm)-coated dressings for burns is also mentioned in a clinical report (Avalos, Haza, Mateo, & Morales, 2014). Since silver nanoparticles are being used for epidermal applications in open wounds and burns and because of the previously mentioned reactions of silver nanoparticles in biological environments, their toxicity on dermal Fibroblast cells is a vital indicator of their toxicity level.

The phenotype of skin Fibroblasts can change due to a number of parameters like duration of the cell culture, the location of the skin biopsies and the age of the donor (Moulin, Mayrand, Laforce-Lavoie, Larochelle, & Genest, 2011). As far as the different body compartments are concerned, there are topographic differences in the expression of genes, for example they have a different capacity to express key extracellular matrix proteins such as collagenase and types I and III procollagen. This can even change from their location within the dermis, the layer of human skin (Mohammad Ali, Bauer, Tredget, & Ghahary, 2004), (Sriram, Bigliardi, & Bigliardi-Qi, 2015). The ideal site of human body for harvesting Fibroblast cells is still under investigation. Fernandes, et al., 2016, studied different human body sites for the harvesting of Fibroblast cells for cell culture. In spite of being from different body parts, their morphology appeared similar, except from the groin area were cells spreading out was not achieved, as

presented in Figure 6.3 below. Fibroblasts isolated from abdominal scar presented higher cell proliferation rates and also higher cells viability after cryopreservation, something that comes to agreement with fibroblasts activity in wound repair, as mentioned before.

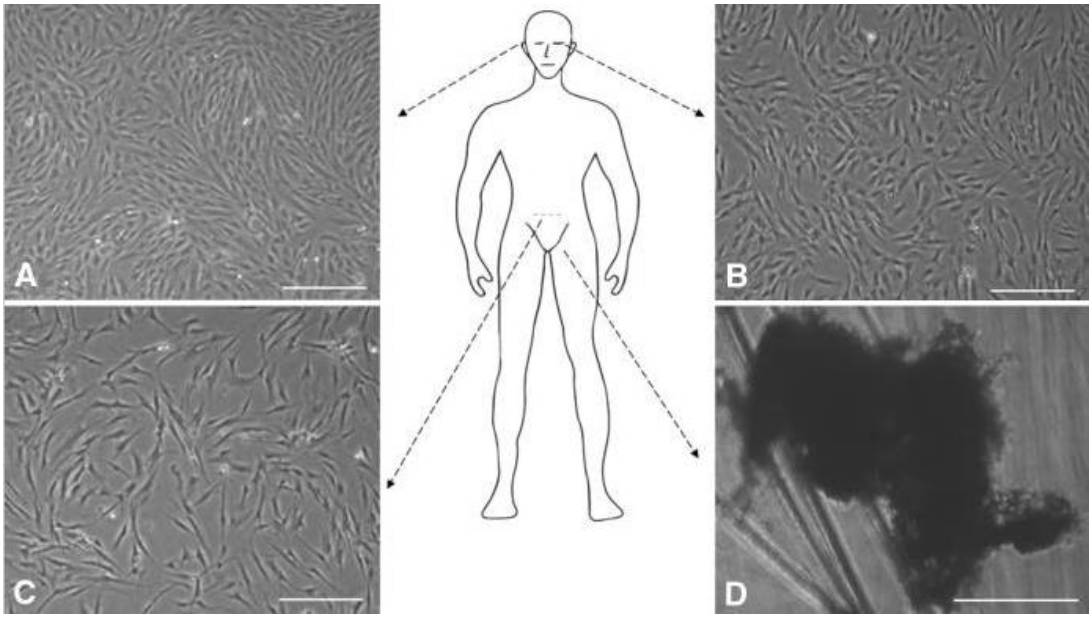

Figure 6.3. *Body sites selected for the harvesting of fibroblast cells: back of ears, eyelid, cesarean scar and groin.* ***A)*** *Fibroblast cultured from the back of the ears (otoplasty) and,* ***B)*** *fibroblast cultured from Eyelid (blepharoplasty),* ***C)*** *fibroblast cultured from Cesarean Scar (abdomen) e,* ***D)*** *Skin tissue from Groin under cell culture conditions, which did not spread cells (Fernandes, et al., 2016).*

Many studies using Fibroblast cell lines have been conducted till now to examine the minimum toxic concentration of AgNPs and their mechanism of toxicity action. Some examples are mentioned below.

- Paknejadi, Bayat, Salimi, & Razavi, 2018, studied AgNPs effect on normal Human Skin Fibroblasts, at different concentrations 2.17 to 69.5 ppm, for exposure time 24 and 48 hours. Nanoparticles used were mainly spherical with an average size of 6.03 nm. A significant dicrease in cells viability appeared in a concentration- and time-dependent manner. IC_{50} values calculated were 30.64 and 14.98 μg/mL for 24 and 48 hours of incubation, respectively. No mechanism of AgNPs cytotoxicity action was proposed.
- Galandáková, et al., 2016, reported that the non-toxic concentrations of AgNPs (synthesis was performed by reduction of $AgNO_3$ with sodium borohydride ($NaBH_4$)) tested on normal human dermal fibroblasts (NHDF), were estimated to be at the range

of 0.25-25 μg/mL after a 24 h treatment, whereas for silver ions also tested on NHDF, non-toxic concentrations were found to be at the range of 0.025–1 μg/mL. Moreover, for these concentrations, no DNA damage appeared under fluorescence microscope. Testing the AgNPs wound healing procedure, no increase of the number of pro-inflammatory markers was observed. The nanoparticles used were a mixture of sizes at the range of 0–40 nm, with a mean size of approximately 10 nm. Alhtough at this study silver nanoparticles seemed to be less toxic than silver ions, the size plays an important role. At this study it was also reported that 5 nm AgNPs were more toxic than Ag^+ and 20 and 50 nm AgNPs were found to be less toxic.

- Wildt, et al., 2016, tested 50 ppm of 10, 50, 100 and 200 nm silver nanoparticles on mouse fibroblast cells (L-929). The highest toxicity was reported by the smallest nanoparticles, likely due to a higher release of silver ions, which is in line with other studies examining the nanoparticles' size-dependent toxicity. In this study, it is also mentioned that all nanoparticles are dissolving extracellularly and the bigger ones are reformed in smaller particles, which have high dissolution. The greatest dissolution occurs intracellularly potentially because of the increased acidity of lysosomes where many AgNPs are mostly gathering. The lower amount of Ag ions release from the larger particles may be controlled through cellular protective mechanisms.

- The same result for the toxicity of the smaller nanoparticles were also obtained at the study by Avalos, Haza, Mateo, & Morales, 2014, who tested the interactions of AgNPs of different sizes on Normal Human Dermal Fibroblasts. In fact, 4.7 nm AgNPs (approximately spherical) showed high decrease in NHDF viability at concentrations 6.72 and 13.45 ppm for all treatment times (24, 48 and 72 h). This study also showed that oxidative stress is the primarily mechanism of toxicity action and the smaller the particle the higher the production of ROS.

7. Experimental Procedure

The aim of this study is the production of different sizes and/or different shapes of nanoparticles to subsequently test their antimicrobial efficacy and their possible cytotoxicity effects. A number of different experimental techniques were utilized in order to achieve that aim. In view of this, the experimental section will be sub-dived into five different sections as follows:

1. synthesis of the nanoparticles' dispersions;
2. purification of the nanoparticles' dispersions;
3. characterization;
4. antimicrobial testing (on Salmonella cells);
5. toxicity testing (on Fibroblast cells).

7.1 Synthesis

In this section, silver nanoparticles dispersions were obtained through the use of different bottom-up methods. These methods include various modified versions of the Turkevich method, wherein reduction of the silver ions is achieved through chemical means and reduction by atmospheric plasma generation, where physical processes are used to achieve the reduction of the silver ions.

7.1.1 Materials used

- Silver Nitrate $AgNO_3$ (Sigma-Aldrich, Steinheim, Germany, 99.8-100.5 %, SZBB0340V), used as the source of silver ions
- Trisodium Citrate, $Na_3C_6H_5O_7$, (Scharlau, Barcelona, Spain, 99.0-101.0%, 1413194) used as the capping agent
- Glycerol, $C_3H_8O_3$ (Honeywell Riedel-de-Haën™, Seelze, Germany, 99.0-101.0%, G323L), used as a solvent and stabilizer
- Sodium Hydroxide, NaOH (Sigma-Aldrich, Steinheim, Germany, 98-100.5%, SZBB3480V)
- Acetone (Fisher scientific, UK, 1413194)
- Glassy carbon (Alpha Aesar, 3 mm in diameter)
- Tungsten wire (0.375 mm in diameter and a purity of 99.95%, supplied by Alfa Aesar)

- 500 mL conical flask
- 500 mL beakers
- A ** g scale with 0.1 g readability (Sartorius TE601, Göttingen),
- An analytical balance with readability 0.1 mg (Sartorius TE64, Göttingen)
- Aluminum foil
- Utility clamps
- Laboratory stirrer (IKA® RW 16, Staufen)
- A hotplate with temperature controller (Wisd WiseStir® MSH-20A).

7.1.2 Modified Turkevich Methods

Various modifications to the Turkevich method were performed with the aim of producing different sizes and /or different shapes of nanoparticles. The modifications performed were (1) using glycerol as a solvent instead of water; (2) carrying out the synthesis at room temperature (with the aid of NaOH) or 70°C instead of 100°C and (3) using different molar ratios of silver nitrate to trisodium citrate.

Modified Turkevich Method at room temperature

200 g of glycerol (weighed using Sartorius TE601, Göttingen balance) were poured in a 500 mL conical flask. This was followed by the addition of 0.20 g of silver nitrate and 3.47 g of trisodium citrate as weighed by a duly calibrated analytical balance (Sartorius TE64, Göttingen). This results in a system having a 1:10 molar ratio between silver nitrate and trisodium citrate. The flask was then covered with aluminum foil except for the neck opening, from which an overhead stirrer was inserted. The flask was immobilized with a utility clamp and the flask contents were stirred at approximately 510 rpm for 1 hour. 0.50 g of NaOH were then added and the contents of the flask were stirred for an additional 15 minutes. The setup used is shown in Figure 7.1.

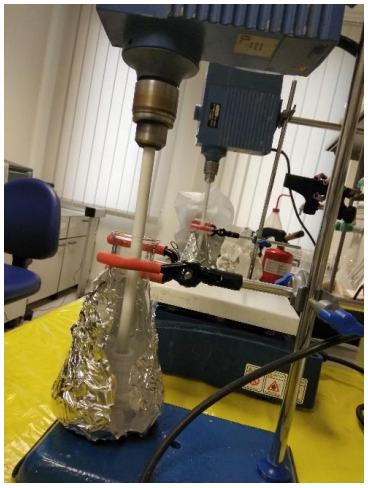

Figure 7.1. *The setup used for the Modified Turkevich Method at room temperature.*

This experiment was then repeated using different molar ratios of silver nitrate: trisodium citrate as indicated in Table 7.1 below.

Table 7.1. The masses of silver nitrate and trisodium citrate used in order to achieve different molar ratios.

Repeat number	$AgNO_3$ (g)	$Na_3C_6H_5O_7$ (g)	$AgNO_3$: $Na_3C_6H_5O_7$
1	0.20	1.74	1:5
2	0.20	0.87	2:5
3	0.20	0.43	4:5
4	0.20	0.22	8:5

Modified Turkevich Method at 70°C

200 g of glycerol (weighed using Sartorius TE601, Göttingen balance) were poured in a 500 mL beaker. This was followed by the addition of 0.20 g of silver nitrate and 3.47 g of trisodium citrate as weighed by a duly calibrated analytical balance (Sartorius TE64, Göttingen). This results in a system having a 1:10 molar ratio between silver nitrate and trisodium citrate (hence forth referred to as MTM_70-1:10). The beaker was then covered with aluminum foil except for its opening, from which an overhead stirrer was inserted. The beaker contents were then stirred at approximately 510 rpm for 1 hour at a temperature of 70°C, which was maintained

using a temperature-controlled hotplate (Wisd WiseStir® MSH-20A). The setup used is shown in Figure 7.2 below.

This experiment was then repeated using a molar ratios of silver nitrate : trisodium citrate of 1:5 (hence forth referred to as MTM_70-1:5) by using 0.20g of silver nitrate and 1.74 g of trisodium citrate.

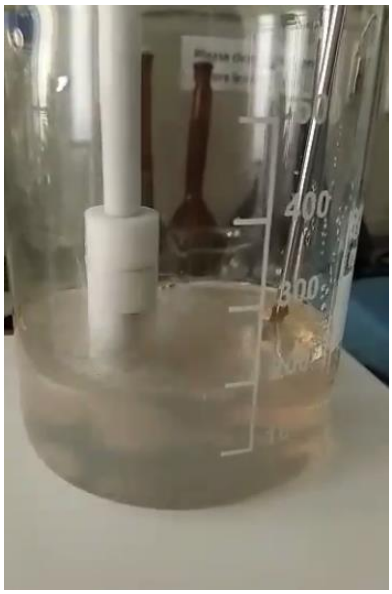

Figure 7.2. *The setup used for the Modified Turkevich Method at 70 ^{o}C.*

7.1.3 Reduction via atmospheric plasma generation

The electrochemical cell used for the production of silver nanoparticles through surface plasma-glycerol interaction under argon atmosphere at room temperature is shown in Figure 7.3. First, a solution of silver nitrate and trisodium citrate in glycerol was prepared. 200 g of glycerol (weighed using Sartorius TE601, Göttingen balance) were poured in a 500 mL beaker. This was followed by the addition of 0.1 g of silver nitrate and 1.73 g of trisodium citrate as weighed by a duly calibrated analytical balance (Sartorius TE64, Göttingen). This results in a system having a 1:10 molar ratio between silver nitrate and trisodium citrate. The beaker was then covered with aluminum foil except for the upper opening, from which an overhead stirrer was inserted.

The contents of the beaker were stirred at approximately 510 rpm for 1 hour. This solution was transferred to a reservoir which was connected to the anodic half cell via a peristaltic pump. The anodic half cell was composed of a syringe with a glassy carbon (3 mm in diameter) anode. This was connected to the cathodic half cell through an electrolytic bridge. The cathodic half

cell was composed of a centrifuge tube (30 mm in diameter) fitted with a quartz tube of 3 mm inner diameter to which the electrolytic bridge was connected to. The cathode was made of a tungsten wire which was manually placed at a distance of circa 7 mm above the surface of the quartz tube. The tungsten and glassy carbon electrodes were connected to a high-voltage power supply with an output volt-ampere parameters of 3-4kV and 5-10 mA. Before the experiment, the glycerol solution was pumped from the reservoir to the anodic area (which was kept under positive pressure by moving the plunger of the syringe down) which then moved to the cathodic area via the electrolytic bridge to the quartz tube until it reached its top. Furthermore, argon gas was flushed through the reaction vessel at a flow rate of 1.6 L/min for 10 minutes in order to remove air from the reaction zone. Argon gas was then left to flow at the same flow rate during the experiment. During the experiment, the silver nanoparticles formed on the surface of the quartz tube and were then moved to the centrifuge tube by pumping 1 drop of solution. This was done in about 5 minutes intervals. All experiments were conducted at room temperature of 22 ^{o}C. No stirring was applied to the solution.

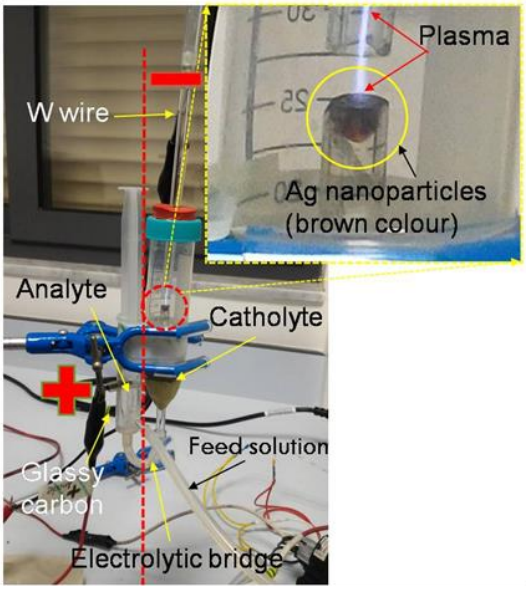

Figure 7.3. *Working prototype of electrochemical cell for synthesis of silver nanoparticles, using surface plasma process under argon atmosphere.*

7.2 Purification Process

After synthesis, the nanoparticles dispersions were first washed with Acetone (Fisher scientific, UK, 1413194) three times, each time using 200 mL of acetone in the case of the modified Turkevic methods and 25 mL in the case of the plasma method. Each time, the supernatant was removed with a disposable pipet.

In the case of the Modified Turkevich method at room temperature, a first centrifugation was done using a Benchtop Sartorious 2e16P Centrifuge (Goettingen, Germany), at 3500 ×5 for 5 minutes. This was done to remove large particles from the suspension (mostly undissolved NaOH). This step was not needed in the case of the modified Turkevich method at 70°C and plasma method, as no NaOH was used.

In all cases, the nanoparticles suspensions obtained were subdivide between a number of 50 mL centrifuge tubes so that each tube contained approximately 12 mL of the nanoparticles' suspension. This was followed by the addition of distilled water (up to 25 mL mark) followed by the addition of acetone (up to 40 mL mark). Centrifugation followed at 13480 ×g for 10 minutes using a bench top Yingtai TG16 Centrifuge (Changsha, China). The supernatant was then removed and the solid was re-dissolved in 2 mL of water followed by the addition of acetone (up to 40 mL mark). This procedure was repeated twice. After the last repeat, and after the removal of the supernatant, the centrifuge tubes were covered with Aluminum foil with small holes opened at the upper side. These tubes were left to dry overnight.

For each experiment, the solid left in the tubes was then re-dissolved in 5 mL water and all of them were placed in an Elmasonic S 60 (H) ultrasound bath (Singen, Germany) for 30 minutes. All the contents were then poured in a graduated round glass reagent bottle which was filled with water up to approximately 100 mL mark in the case of the Turkevich methods and approximately 30 mL mark in the case of the plasma method. The reagent bottle was then placed again in Ultrasound for an additional 15 minutes.

The content of the reagent bottle was then slowly taken with a syringe (20 mL per time) and was filtered with 200 nm microfilters (Kinesis, KX Syringe filters, SFS-PES-25-022, 1706260007) and placed in another reagent bottle, covered with Aluminum foil. The nanoparticles were stored in a fridge, at 4°C. A summary of the purification method is shown in Figure 7.4.

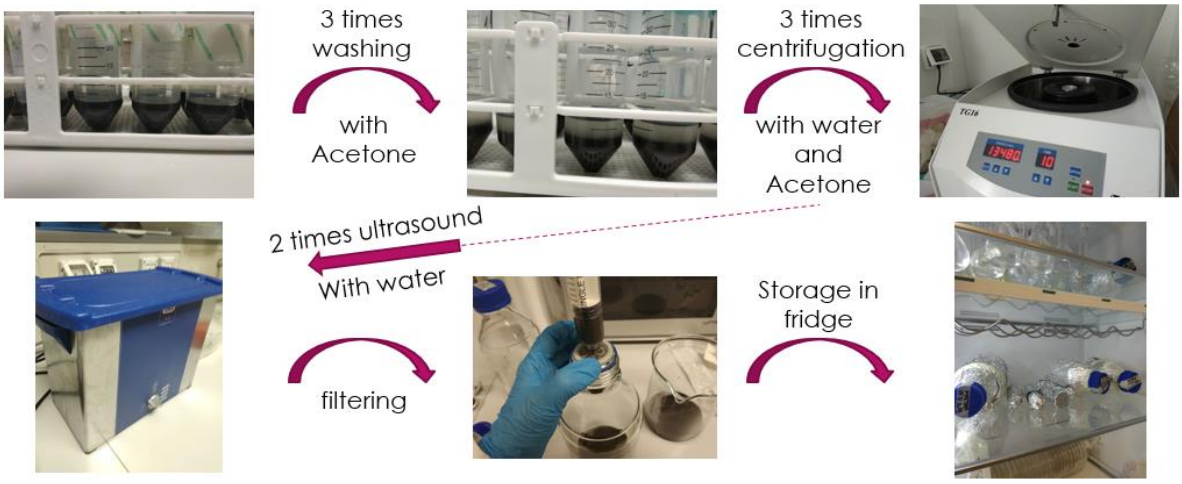

Figure 7.4. *The purification steps followed, diagrammatically.*

7.3 Characterization methods

After purification, characterization of the sample followed. The instruments used for this purpose were:

- Ultraviolet-visible (UV-vis) spectrophotometer (Shimadzu Single monochromator UV-2600, Japan) that was processed in the range of 200–900 nm, to confirm the nature of nanoparticles and obtain a picture of possible size and shape,
- Inductively Coupled Plasma-Mass (ICP-M) spectrophotometer, to define the concentrations (the results were obtained from Malta's Water Services Corporation),
- Transmission Electron Microscopy (TEM), to define with accuracy size and morphology (the results were obtained from University of Nottingham).

7.4. Antimicrobial Testing

For the microbiological testing of silver nanoparticles dispersions, *Salmonella enterica*, serotype Abony 6017, was used (available at lab of Food Microbiology of the University of Malta), previously obtained from the National Collection of Types Cultures (Health Protection Agency, Salisbury, England) in a lyophilised form. The bacterial cultures were stored in vials in a freezer at -80°C. A bead was taken from the vial and was streaked on Tryptic Soya Agar (TSA) (Oxoid, UK) plates, which were later incubated for 24 ± 2 h at 37°C, to obtain single colonies. Thereafter, the plates were stored at 4°C for a maximum of one month.

2 different colonies were picked under sterile conditions from the stock with a 10 μL loop and were transferred to 2 different tubes with 9 mL of Tryptic Soya Broth without dextrose (TSB-D) (Scharlau, Spain). The tubes were then incubated again for 24 ± 2 h at 37°C, allowing the bacteria to reach stationary phase (108-109 log CFU/mL).

To obtain the final inoculum, 5 mL of the suspension of each tube (after stirring it with Vortex) was centrifuged (6400 g) for 20 min (Benchtop Centrifuge 2e16P, Sartorious, Goettingen, Germany) and the supernatants were discarded. The same volume of sterile water was added in each centrifuge tube, under sterile conditions, resulting in a concentration of 10^6 CFU/mL.

1 mL of each inoculum was transferred to 9 mL of nanoparticles' dispersion and another 1 mL of each inoculum was transferred to 9 mL of distilled water. The tubes with the nanoparticles' dispersion are covered with Aluminum foil. Duplicated samples from each inoculum (the blank and the one with the nanoparticles' dispersion) were diluted and were plated (spread on TSA plates with an L-shaped disposable spreader to create a confluent lawn) for time intervals: 0, 2, 4, 6 h. The dilutions were made with Ringer's solution (Scharlau, Sentmenat, Spain).

The whole procedure was followed for all the nanoparticles' dispersions, from every method of synthesis, for 2 different concentrations: 3.9 ppm and 6.2 ppm for the samples of Modified Turkevich Method and 0.39 ppm and 3.9 ppm for the sample of Plasma generation Method.

After the plating of the samples and their incubation for 24 ± 2 h at 37°C, visual counting of the colonies on plates followed. Based on the dilution factor, the volume plated (0.1 mL), and the number of colonies on the plate, the count of microorganisms was calculated using the following equation (1) (Yousef & Carlstrom, 2003):

$$Count\left(\frac{CFU}{ml} or \frac{CFU}{g}\right) = \frac{number\ of\ colonies}{dilution\ factor\ \times volume\ plated} \quad (1)$$

The number of colonies is the average of duplicate plates in each case and therefore the standard deviation was also calculated.

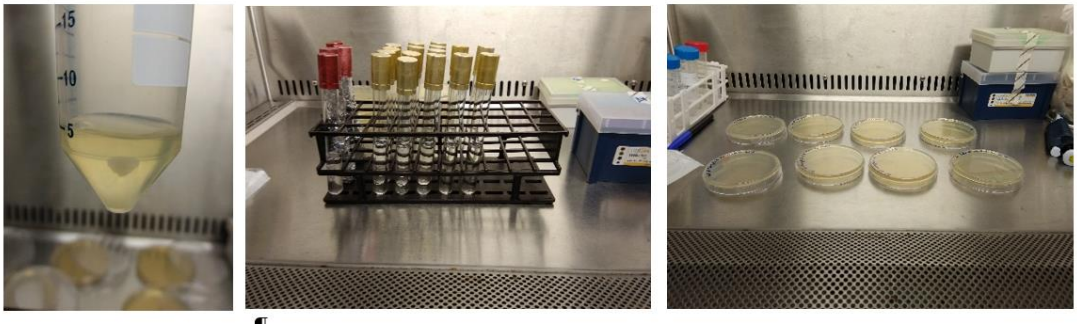

(a) **(b)** **(c)**

Figure 7.5. *Antimicrobial Testing. (a) Inoculum after centrifugation, (b) Dilutions with Ringer's solutions and nanoparticles' dispersions of the final inoculum, (c) Plating (TSA).*

7.5 Cytotoxicity testing

A cell culture flask of Normal Human Dermal Fibroblasts (NHDF) (Passage number: P=12, already subcultured), incubating with DMEM (Dulbecco's Modified Eagle Medium, Invitrogen, California, USA), in 37°C was received. Firstly, a macroscopic observation of the media was done to examine possible signs of contamination (the media would have changed colour from phenol red to yellow or purple due to pH shifts, or would have been cloudy). A microscopic observation was then done with an inverted microscope at low temperature (Motic, Hong Kong) to confirm there is no contamination (movement is a sign, since fibroblasts are adherent cells and do not move, as well as shimmering black dots or rounded particles) and to examine their confluency (must be at least 80% confluent). The media, DMEM was emptied from the flask, under sterile conditions, and the flask was washed with PBS (Phosphate Buffer Saline, Sigma Aldrich, Germany). 3-5 mL of Trypsin (Invitrogen, California, USA) were then added (to suspend the cells) and the flask was left again in the incubator (37°C) for 2-3 min. The flask was then examined under the microscope to confirm the suspension of all cells (by the movement). The content of the flask was then collected in a centrifuge tube of 15 mL, under sterile conditions, and the flask was washed with PBS that was then also added in the centrifuge tube.

Centrifugation followed (Eppendorf, Italy) at 1500 rpm for 5 minutes. After discarding the supernatant, under sterile conditions, 5 mL of PBS were added, and a second centrifugation followed. After discarding the supernatant, 10 mL of media were added, under sterile conditions. Mixing followed.

A small amount of cell suspension (a drop) was added to the edge of a counting chamber of a hemocytometer. The hemocytometer was then placed under the inverted microscope and was viewed at 40x magnification. The number of cells was counted at 4 quadrants and the average number was calculated and multiplied by the dilution number (10^4 cells/mL). $2x10^3$ was needed per well, in 100 μL. The appropriate amount of complete media (DMEM media supplemented with 10% fetal bovine serum and 0.1% penicillin and streptomycin), for all wells needed, was added in the centrifuge tube, under sterile conditions, and after mixing, it was discarded in a clean waste container.

The cell suspension was then taken and added in three 96-well tissue culture plates, one for each day of AgNPs exposure study (24, 48, 72 h), with a multipipette (Gilson, Middleton, USA). The outer wells, the ones at the perimeter of the plates, were filled with distilled water instead, to prevent contamination. 5 wells in the center of a fourth multiwell plate were also filled with the suspended cells, to test the conditions used (positive and negative controls) at day 0. The plates were incubated again overnight at 37°C under 5% CO_2: 95% conditions.

The next day, the cells were dose the four synthesized AgNPs dispersions, at a range of concentrations, for 72 h (3 replicates in each days' plates for each concentration were tested). Nanoparticles' dispersions were diluted at least 1:10 with media, so that the water will not affect the cells. Media was used as a negative control and DMSO (Sigma Aldrich, Germany) and $AgNO_3$ 250 μM (Sigma Aldrich, Germany) were used as positive. Silver nitrate at this particular concentration (250 μM) has been proven cytotoxic to H-ras transformed 5RP7 cells, from a previous study (Kaplan, Ciftci, & Kutlu, 2016). The plates with the nanoparticles' dispersions were left in the incubator, whereas the plate with the negative and positive controls (day 0) proceeded with the MTT assay.

20 μL of 10 mM MTT (Sigma Aldrich, Germany) were added in each well, under sterile conditions, and the plate was left in the incubator for 4 h. The initial colour of MTT solution is yellow, and the colour changes to purple (cause 3-(4,5-Dimethylthiazol-2-yl)-2,5-diphenyltetrazolium bromide, a tetrazole, is reduced to purple formazan in the mitochondria of the living cells). The plate was afterwards taken from the incubator and was balanced with another plate for centrifugation. After centrifugation, at 2000 rpm for 10 min, the plate was turned upside-down on a dry tissue, so that both media and MTT are removed (sterile conditions not obligatory). 120 μL of DMSO were then added in each well, under sterile conditions. The plate was then shaken on a plate shaker (Eppendorf, Italy), at 570 rpm for 5

min. Finally, the plate was placed in a spectrophotometer (SPECTROstar nano, BMG LABTECH GmbH, Ortenberg, Germany), that read the absorbance in a wavelength of 562 nm. This procedure was repeated for every multiwell plate, at day 1, 2 and 3.

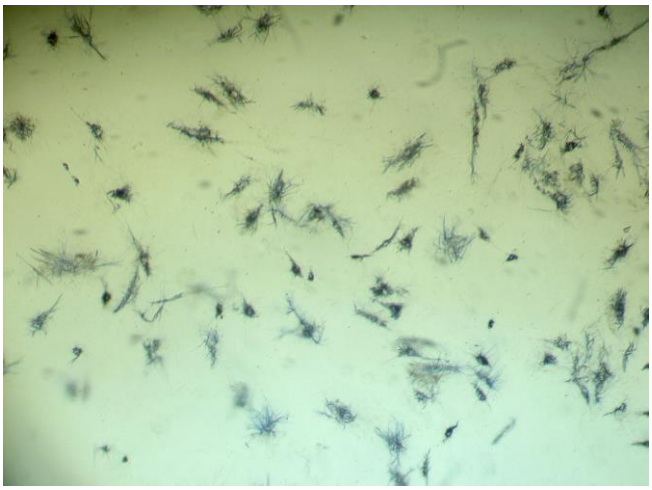

Figure 7.6. *Microscopic observation of Normal Human Dermal Fibroblasts with an inverted microscope, at low temperature.*

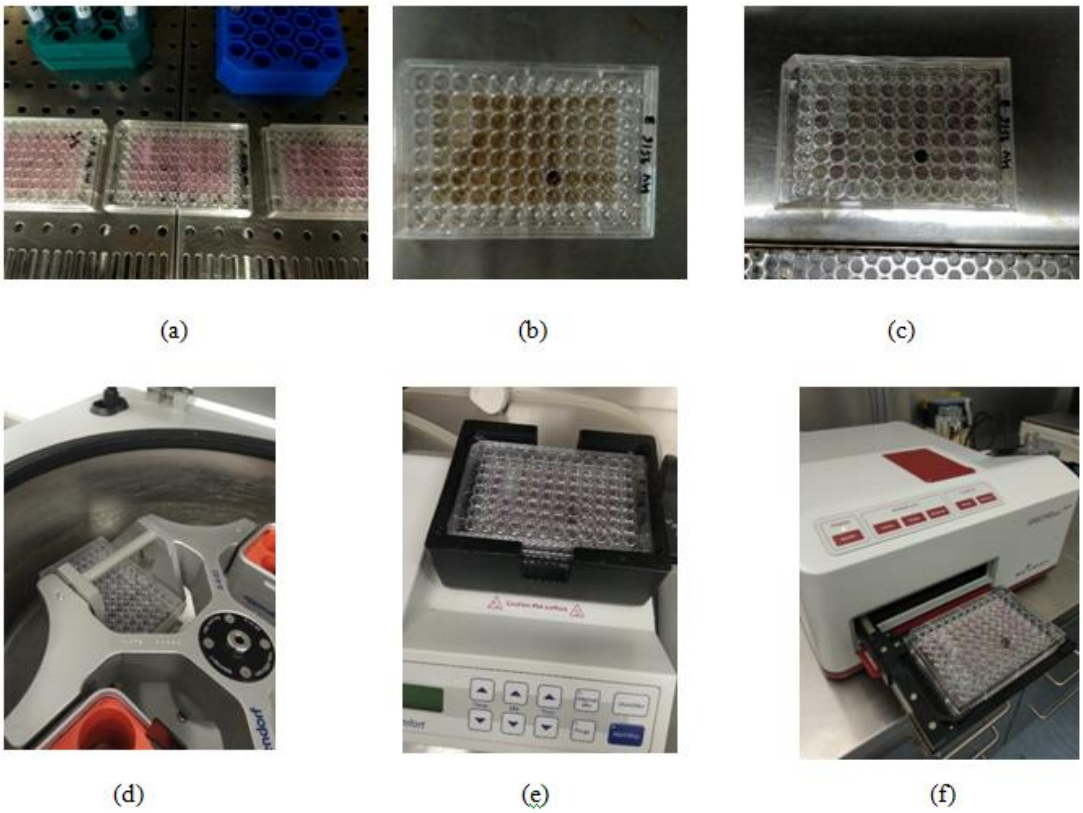

Figure 7.7. *Cytotoxicity testing. (a) 96-well tissue culture plates after AgNPs dose at a range of concentrations, (b) wells after MTT addition (0 h), (c) wells after MTT addition (4 h), (d) centrifugation, (e) shaking of the cells on plate shaker, (f) Optical Density reading at a spectrophotometer.*

8. Results

8.1 Visual observation

For all methods of synthesis used in this study, (Modified Turkevich Method at room temperature, Modified Turkevich Method at 70°C and Reduction via atmospheric plasma generation), formation of silver nanoparticles (and thus reduction of Ag^{+} to Ag^{0}) was initially established by the characteristic colour change, expected when a suspension of silver nanoparticles is formed. In fact, the reaction mixture changed from colourless to green, yellow or red (depending on the methodology employed), as shown in the following figures (Figure 7.1, Figure 7.2 and Figure 7.3).

(a) **(b)** **(c)**

Figure 7.1. *Colour change, from colourless to green, for AgNPs dispersion synthesized by the Modified Turkevich Method at room temperature. (a) Colourless, before the addition of NaOH, (b) Green, after the addition of NaOH, and (c) all ratios of silver nitrate: trisodium citrate (1:10, 1:5, 2:5, 4:5, 8:5).*

(a) **(b)**

Figure 7.2. *Colour change, from colourless to red, for AgNPs dispersion synthesized by the Modified Turkevich Method at 70ºC. (a) Colourless, at the beginning (b) Yellow, after the passing of half an hour.*

Figure 7.3. *The final reaction mixture of AgNPs, synthesized by reduction via atmospheric plasma generation, coloured yellow.*

8.2 Characterization and quantification of silver nanoparticles

As discussed in the "Experimental Procedure" section (Chapter 7), three different methods (UV-Vis, ICP-Ms, TEM) were used to obtaining the necessary information on the nature, concentration, morphology and size of the nanoparticles' dispersions produced in this study. The results obtained using each method will be discussed in detail below.

8.2.1. UV-Vis analysis

UV-Vis analysis is a useful tool to confirm nanoparticles' formation and determine some of their properties. As mentioned in Chapter 2, radiation in the UV-Vis region interacts with the nanoparticles due to the Surface Plasmon Resonance (SPR). The absorbance of the nanoparticles is influenced by many factors like size, shape, interparticle interactions, free electron density and surrounding medium (Desai, Mankad, Gupta, & Jha, 2012). Therefore, the shape of the UV-Vis spectrogram may be used for characterization of the silver nanoparticles obtained.

In the case of the experiments conducted during this study, all UV-Vis spectra obtained (*see* Figure 8.4) show a strong absorbance peak in the range of 350-600 nm. This absorbance is characteristic for the SPRs of colloidal silver nanoparticles (Saeb, Alshammari, Al-Brahim, & Al-Rubeaan, 2014), thereby confirming the presence of silver nanoparticles. The UV-Vis spectra obtained for each methodology used will be discussed in more detail below.

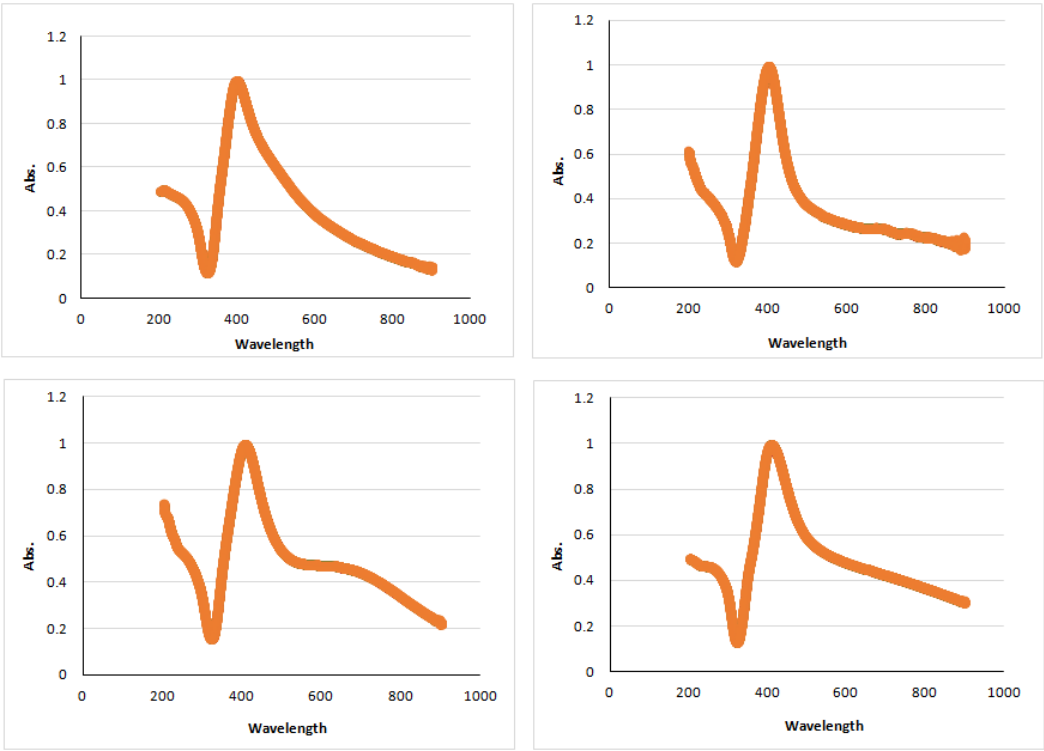

Figure 8.4. *Representative spectra of UV-Vis analysis for each of the method used (a) MTM-R_1:10, (b) MTM-70_1:10, (c) MTM-70_1:5, and (d) PL_1:10.*

<u>Modified Turkevich Method at room temperature</u>

As detailed in the "Experimental Procedure" section (Chapter 7), 5 different experiments were conducted using this methodology, whereby different ratios of silver nitrate to trisodium citrate were used. When using molar ratios of 1:10 and 1:5, a homogeneous dispersion of silver nanoparticles was obtained. However, for the other 3 molar ratios used (2:5, 4:5 and 8:5), agglomerated nanoparticles appeared in the reaction vessel, as it is shown in Figure 7.5. Thus, further analyses were only done for molar ratios of 1:10 and 1:5 (silver nitrate: trisodium).

Figure 8.5. *Agglomerated nanopartiles appeared at AgNPs dispersion, synthesized by the Modified Turkevich method at room temperature, for molar ratios 2:5, 4:5 and 8:5 of silver nitrate: trisodium citrate.*

The raw data and normalized data obtained for these two ratios are shown in Figures 8.6 and 8.7 below.

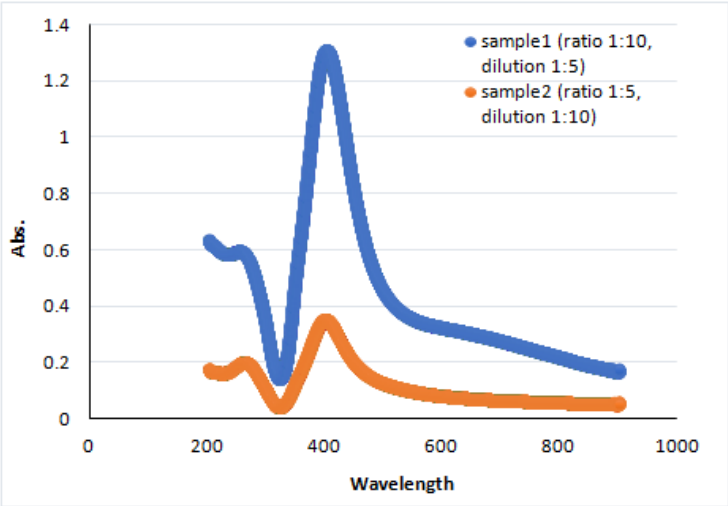

Figure 8.6. *UV-Vis absorption spectrum of AgNPs synthesized by the Modified Turkevich Method at room temperature, for molar ratios 1:10 (sample 1) and 1:5 of silver nitrate : trisodium citrate (sample 2), after dilution with water 1:5 of nanoparticles' suspension: water for sample 1 and 1:10 of nanoparticles' suspension: water for sample 2.*

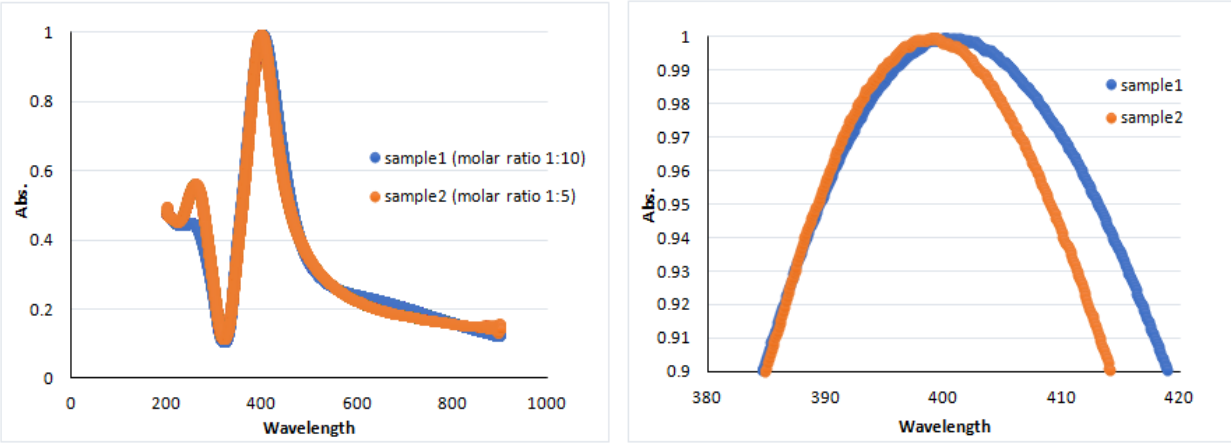

(a) **(b)**

Figure 8.7. *UV-Vis absorption spectrum of AgNPs synthesized by the Modified Turkevich Method at room temperature, for molar ratios 1:10 (sample 1) and 1:5 (sample 2) of silver nitrate : trisodium citrate, after normalization of the experimental data at 300-600 nm. (a) the complete absorbance spectrum band at 200-900 nm (b) the absorption peaks at 380-430 nm.*

The maximum absorbance for sample 1, the one with a ratio of 1:10 of silver nitrate to trisodium citrate, appears at 400 nm, whereas the maximum absorbance for sample 2, the one with ratio 1:5 of silver nitrate to trisodium citrate, appears at 398.9 nm. Since the two samples followed different dilutions (for absorbance to be below 1-1.2 max), no conclusions can be made in regards to the nanoparticles' concentration (the stronger the absorbance, the bigger the concentration of nanoparticles synthesized (Desai, Mankad, Gupta, & Jha, 2012)). Furthermore, when normalized, the spectrographs of both experiments follow the same curve profile. This indicates that both experiments resulted in very similar nanoparticles in terms of size and shape. For that reason, only the sample with molar ratio 1:10 (sample 1) was further tested (hereby named as MTM_R-1:10).

The stability of the obtained silver nanoparticles dispersion was then tested using UV-Vis analysis. This was important as different tests on the nanoparticles were conducted at different times. The complete absorbance spectrum band at 200-900 nm and the absorption peaks after normalization are presented in Figure 8.8 below.

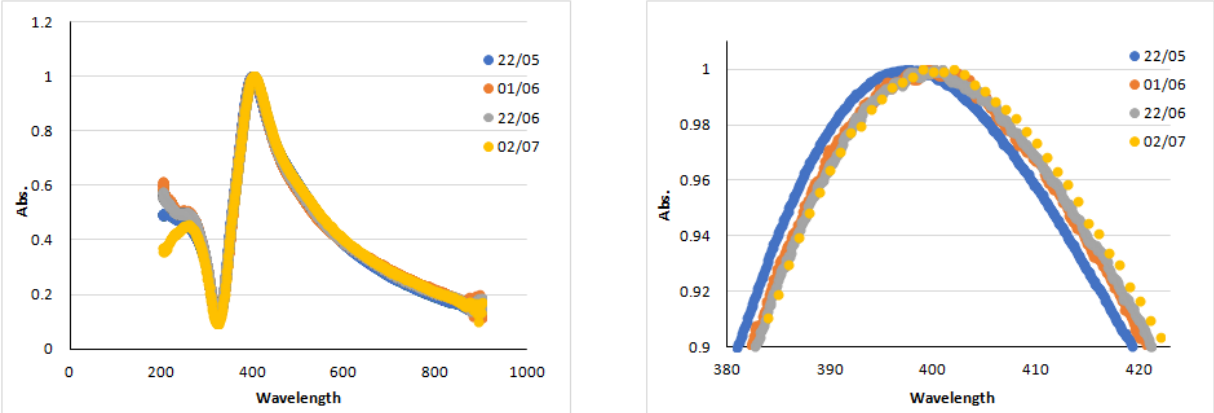

(a) **(b)**

Figure 8.8. *Stability test on 4 different dates (22/05/18, 01/06/18, 22/06/18 and 02/07/18) via UV-vis analysis, of silver nanoparticles' dispersion synthesized by Modified Turkevich Method at room temperature, with molar ratio 1:10 of silver nitrate to trisodium citrate, after normalization at 300-600 nm. (a) the complete absorbance spectrum band at 200-900 nm (b) the absorption peaks at 380-430 nm.*

Referring to Figure 8.8 above, it is evident that silver nanoparticles produced via this method are stable, with UV-Vis profile remaining constant even after one month.

<u>Modified Turkevich Method at 70ºC</u>

As detailed in the "Experimental Procedure" section (Chapter 7), two molar ratios of silver nitrate to trisodium citrate, namely 1:10 (MTM_70-1:10) and 1:5 (MTM_70-1:5), were used for this procedure. The UV-Vis spectra obtained for the latter experiments are shown in Figure 7.9 (a), whilst the data after normalization is shown in Figure 8.9 (b).

From the normalized data (Figure 8.9b) one may note that there is a difference in the secondary band area (above 600 nm) between the two samples which is an indication that different shapes of nanoparticles might have been produced. The secondary band area above 600 nm, could be attributed to quadrupole plasmon resonance and therefore its arising is a sign of nonspherical particles (Desai, Mankad, Gupta, & Jha, 2012). For that reason, since nanoparticles synthesized with a molar ratio 1:5 silver nitrate to trisodium citrate have a higher absorbance in the secondary band, they are expected to be non-spherical.

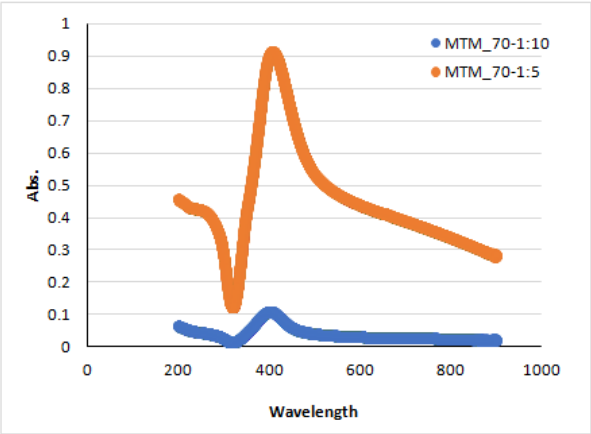

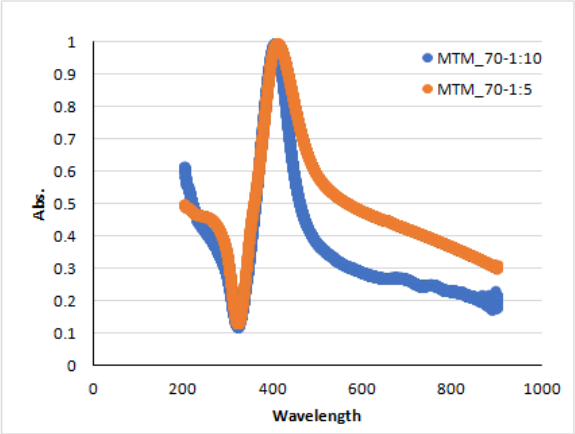

(a) **(b)**

Figure 8.9. *UV-vis absorption spectrum of AgNPs synthesized by MTM_70-1:10 and MTM_70-1:5, after dilution with water 1:10 of nanoparticles' suspensions: water (a) before normalization and (b) after normalization of experimental data.*

Since the dilution factor in both cases was 10, the concentration of the synthesized nanoparticles' suspension obtained using a 1:5 and 1:10 molar ratios of silver nitrate to trisodium citrate can be compared, according to figure 8.9 (a). In this case, when using a 1:5 ratio, larger amounts of nanopartilces were produced (nearly double).

These samples were also further tested for their stability (*see* Figures 8.10).

From Figures 8.10 (a), (b), (c) and (d), a good stability of both samples is observed even after the passing of one month. Only a small transposition of the peak appears in Figure 8.10 (d) for AgNPs synthesized by MTM_70-1:5 on the last date (02/07/2018).

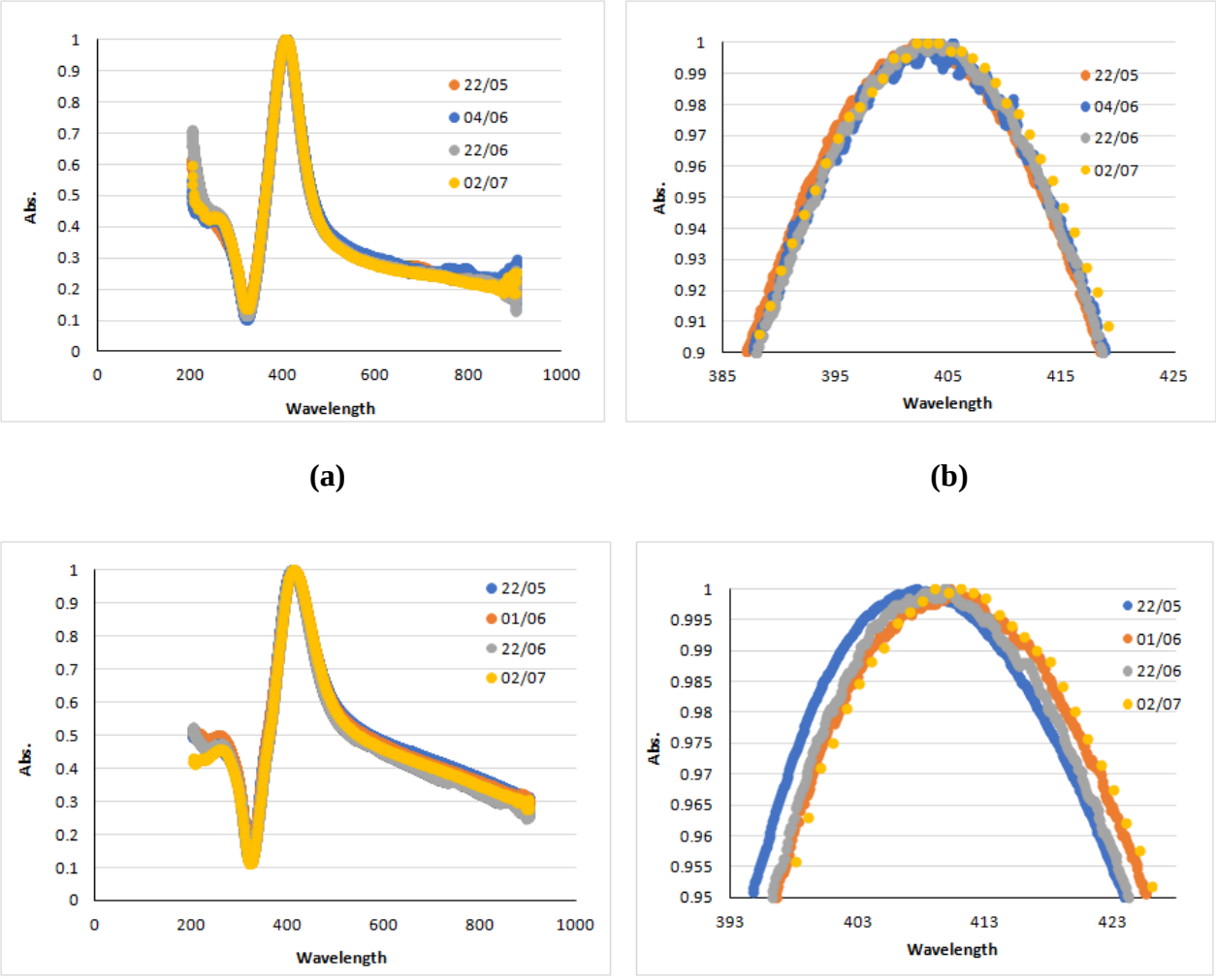

Figure 8.10. *Stability test on different dates (22/05/2018-02/07/2018), via UV-vis analysis, of silver nanoparticles' dispersion synthesized by (a), (b) MTM_70-1:10 and by (c), (d) MTM_70-1:5, after normalization at 300-600 nm. (a), (c) the complete absorbance spectrum band at 200-900 nm (b), (d) the absorption peaks at 380-425.*

<u>Reduction via atmospheric plasma generation (plasma)</u>

The sample obtained, after the purification procedure, was analyzed with UV-vis spectrophotometer. The results are shown in Figure 8.11.

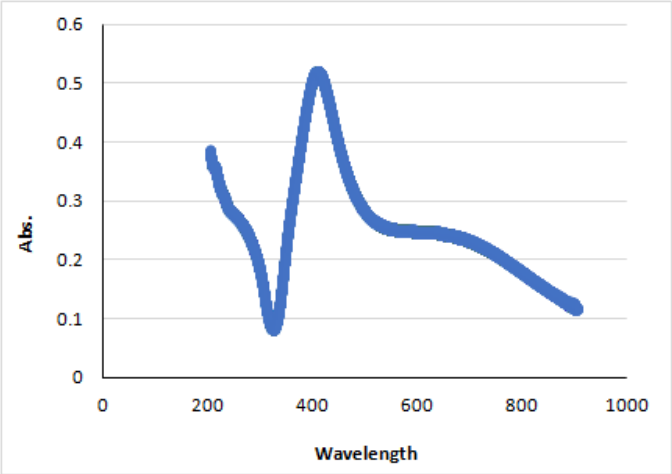

Figure 8.11. *UV-vis absorption spectrum of AgNPs synthesized via atmospheric plasma generation, for molar ratio 1:10 of silver nitrate: trisodium citrate. No dilution was needed.*

From Figure 8.11, it seems the absorbance peak appears at 405.3 nm.

Stability test was also performed, as shown in Figures 8.12 (a) and (b) below.

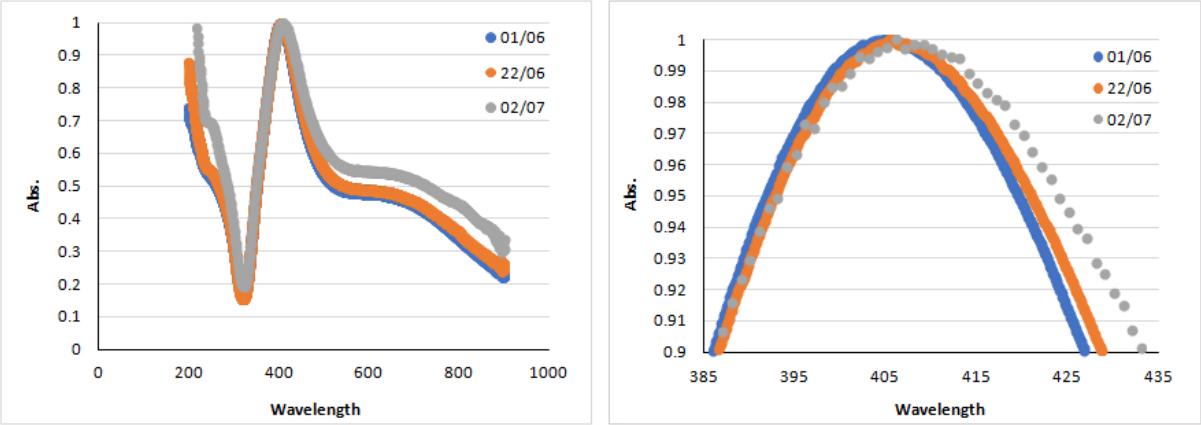

(a) **(b)**

Figure 8.12. *Stability test on different dates (01/06/2018-02/07/2018) via UV-vis analysis, of silver nanoparticles' dispersion synthesized by reduction via atmospheric plasma generation with molar ratio 1:10 of silver nitrate to trisodium citrate, after normalization at 300-600 nm. (a) the complete absorption spectrum band at 200-900 nm (b) the absorption peaks at 385-435 nm.*

From Figures (8.12 (a) and (b)) it seems that AgNPs synthesized by reduction via atmospheric plasma generation remained stable during the passing of one month, with only a small transposition of the tailing on the last date (02/07/2018) and a small broadening of the bandwidth. That means that the shapes of the synthesized AgNPs slowly change and the size distribution grows.

**It must be stated that in all samples, from all methods of synthesis, in the last stability test (date: 02/07/2018), a different rate of absorbance was used in UV-vis analysis.*

Comparison of all methods

Figures 8.13 (a), (b) and (c) below, contain the absorption spectrum band of all methods at 200-900 nm for better comparison.

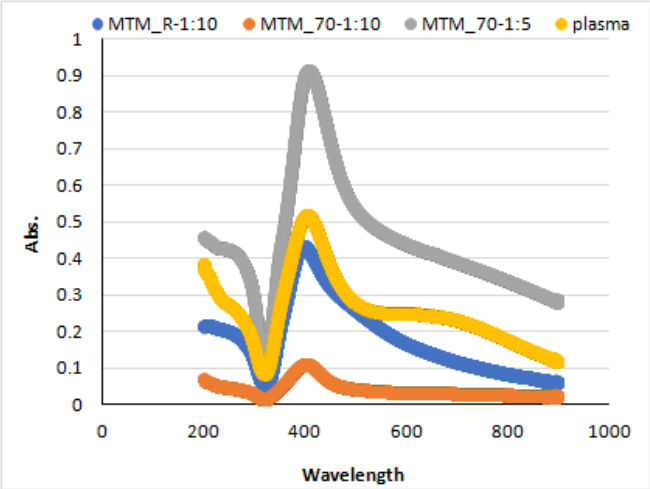

(a)

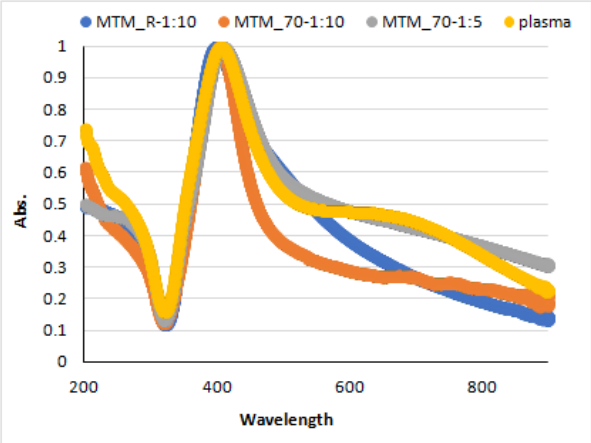

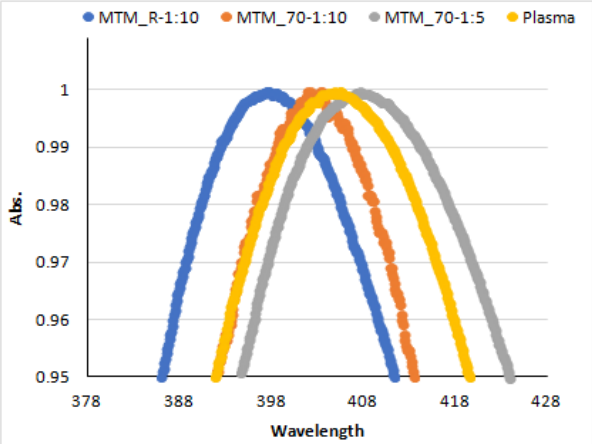

(b) **(c)**

Figure 8.13. *UV-Vis absorption spectrum band for all methods of synthesis of silver nanoparticles (MTM_R-1:10, MTM_70-1:10, MTM_70-1:5 and plasma) (a) the complete absorption band at 200-900 nm before normalization, (b) the complete absorption band at 200-900 nm after normalization of experimental data and (c) the absorption peaks at 385-425 nm after normalization of experimental data.*

From Figure 8.13 (a), no conclusions can be made since the samples followed different dilutions with water. On the other hand, after normalization of the experimental data, it is clear that the absorption peaks, the bandwidth as well as the secondary absorption band after 600 nm, are different in all cases (*see* Figures 8.13 (b) and (c)). Therefore, different sizes, size distributions and shapes can be expected among all methods.

More specifically, the smallest sizes are expected in the case of silver nanoparticles synthesized by Modified Turkevich Method at room temperature with a molar ratio of 1:10 (silver nitrate to trisodium citrate), whereas the biggest sizes are expected in the case of silver nanoparticles synthesized by Modified Turkevich Method at 70°C with molar ratio of 1:5. This is due to the fact that a blue shift is a sign that smaller particles are being produced. Note that by term 'red shift' one understands a change in absorbance to a longer wavelength whereas by the term 'blue shift' one understands a change in absorbance to a shorter wavelength.

Moreover, spherical nanoparticles are expected in the case of AgNPs synthesized by Modified Turkevich Method at 70°C with molar ratio 1:10 of silver nitrate to trisodium citrate (low absorbance above 600 nm) whereas different shapes are expected in all the other cases. The narrowest size distribution is expected in the former method too.

<u>Other tests with UV-vis analysis</u>

One of the factors that can strongly influence the stability of the samples is light. This is why for one of the samples made, (using the modified Turkevich Method at room temperature with a 1:10 ratio molar ratio of silver nitrate to trisodium citrate), the effect of light on the stability of silver nanoparticles was investigated. The results obtained are shown in Figure 8.14.

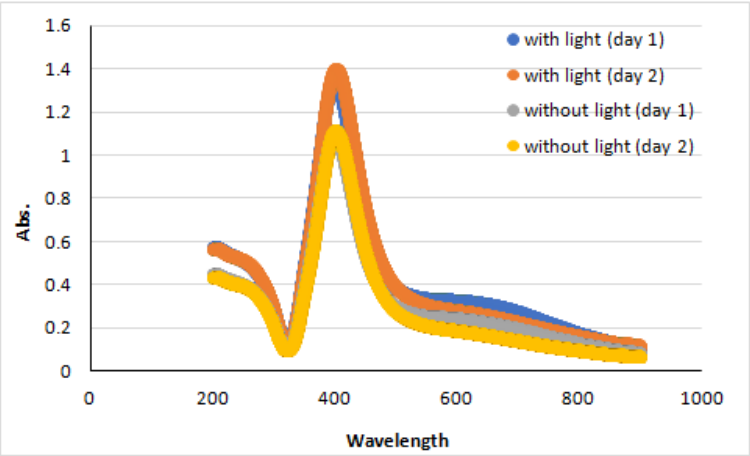

Figure 8.14. *Change of maximum absorbance peak for AgNPs synthesized by Modified Turkevich method at room temperature, according to sample's exhibition to light, at 2 days' time.*

From this figure, it seems that in all cases, the maximum absorbance is about 400 nm. However, the samples which were in light exposure, show a slight increase in the maximum absorbance peak, while the overall profile of the spectrogram remains approximately constant (1.3534 for the one with light at day 1, 1.0938 for the one without light at day 1, 1.4043 for the one with light at day 2 and 1.1165 for the one without light at day 2). This may indicate that a photochemical reduction of silver ions to silver nanoparticles is taking place in the light (Babaahmadi, Montazer, Toliyat, & Ghanbarafjeh, 2011). Because of this possible photochemical process, all samples were kept refrigerated in the dark (with aluminum foil) between all stability tests.

Other factors that may influence the profile of the curve are the presence of silver ions and trisodium citrate (which may be present in small concentrations). These two factors were tested separately, by measuring the UV-Vis absorption of an $AgNO_3$ solution in glycerol and a Trisodium Citrate solution in glycerol. The spectrographs obtained are shown in Figures 7.15 (a) and (b).

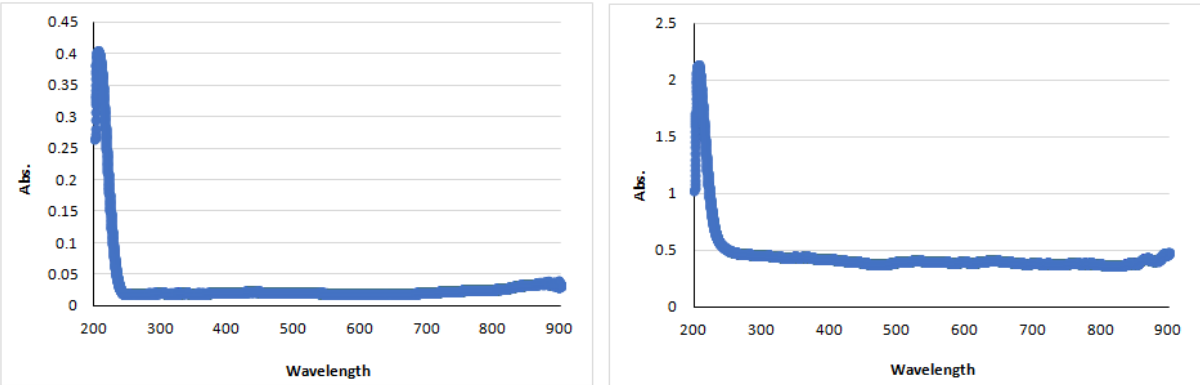

(a) **(b)**

Figure 8.15. *UV-vis absorption spectrum of (a) Glycerol-$AgNO_3$ solution and (b) Glycerol-$Na_3C_6H_5O_7$ solution.*

From these Figures it seems that the effect of trisodium citrate ($Na_3C_6H_5O_7$) is very strong for UV-Vis absorbance at 200-250 nm, although in the region of interest for silver nanoparticles (350 nm to 800 nm), no peaks are observed. This means that these two reagents are not interfering with the identification of silver nanoparticles using UV-Vis.

8.2.2 ICP-MS analysis

ICP-Ms analysis is a precise and analytical method that exhibits limits of detection in the parts-per-trillion range (Poitras, et al., 2014). This analysis was used for the quantification of the AgNPs samples and the results are shown in Table 8.1 below.

Table 8.1. ICP-MS analysis results for diluted AgNPs samples, 1:10 of AgNPs dispersions: water, except Plasma sample where no dilution was done. (1) MTM_R-1:10 (2) MTM_70-1:10 (3) MTM_70-1:5 (4) Plasma.

Number	Sample	Concentration (ppm)
1	MTM_R-1:10	6.2261
2	MTM_70-1:10	3.9361
3	MTM_70-1:5	8.1543
4	Plasma	3.9000

It may be observed that sample MTM_70-1:5 had the highest concentration, followed by MTM_R-1:10, MTM_70-1:10 and the sample synthesized by reduction via plasma generation. The concentration of AgNPs synthesized at 70°C with molar ratio 1:5 of silver nitrate to trisodium citrate is twice the concentration of those synthesized at 70°C with molar ratio 1:10, exactly how it was expected from their UV-Vis spectrum band in Figure 8.9 (a) (these samples followed the same dilution).

Since samples MTM_R-1:10, MTM_70_1:10 and MTM_70_1:5 were diluted 10 times before the ICP-MS analysis, their initial concentration is 10 times more. The same does not apply to AgNPs sample synthesized by Reduction via plasma generation, since nanoparticles' dispersion prepared was much less concentrated and thus no dilution was needed.

8.2.3 TEM analysis

To obtain more information on the surface morphology and on the size of the colloidal AgNPs prepared, TEM analysis followed for all samples.

Modified Turkevich Method at room temperature

The morphology and size of the AgNPs dispersion prepared with this method and with a molar ratio of 1:10 of silver nitrate: trisodium citrate, is much clearer in the figure below, Figure 8.16.

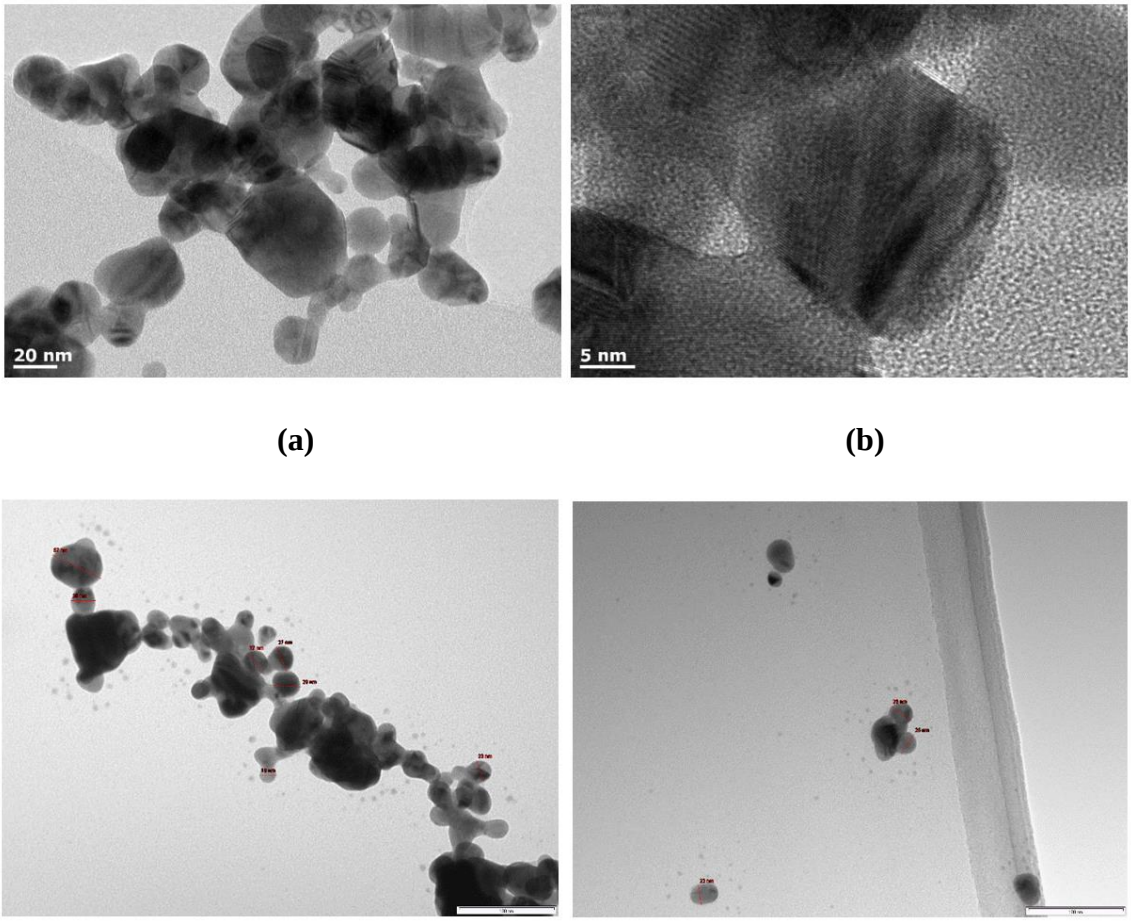

(a) **(b)**

(c) **(d)**

Figure 8.16. *TEM images of AgNPs dispersion synthesized by Modified Turkevich Method at room temperature with molar ratio 1:10 of silver nitrate: trisodium citrate (MTM_R-1:10). (a) 20 nm (b) 5 nm (c),(d) 100 nm (more diluted sample) magnification.*

From Figures 8.16 (a)-(d), it is clear that MTM_R-1:10 sample of AgNPs dispersion, consists of a mixture of shapes, but mostly spherical, with a size distribution in the range of 18-57 nm. This is as expected from the UV-vis profile. Thus, the two methodologies are in agreement.

Modified Turkevich Method at *70°C*

The morphology and size of the AgNPs dispersion prepared with this method and with molar ratio 1:10 of silver nitrate to trisodium citrate, are shown in Figure 8.17 below.

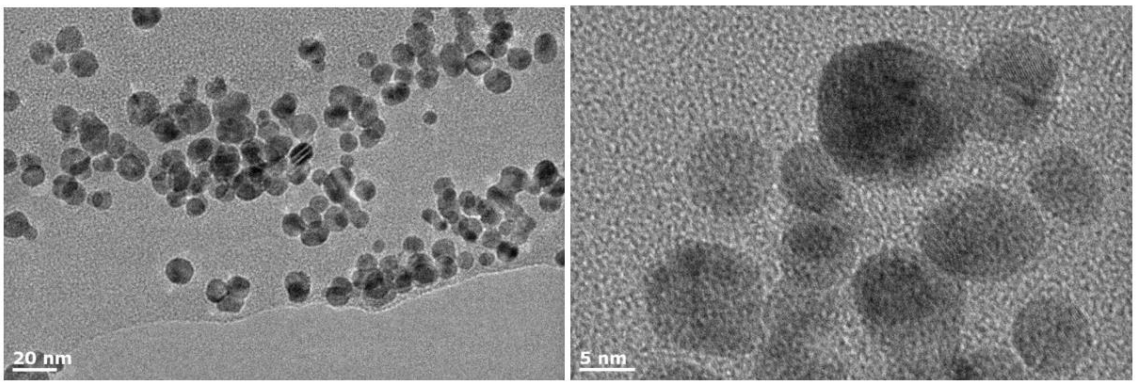

(a) **(b)**

Figure 8.17. *TEM images of AgNPs dispersion synthesized by Modified Turkevich Method at 70°C with molar ratio 1:10 of silver nitrate: trisodium citrate. (a) 20 nm (b) 5 nm magnification.*

From the images above, it is obvious that the MTM_70-1:10 sample of silver nanoparticles' dispersion consists of spherical shaped particles, as it was predicted with UV-Vis analysis, with a size distribution in the range of 7-15 nm.

The morphology and size of the AgNPs dispersion prepared with the same method and with molar ratio 1:5 of silver nitrate: trisodium citrate, are shown in Figure 8.18 below.

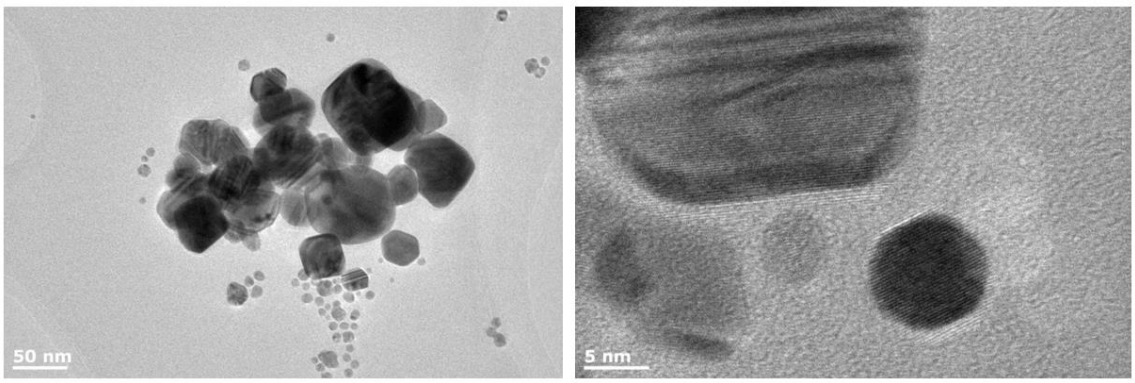

(a) **(b)**

Figure 8.18. *TEM images of AgNPs dispersion synthesized by Modified Turkevich Method at 70°C with molar ratio 1:5 of silver nitrate: trisodium citrate, for (a) 50 nm (b) 5 nm magnification.*

From Figures 8.18 (a) and (b), it is obvious that the MTM_70-1:5 sample of silver nanoparticles' dispersion consists of a mixture of shapes, mostly pyramidal, with a large size distribution in the range of 6-84 nm.

As far as synthesis by Reduction via Plasma generation is concerned, the sample could not be properly analysed due to time constrains.

Comparing these results with the results that were expected with UV-Vis analysis, it seems that in the end, the smallest nanoparticles produced were those synthesized by Modified Turkevich method at 70°C with molar ratio 1:10 of silver nitrate to trisodium citrate and not those synthesized at room temperature. The former were indeed spherical shaped particles and had the narrowest size distribution. Nevertheless, nothing specific is known for nanoparticles synthesized by atmospheric plasma.

8.3 Antimicrobial testing

ICP-MS analysis results were used to decide on the concentrations that were tested on *Salmonella enterica* cells for each sample prepared by all methods of synthesis and these were:

- ✓ 3.9 ppm and 6.2 ppm (for the samples of Modified Turkevich Method),
- ✓ 0.39 ppm and 3.9 ppm (for the sample produced with Plasma generation Method),

as mentioned above in the "Experimental Procedure" section (Chapter 7).

The results (microbial counts expressed in logarithmic scale), for each time interval representing the exposure time, for all methods of synthesis of silver nanoparticles' dispersion, are presented in Figure 8.19 for a concentration of 3.9 ppm (including plasma generated nanoparticles) and Figure 8.20 for 6.2 ppm.

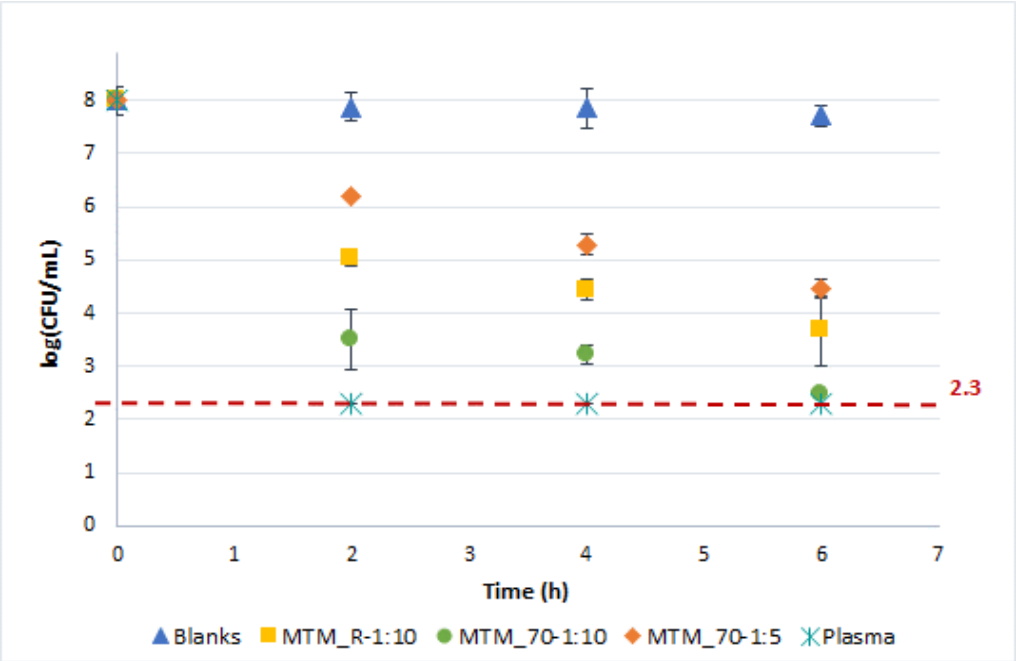

Figure 8.19. *Antimicrobial action of AgNPs synthesized by different methods on Salmonella enterica, for 3.9 ppm concentration and 0-6 h time exposure. Blanks: inoculum in distilled water. Detection limit: 2.3 log(CFU/mL).*

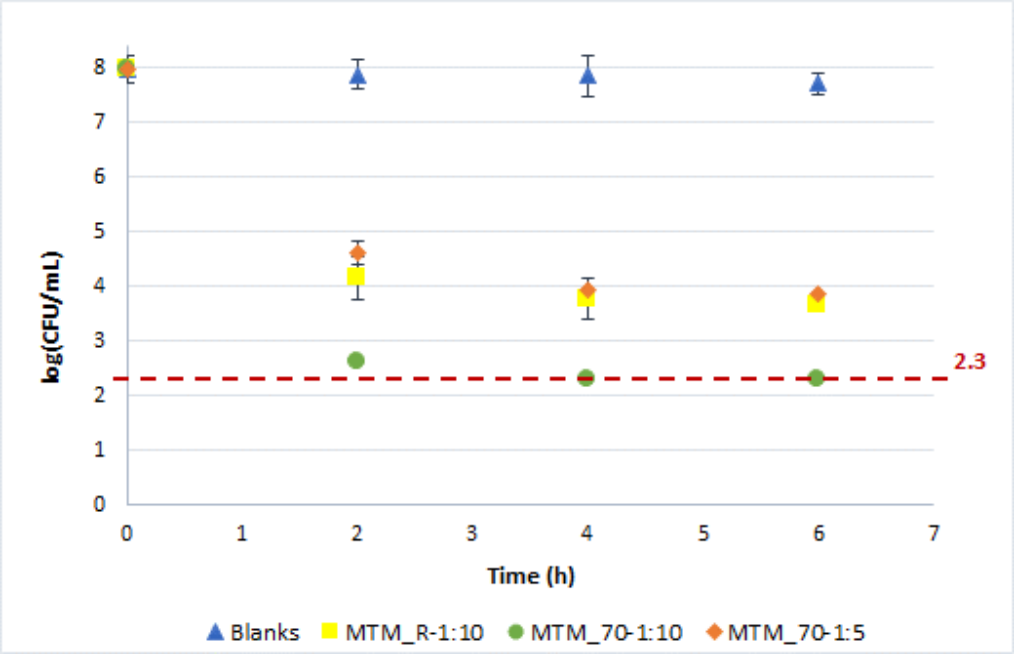

Figure 8.20. *Antimicrobial action of AgNPs synthesized by different methods on Salmonella enterica, for 6.2 ppm concentration and 0-6 h time exposure. Blanks: inoculum in distilled water. Detection limit: 2.3 log(CFU/mL).*

From Figures 8.19 and 8.20, a strong inhibition of bacterial levels can be observed for all silver nanoparticles' dispersions synthesized by all methods. On one hand, the strongest antibacterial action at a concentration of 3.9 ppm was achieved with the plasma sample of AgNPs dispersion, followed by MTM_70-1:10 sample. On the other hand, AgNPs of 6.2 ppm of MTM_70-1:10 sample, still presented the strongest antibacterial action followed by MTM_R-1:10 sample of AgNPs dispersion of the same concentration. The latter concentration was not tested for AgNPs synthesized by plasma, as it is mentioned in the "Experimental Procedure" section (Chapter 7).

At Table 8.2, the microbial counts in logarithmic scale, for AgNPs synthesized by all the above methods, except plasma, are tabulated.

Table 8.2. *Salmonella enterica* counts in logarithmic scale (log CFU/mL) for a) MTM_R-1:10, b) MTM_70-1:10 and, c) MTM_70-1:5 samples of AgNPs dispersions at concentrations: 6.2 ppm, 3.9 ppm and 0 ppm (blank sample).

Method	**C_{NPs} (ppm)**	**Exposure time (h)**			
		0	**2**	**4**	**6**
MTM_R-1:10	**0**	7.99^{i} (±0.25)	7.87^{i} (± 0.27)	7.85^{i} (± 0.37)	7.71^{i} (± 0.18)
	3.9	7.99^{i} (±0.25)	5.01^{g} (± 0.11)	4.43^{efg} (± 0.20)	3.67^{cde} (± 0.65)
	6.2	7.99^{i} (±0.25)	4.13^{def} (± 0.39)	3.77^{cdef} (± 0.37)	3.63^{cde} (± 0.00)
MTM_70-1:10	**0**	7.99^{i} (±0.25)	7.87^{i} (± 0.27)	7.85^{i} (± 0.37)	7.71^{i} (± 0.18)
	3.9	7.99^{i} (±0.25)	3.51^{cd} (± 0.58)	3.22^{bc} (±0.19)	2.46^{ab} (± 0.00)
	6.2	7.99^{i} (±0.25)	2.61^{ab} (± 0.00)	$< 2.30^{a}$ (± 0.00)	$< 2.30^{a}$ (± 0.00)
MTM_70-1:5	**0**	7.99^{i} (±0.25)	7.87^{i} (± 0.27)	7.85^{i} (± 0.37)	7.71^{i} (± 0.18)
	3.9	7.99^{i} (±0.25)	6.21^{h} (± 0.03)	5.29^{g} (± 0.19)	4.46^{efg} (± 0.18)
	6.2	7.99^{i} (±0.25)	4.62^{fg} (± 0.22)	3.92^{cdef} (± 0.00)	3.85^{cdef} (± 0.00)

The different letters among samples show statistical differences ($p<0.05$) according to post-hoc Tukey's test.

These results show that there is statistical difference on microbial survival among the methods of nanoparticles synthesis, as well as among concentrations and time intervals, and therefore all factors affect the inhibition of *Salmonella enterica* (significance level $p<0.001$). More

specifically, the mean values of log(CFU/mL) for each method, show that the greatest inhibition of *Salmonella enterica* is achieved by silver nanoparticles produced by Modified Turkevich Method at 70°C with molar ratio 1:10 of silver nitrate: trisodium citrate, followed by AgNPs synthesized at room temperature with the same molar ratio. As far as concentration is concerned, the increase of nanoparticles concentration results in subsequent increase in the inhibition of the microorganism. This decrease, following exposure to twice the concentration of silver nanoparticles, is not proportional (5.18 log(CFU/mL) for 3.9 ppm and 4.59 log(CFU/mL) for 6.2 ppm). Last but not least, increase of the exposure time of *Salmonella enterica* cells to silver nanoparticles, increased the inhibition of the microorganism, resulting in almost half of the initial population after 6 hours, i.e., 7.99 log(CFU/mL) at 0 hours to 4.83 log(CFU/mL) in 6 hours.

At the lower concentration of 3.9 ppm, it appears that *Salmonella enterica* exposed to two AgNPs samples, i.e., MTM_R-1:10 and MTM_70-1:5, has not been inactivated after 6 hours. For that reason, the exposure time was extended to 26 hours to assess whether these samples could inhibit *Salmonella enterica* similarly to the inhibition achieved at 6.2 ppm concentration. The results are presented at Figure 8.21.

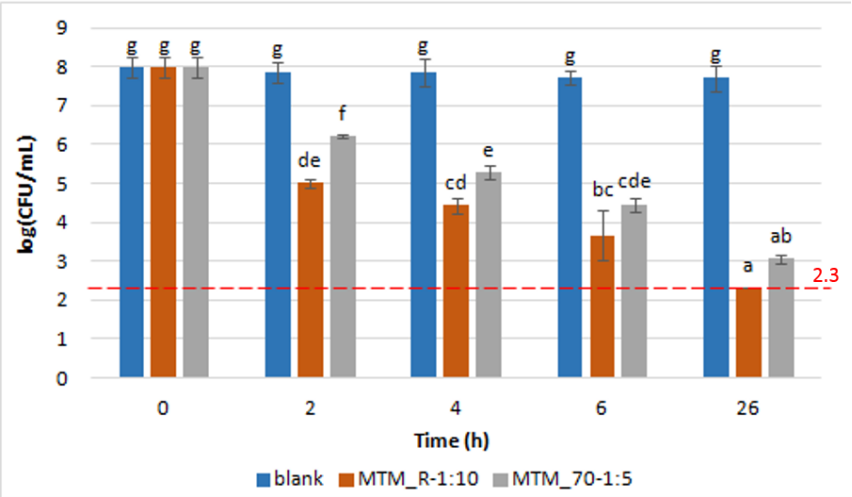

Figure 8.21. *Antimicrobial action of AgNPs synthesized by different methods on Salmonella enterica, for concentration 3.9 ppm and time exposure of 0, 2, 4, 6, 26 h. Blanks: inoculum in distilled water. Detection limit: 2.3 log(CFU/mL). The different letters among samples show statistical differences (p<0.05) according to post-hoc Tukey's test.*

It is clear that after 26 hours, both samples achieve a good inhibition of *Salmonella enterica* growth.

The statistical analysis of the obtained results revealed that each design factor individually (the different methods used – Blanks, MTM_R-1:10 and MTM_70-1:5 –, nanoparticles' concentration – 0 and 3.9 ppm – and time of exposure) had a significant effect on the inhibition of *Salmonella enterica* ($p<0.001$) whereas the interaction of all design factors exhibited no significant effect. The sample that resulted in the greatest inhibition of *Salmonella enterica* is MTM_R-1:10, according to the mean values of log(CFU/mL). Moreover, as the time of exposure to silver nanoparticles increases, the inhibition of the microorganism also increases, i.e., from 7.99 log(CFU/mL) at 0 hours to 2.3 log(CFU/mL) at 26 hours.

For AgNPs synthesized by the reduction via plasma generation method, two concentrations were tested: 3.9 ppm and 0.39 ppm. Table 7.3 summarizes all the results for all samples at 3.9 ppm concentration.

Table 8.3. *Salmonella enterica* counts in logarithmic scale (log(CFU/mL)) for a) MTM_R-1:10, b) MTM_70-1:10, c) MTM_70-1:5 and, d) plasma samples of AgNPs dispersions at concentrations: 3.9 ppm and 0 ppm (blank sample).

Method	**C_{NPs} (ppm)**	**Exposure time (h)**			
		0	2	4	6
Sample1	**0**	7.99^{g} (±0.25)	7.87^{g} (± 0.27)	7.85^{g} (± 0.37)	7.71^{g} (± 0.18)
	3.9	7.99^{g} (±0.25)	5.01^{e} (± 0.11)	4.43^{de} (± 0.20)	3.67^{cd} (± 0.65)
70_1:10	**0**	7.99^{g} (±0.25)	7.87^{g} (± 0.27)	7.85^{g} (± 0.37)	7.71^{g} (± 0.18)
	3.9	7.99^{g} (±0.25)	3.51^{c} (± 0.58)	3.22^{bc} (±0.19)	2.46^{ab} (± 0.00)
70_1:5	**0**	7.99^{g} (±0.25)	7.87^{g} (± 0.27)	7.85^{g} (± 0.37)	7.71^{g} (± 0.18)
	3.9	7.99^{g} (±0.25)	6.21^{f} (± 0.03)	5.29^{e} (± 0.19)	4.46^{de} (± 0.18)
Plasma	**0**	7.99^{g} (± 0.25)	7.87^{g} (± 0.27)	7.85^{g} (± 0.37)	7.71^{g} (± 0.18)
	3.9	7.99^{g} (± 0.25)	$< 2.30^{a}$ (± 0.00)	$< 2.30^{a}$ (± 0.00)	$< 2.30^{a}$ (± 0.00)

The different letters among samples show statistical differences ($p<0.05$) according to post-hoc Tukey's test.

These results show that there is statistical difference between the microorganism levels among the methods of nanoparticles synthesis, as well as between concentrations and among time

intervals, and therefore all factors affect the inhibition of *Salmonella etnerica* (significance level $p<0.001$).

More specifically, the mean values of log(CFU/mL) for each method, show that the greater inhibition of *Salmonella enterica* is achieved by plasma sample of AgNPs, followed by MTM_70-1:10. Last but not least, as the time of exposure to silver nanoparticles increases, the inhibition of bacteria also increases, i.e., 7.99 log(CFU/mL) at 0 hours to 2.3 log(CFU/mL) at 6 hours).

Regarding the antimicrobial effect of AgNPs synthesized with plasma, which is resulted in a concentration of 0.39 ppm, this leads to the microbial levels presented in Figure 8.22, according to the values tabulated in Table 8.4.

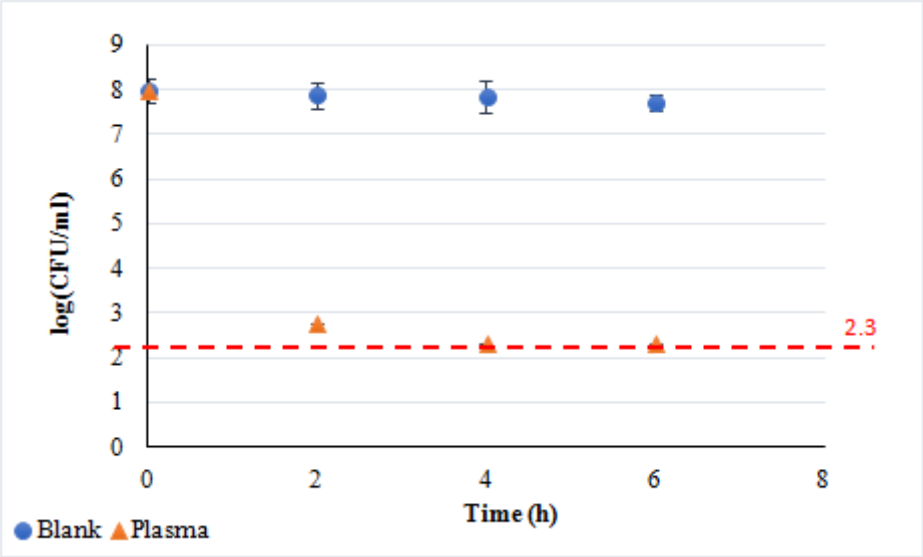

Figure 8.22. *Antimicrobial action of silver nanoparticles synthesized by Reduction via plasma generation, for AgNPs concentration 0.39 ppm and time intervals 0, 2, 4 and 6 hours (Blanks: inoculums in distilled water). Detection limit: 2.3 log(CFU/mL).*

Table 8.4. *Salmonella enterica* counts in logarithmic scale (log(CFU/mL)) for AgNPs synthesized by reduction via plasma generation with molar ratio 1:10 of silver nitrate: trisodium citrate, for nanoparticles concentrations: 3.9 ppm and 0 ppm (blank sample).

Method	**C_{NPs} (ppm)**	**Exposure time (h)**			
		0	**2**	**4**	**6**
	0	7.99^{b} (± 0.25)	7.87^{b} (± 0.27)	7.85^{b} (± 0.37)	7.71^{b} (± 0.18)
Plasma	**0.39**	7.99^{b} (± 0.25)	2.79^{a} (± 0.00)	$< 2.30^{a}$ (± 0.00)	$< 2.30^{a}$ (± 0.00)
	3.9	7.99^{b} (± 0.25)	$< 2.30^{a}$ (± 0.00)	$< 2.30^{a}$ (± 0.00)	$< 2.30^{a}$ (± 0.00)

The different letters among samples show statistical differences ($p<0.05$) according to post-hoc Tukey's test.

These results show that the exposure time had a significant impact to the microbial levels. When comparing the two tested concentrations, no significant effect was observed. There is a great reduction to *Salmonella enterica* levels during the 2 hours exposure after which, bacteria reach the detection limit.

8.4 Cytotoxicity testing

After measuring the Optical Density (OD) in spectrophotometer, having as control samples Untreated cells only with media (DMEM, negative control), $AgNO_3$ 250 μM (positive control) and DMSO 1.6 % (positive control), as mentioned before in the "Experimental Procedure" (Chapter 7), cells viability in 3 days time can be examined. For that reason, the OD percentage of the negative control (Untreated) on day 0 was calculated in each case of AgNPs sample. The percentages derive from the mean value of 3 replicates. It must be stated that a decrease in optical density can be interpreted as loss of cells viability.

Modified Turkevich Method at room temperature

The cell viability of human Fibroblasts after exposure to AgNPs synthesized by Modified Turkevich Method at room temperature with molar ratio 1:10 of silver nitrate to trisodium citrate, at a range of concentrations, over 3 days, is presented in Figure 8.23.

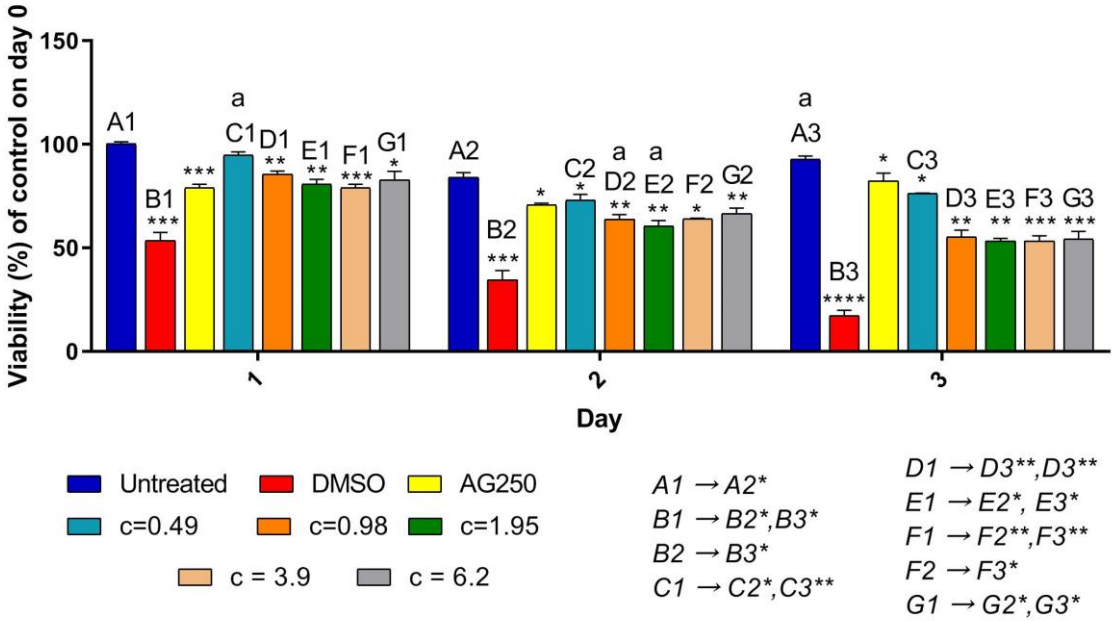

Figure 8.23. *Fibroblast cells viability, as percentage of Untreated (negative control) ± SD (3 replicates measured), after exposure to MTM_R-1:10 sample of AgNPs dispersion, at a range of concentrations, over a 3 day period. $AgNO_3$ 250 μM and DMSO 1.6 % were used as positive controls. Statistical significance with the Untreated is annotated by black stars (*) and the level of significance is given as follows: * p<0.05, **p<0.01, *** p<0.001 and ****p<0.0001. Significant differences over time are annotated by capital letters and significance is given below the graph in the legend. Letter (a) signifies that SD was taken from only 2 replicates. Data were analyzed by Two-way Anova and Tukey's post-hoc multi-comparison test. Cell viability is measured by MTT assay.*

From figure 8.23, it seems that both time and treatment had a significant effect on % viability ($p<0.0001$). More specifically, a time-dependent reduction in % viability can be observed, especially in the first 2 days of AgNPs exposure. $AgNO_3$ solution is the only exception to that observation since it remained stable at all exposure times. It must be stated of course, that the significant reduction of cells viability of the Untreated ($p<0.05$), from the 1st to the 2nd day of exposure, could have been caused from small experimental errors, like the scratching of the wells or small pipetting errors resulting to slightly smaller number of cells seeded in that particular well, since it does not follow the overall behavior of Untreated in the rest 2 days. As far as cells viability from the 2nd to the 3rd day of exposure is concerned, no significant reduction

can be observed, except in the cases of DMSO and 3.9 ppm concentration of MTM_R-10 AgNPs. As far as AgNPs concentration is concerned, all concentrations presented a significant reduction of cells viability compared to the Untreated of the same day (significance is presented in all cases at the legend below 8.23 graph), but this reduction does not seem to be in accordance with concentration. That means, that even when concentration increases, the reduction of cells viability caused, remains stable at a certain point, namely in the range of 15-21% at all concentrations on the 1st day and 53-55% at all concentrations on the last day of exposure. Exception is 0.49 ppm concentration that did not show a significant reduction of cells viability compared to the Untreated on the 1st day of exposure ($p<0.05$), and it did not follow the same % viability reduction with the rest of the concentrations. Therefore, all MTM_R-1:10 AgNPs concentrations are assumed to be cytotoxic, during the whole exposure time.

DMSO seems to have effectively killed half the population of cells over the 3 day period and challenge with $AgNO_3$ was as cytotoxic as nanoparticles (no significant difference in % viability was observed among them) over the first 2 days of exposure. Exception to that, is 0.49 ppm concentration that presented significantly higher cells viability than $AgNO_3$ on the 1st day of exposure ($p<0.01$) and 1.95 ppm concentration that presented significantly lower cells viability than $AgNO_3$ on the 2nd day of exposure ($p<0.05$). On the 3rd day though, all AgNPs concentrations, except 0.49 ppm, had significantly reduced % viability compared to $AgNO_3$ solution ($p<0.05$).

Modified Turkevich Method at 70°C

Cells viability of human Fibroblasts after exposure to AgNPs synthesized by Modified Turkevich Method at 70°C with molar ratio 1:10 of silver nitrate to trisodium citrate, at a range of concentrations, over 3 days, is presented in Figure 8.24.

From this figure (8.24), it seems that both time and treatment had a significant effect on % viability ($p<0.0001$). More specifically, a time-dependent reduction in % viability can be observed in the case of the Untreated and DMSO (as before), and in the cases of 1.95, 3.9 and 6.2 ppm concentrations. All the other treatments did not show a significant reduction of % viability over time. As far as AgNPs concentration is concerned, there is a clear concentration-dependent reduction of cells viability. 1.95, 3.9 and 6.2 ppm concentrations, presented statistical significance with the Untreated at all exposure times (significance is presented on the graph). On the last day of exposure (3rd day) in particular, 6.2 ppm reduced viability more

than 50% (71%, specifically), followed by 3.9 ppm concentration that reduced viability almost up to 50% (48% reduction of the Untreated). 0.49 and 0.98 ppm concentrations, presented a significant difference with the Untreated on the 1st and the 3rd day of exposure (significance is presented on the graph) but no significant difference was observed on the 2nd day. However, having in mind the possible experimental errors related to the Untreated on the 2nd day, as mentioned before, this non-significant reduction would in other case be significant. Paradoxically, on the 3rd day, 0.49 ppm concentration of AgNPs, not only it did not reduce % viability but viability actually increased, something that could be explained from the natural variations of cellular metabolism or from small pipetting errors leading to slightly more cells seeded in that well. Therefore, all MTM_70-1:10 AgNPs concentrations are assumed to be cytotoxic, during the whole exposure time.

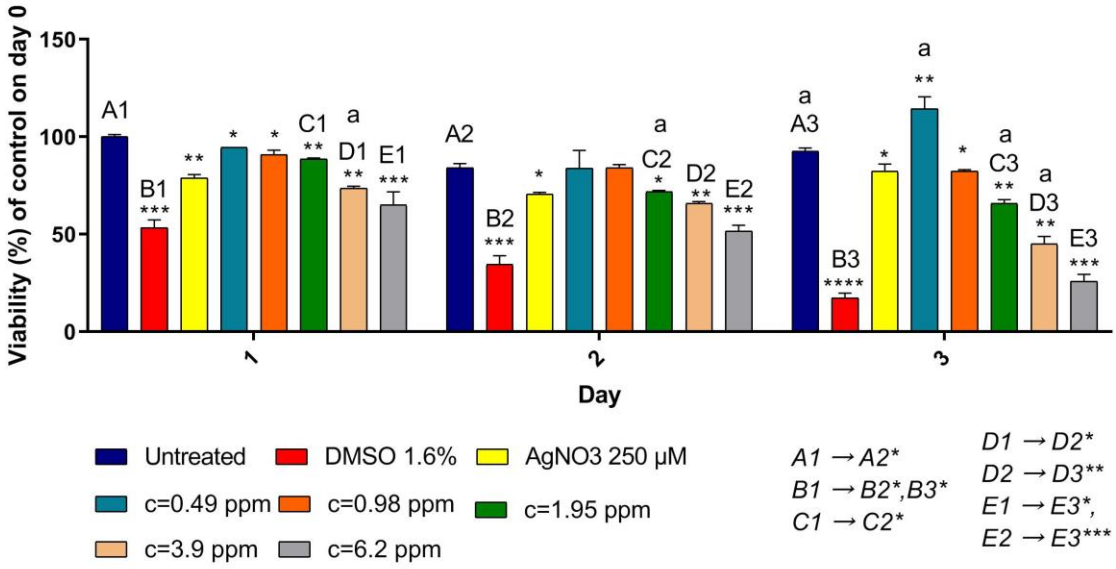

Figure 8.24. *Fibroblast cells viability, as percentage of Untreated (negative control) ± SD (3 replicates measured), after exposure to MTM_70-1:10 sample of AgNPs dispersion, at a range of concentrations, over a 3 day period. $AgNO_3$ 250 μM and DMSO 1.6 % were used as positive controls. Statistical significance with the Untreated is annotated by black stars (*) and the level of significance is given as follows: * p<0.05, **p<0.01, *** p <0.001 and ****p<0.0001. Significant differences over time are annotated by capital letters and significance is given below the graph in the legend. Letter (a) signifies that SD was taken from only 2 replicates. Data were analyzed by Two-way Anova and Tukey's post-hoc multi-comparison test. Cell viability is measured by MTT assay.*

Challenge with $AgNO_3$ on the 1st day presented a significantly higher reduction of % viability compared to AgNPs with concentrations 0.49, 0.98 and 1.95 ppm ($p<0.05$). On the 2nd day though, $AgNO_3$ solutions presented a significantly higher reduction of % viability only compared to 0.98 ppm concentration of AgNPs ($p<0.05$), whereas it presented a lower

reduction of cells viability compared to 3.9 and 6.2 ppm concentrations of AgNPs ($p<0.05$). On the 3rd day, $AgNO_3$ presented a significantly higher cells viability than 3.9 and 6.2 ppm concentration of AgNPs ($p<0.001$), but no significant difference was observed for all the other nanoparticles dispersions.

Cells viability of human Fibroblasts after exposure to AgNPs synthesized by Modified Turkevich Method at 70ºC with molar ratio 1:5 of silver nitrate to trisodium citrate, at a range of concentrations, over 3 days, is presented in Figure 8.25.

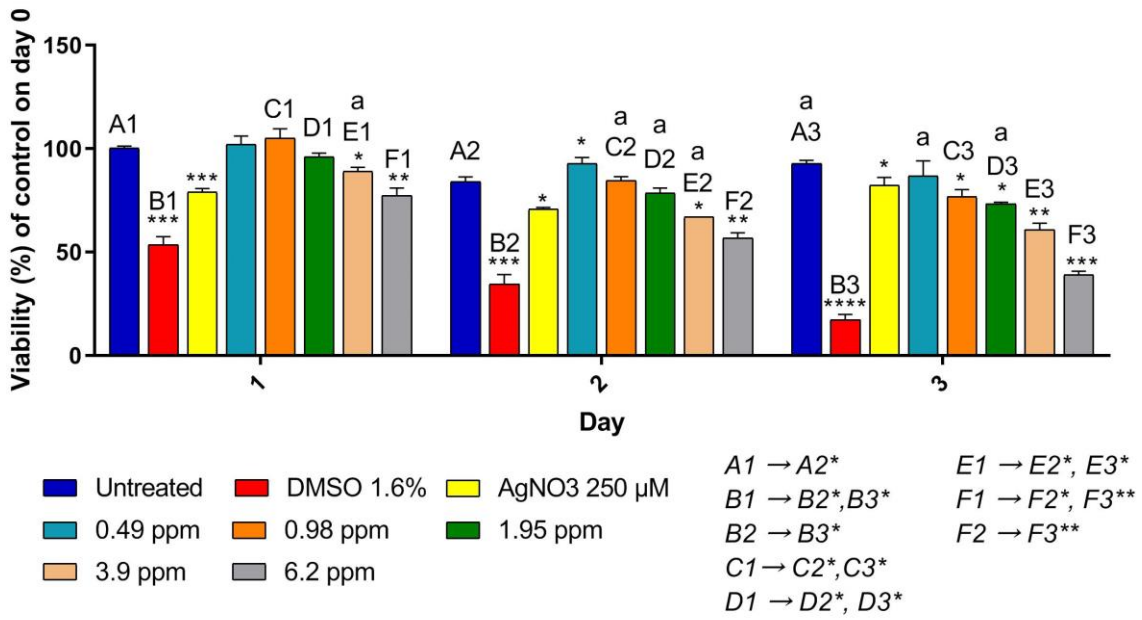

Figure 8.25. *Fibroblast cells viability, as percentage of Untreated (negative control) ± SD (3 replicates measured), after exposure to MTM_70-1:5 sample of AgNPs dispersion, at a range of concentrations, over a 3 day period. AgNO3 250 µM and DMSO 1.6 % were used as positive controls. Statistical significance with the Untreated is annotated by black stars (*) and the level of significance is given as follows: * p<0.05, **p<0.01, *** p <0.001 and ****p<0.0001. Significant differences over time are annotated by capital letters and significance is given below the graph in the legend. Letter (a) signifies that SD was taken from only 2 replicates. Data were analyzed by Two-way Anova and Tukey's post-hoc multi-comparison test. Cell viability is measured by MTT assay.*

From this figure (8.25), it seems that both time and treatment had a significant effect on % viability ($p<0.0001$). More specifically, a time-dependent reduction in % viability can be observed. Exceptions to that observation though are $AgNO_3$ solution and concentration 0.49 ppm of MTM_70-1:5 AgNPs sample, that did not present a significant reduction in % viability over time. Furthermore, there is a clear concentration-dependent reduction of cells viability, with 6.2 ppm concentration having reduced viability more than 50% (56 % reduction of the

Untreated), on the 3rd day. 3.9 ppm concentration of AgNPs also presented a significant reduction of cells viability compared to the Untreated on all days of exposure (significance is presented on the graph at all days). 1.95 ppm concentration significantly reduced cells viability compared to the Untreated only on the 3rd day ($p<0.05$). However, bearing in mind the possible experimental errors related to the Untreated of the 2nd day, as mentioned before, this non-significant reduction would in other case be significant. 0.98 ppm concentration, also presented a significant reduction of cells viability only the 3rd day, with a possible cytotoxic effect on the 2nd day also, for the same reason. 0.49 ppm concentration did not present a significant reduction of cells viability compared to the Untreated at any day of exposure. Therefore, all MTM_70-1:5 concentrations are assumed to be cytotoxic, except 0.49 ppm.

A significantly lower cells viability appeared when cells were challenged with $AgNO_3$ solution compared to the challenge with 0.49 ppm ($p<0.05$), 0.98 ppm ($p<0.01$) and 1.95 ppm ($p<0.05$) of AgNPs on the 1st day. On the 2nd day, $AgNO_3$ presented a significantly lower viability than 0.49 and 0.98 ppm concentration of AgNPs ($p<0.05$), but significantly higher than 6.2 ppm concentration ($p<0.05$). On the 3rd day, cells viability when challenged with $AgNO_3$ was significantly higher than that one in the cases of 3.9 and 6.2 ppm concentration of AgNPs ($p<0.05$ for both).

Reduction via atmospheric plasma generation

The cell viability of human fibroblasts after exposure to AgNPs synthesized by Reduction via plasma generation with molar ratio 1:10 of silver nitrate to trisodium citrate, at a range of concentrations, over 3 days, is presented in Figure 8.26.

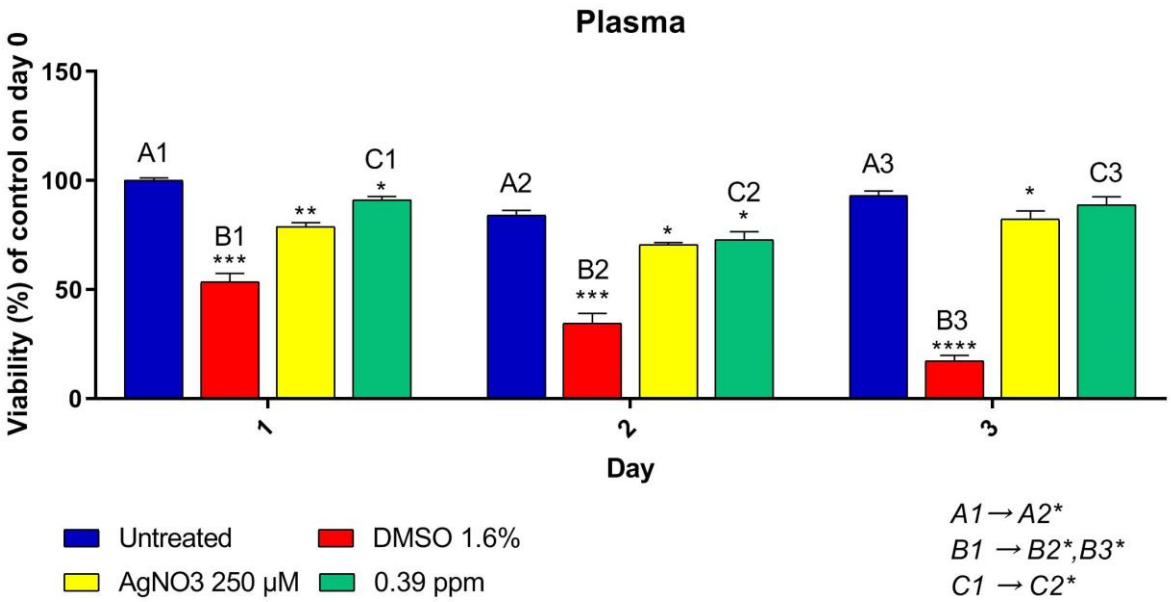

Figure 8.26. *Fibroblast cells viability, as percentage of Untreated (negative control) ± SD (3 replicates measured), after exposure to plasma sample of AgNPs dispersion, at a range of concentrations, over a 3 day period. $AgNO_3$ 250 μM and DMSO 1.6 % were used as positive controls. Statistical significance with the Untreated is annotated by black stars (*) and the level of significance is given as follows: * p<0.05, **p<0.01, *** p <0.001 and ****p<0.0001. Significant differences over time are annotated by capital letters and significance is given below the graph in the legend. Letter (a) signifies that SD was taken from only 2 replicates. Data were analyzed by Two-way Anova and Tukey's post-hoc multi-comparison test. Cell viability is measured by MTT assay.*

From figure 8.26, it seems that both time and treatment had a significant effect on % viability ($p<0.0001$). More specifically, a time-dependent reduction in % viability can be observed except for $AgNO_3$ solution. 0.39 ppm concentration of AgNPs presented a significant reduction of cells viability compared to the Untreated on the first two days of exposure ($p<0.05$ in both days). Paradoxically, it did not present a significant difference with the Untreated, on the 3rd day of exposure.

Challenge with AgNO3 solution presented a significantly lower cells viability on the 1st day compared to 0.39 ppm concentration of AgNPs ($p<0.001$). On the other two days, the two samples presented no significant difference, as far as cells viability is concerned.

Concentration 3.9 ppm of all AgNPs samples (except plasma)

Cells viability of human fibroblasts after exposure to AgNPs synthesized by all the above methods (except plasma), at 3.9 ppm concentration, over 3 days, is presented in Figure 8.27 below.

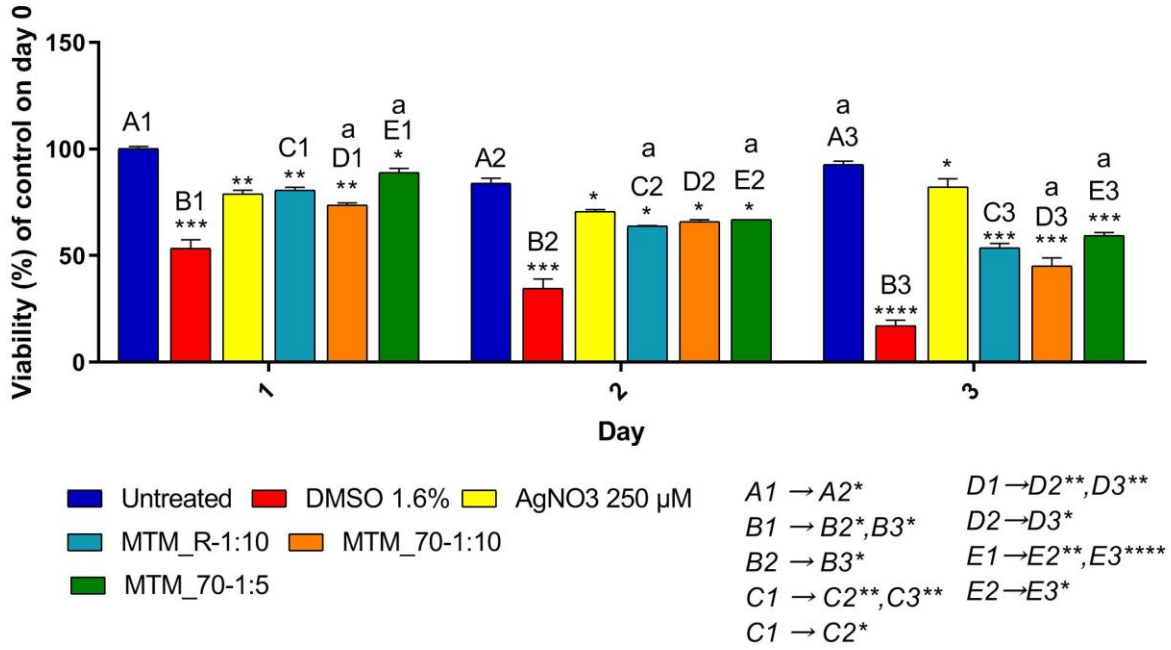

Figure 8.27. *Fibroblast cells viability, as percentage of Untreated (negative control) ± SD (3 replicates measured), after exposure to a)MTM_R-1:10, b)MTM_70-1:10 and c) MTM_70-1:5 samples of AgNPs dispersions, at 3.9 ppm concentration, over a 3 day period. $AgNO_3$ 250 μM and DMSO 1.6 % were used as positive controls. Statistical significance with the Untreated is annotated by black stars (*) and the level of significance is given as follows: * p<0.05, **p<0.01, *** p <0.001 and ****p<0.0001. Significant differences over time are annotated by capital letters and significance is given below the graph in the legend. Letter (a) signifies that SD was taken from only 2 replicates. Data were analyzed by Two-way Anova and Tukey's post-hoc multi-comparison test. Cell viability is measured by MTT assay.*

From figure 8.27, it seems that both time and treatment had a significant effect on % viability ($p<0.0001$). A time-dependent reduction in % viability can be observed in all cases, except cells challenge with $AgNO_3$ solution. Furthermore, all AgNPs samples presented a significant reduction of cells viability, compared to the Untreated, during the whole time of exposure. Hence, all AgNPs samples are cytotoxic at 3.9 ppm concentration.

Challenge with $AgNO_3$ solution on the 1st day of exposure, presented significantly lower cells viability than MTM_70-1:5 ($p<0.05$) but significantly higher cells viability than MTM_70-1:10 and on the last 2 days, it presented significantly higher cells viability than all AgNPs samples ($p<0.05$ on the 2nd day and $p<0.001$ on the 3rd day).

All AgNPs samples on the 3rd day (except plasma)

Cells viability of human fibroblasts after exposure to AgNPs synthesized by all the above methods (except plasma), at a range of concentrations, on the 3rd day of exposure, is presented in Figure 8.28.

From this figure (8.28), it seems that both AgNPs concentration and method of treatment had a significant effect on % viability ($p<0.0001$). More specifically, there is a clear concentration-dependent reduction of % cells viability in all cases (Untreated, DMSO and $AgNO_3$ remained constant since they change only according to time, as controls). At all concentrations, all AgNPs samples seem to have significantly lower % viability compared to the Untreated (significance is presented on the graph), except MTM_70-1:5 at 0.49 ppm concentration. MTM_70-1:10 at 0.49 ppm concentration not only did not present a reduction of cells viability but it actually presented a significant increase compared to the Untreated ($p<0.0001$). This increase, as mentioned before, could either be explained from the natural variations of cellular metabolism or from small pipetting errors leading to slightly more cells seeded in that well. In conclusion, on the 3rd day, all samples are cytotoxic, except for 0.49 ppm of MTM_70-1:10 and MTM_70-1:5.

Challenge with $AgNO_3$ solution showed a significantly lower cells viability than 0.49 ppm concentration of MTM_70-1:10 ($p<0.0001$) and a significantly higher cells viability than 0.98 ppm of MTM_R-1:10 ($p<0.0001$). Compared to all the other concentrations of all AgNPs samples, it presented significantly higher % viability ($p<0.0001$).

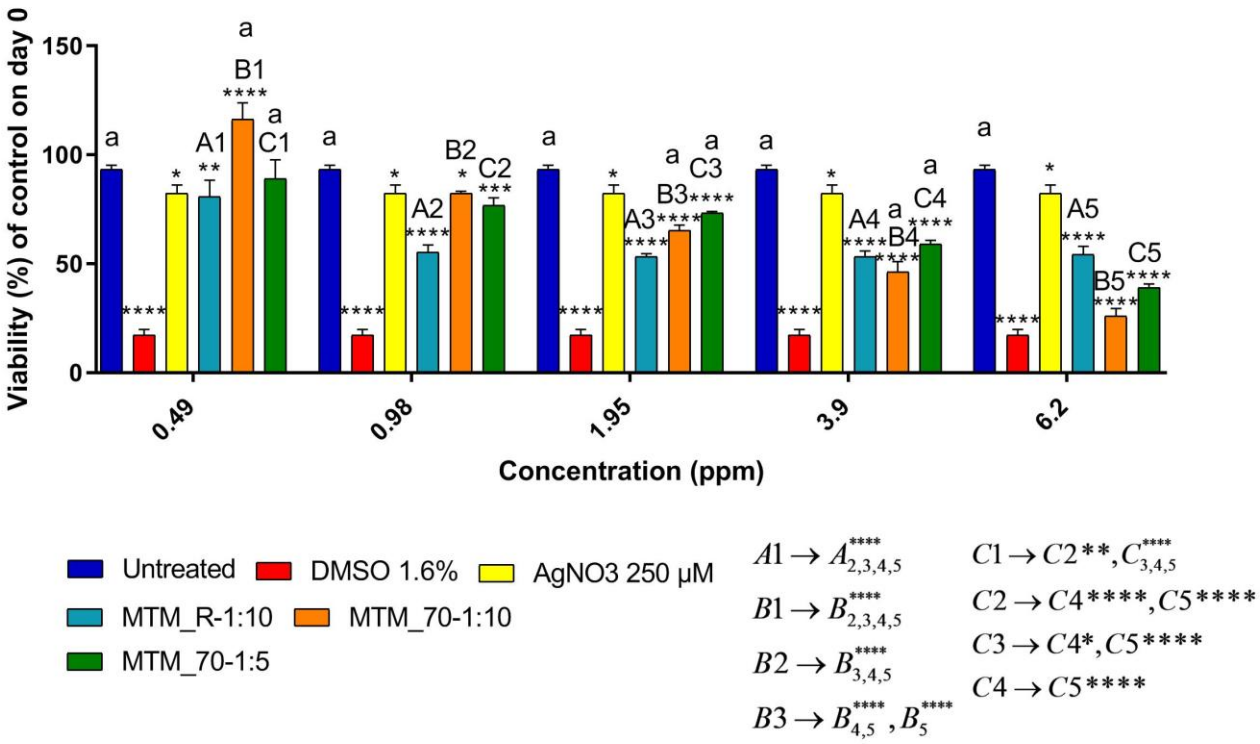

Figure 8.28. *Fibroblast cells viability, as percentage of Untreated (negative control) ± SD (3 replicates measured), after exposure to a)MTM_R-1:10, b)MTM_70-1:10 and c) MTM_70-1:5 samples of AgNPs dispersions, at a range of concentrations, on the 3rd day of exposure. $AgNO_3$ 250 μM and DMSO 1.6 % were used as positive controls. Statistical significance with the Untreated is annotated by black stars (*) and the level of significance is given as follows: * p<0.05, **p<0.01, *** p <0.001 and ****p<0.0001. Significant differences over concentration are annotated by capital letters and significance is given below the graph in the legend. Letter (a) signifies that SD was taken from only 2 replicates. Data were analyzed by Two-way Anova and Tukey's post-hoc multi-comparison test. Cell viability is measured by MTT assay.*

IC_{50} values

To compare all AgNPs dispersions better, the IC_{50}[7] values for all AgNPs samples according to their % viability at all time exposures (1st, 2nd and 3rd day), were also calculated and they are presented at the table below (Table 8.5).

Table 8.5. IC_{50} values of a) MTM_R-1:10, b) MTM_70-1:10 and c) MTM_70-1:5 of Fibroblast viability, after 24, 48 and 72 h exposure. A linear curve was used as a dose-response curve to fit the data.

Number	Method	IC_{50} values		
		24 h	**48 h**	**72 h**
1	MTM_R-1:10	-	-	-
2	MTM_70-1:10	8.96	8.11	4.40
3	MTM_70-1:5	13.54	9.09	5.66

The linear regression used, was not a good model for all samples at all time exposures, especially for MTM_R-1:10. At this AgNPs sample, it seems that there is a linear reduction of cells viability according to concentration only at the lowest concentrations used (0.49-1.95 ppm). At the highest concentrations used, cells viability remained stable and the behavior of the sample at even higher concentrations cannot be predicted. Therefore, the range of concentrations tested, was not wide enough to obtain an exact dose-response model. From Figure 8.23 though, it is clear that a higher concentration than 6.2 ppm is needed for a 50% drop of viability for MTM_R-1:10, at all exposure times. From the other 2 samples, the smallest IC_{50} value appeared from MTM_70-1:10, at all exposure times. It seems that IC_{50} values decreased as the time of exposure increased. These values come in agreement with figures 8.24-8.25, since it is clear that a higher concentration than 6.2 ppm is needed for a 50% drop of viability for MTM_70-1:10 and MTM_70-1:5 on the first 2 days, whereas a concentration between 3.9 and 6.2 ppm is needed on the 3rd day for a half maximal inhibition, for both samples. It is also clear that all IC_{50} values are lower than 100 ppm. Even IC_{50} value of MTM_R-1:10 is expected to be in the range of 6.2-100 ppm.

[7] Half maximal Inhibitory Concentration

9. Discussion

After the discovery that size influences the physicochemical properties and that, therefore, nanoparticles differ from the bulk material and demonstrate unique properties, nanoparticles started being used in a variety of applications, such as, but not limited to, bioimaging, drug delivery and food packaging (*see* Figure 2.1, Chapter 2) (Zaman, Ahmad, Qadee, Rabbani, & Khan, 2014) . Their properties change in accordance to size and shape variations, since their morphology change. This is why narrow size distribution and uniform shape of the particles are required for their applications and it is one of the most difficult tasks of nanoparticles production, along with high yield, low energy consumption and low environmental and cyto-toxicity. The capping agent used, as well as the ratio between capping agent and % nanoparticles concentration, play also a vital role in nanoparticles' final properties (Inmaculada López-Lorente & Valcárcel, 2014), (Khan, Saeed, & Khan, 2017).

Metal nanoparticles, have been used in many applications due to their large surface-area-to-volume ratio. This property makes them highly reactive and therefore more favorable to be used in many applications (*see* Figure 3.1, Chapter 3) (Christian, Von der Kammer, Baalousha, & Hofmann, 2008). Silver nanoparticles in particular, are extensively studied and used, mostly due to their proven antimicrobial efficacy against both Gram-positive and Gram-negative bacteria, viruses and other eukaryotic micro-organisms (Rai, Yadav, & Gade, 2009) (for applications and consumer products *see* Figures 4.1, 4.2, Chapter 4).

The exact mechanism of their antimicrobial action has not yet been completely understood. There are many contradictive studies, reporting that it is due to either silver-ions release from their oxidized surface (Bondarenko, Ivask, Käkinen, Kurvet, & Kahru, 2013) or mechanical disruption of bacteria cell wall by AgNPs itself (Mosselhy, et al., 2015) or a combination of both. Many studies have also reported that Ag^+ (by the form of $AgNO_3$), has higher toxicity than AgNPs (Mosselhy, et al., 2015), (Seong & Lee, 2017), (Mallevre, et al., 2016). Nevertheless, DNA damage, formation of ROS and intracellular increase of Ca^+ levels have been observed (Radzig, et al., 2013), (Lee, Kim, & Lee, 2014), (Seong & Lee, 2017).

As far as silver nanoparticles antimicrobial effect on *Salmonella enterica* is concerned, depolarization of the inner membrane without disruption of the outer membrane (only penetration) and eventually cell death, were observed in small concentration. At exposure in high concentrations, membrane disruption was also observed (Seong & Lee, 2017). Also, some

serotypes of *Salmonella enterica* seem to be more sensitive comparing to AgNPs effect on them, with S. Enteritidis to be one of them (Berton, et al., 2014). From previous studies, MICs of AgNPs on *Salmonella enterica* have been found in a range of 3.12-16 ppm for various serotypes (*see* Table 4.4, Chapter 4).

From the methods of synthesis used till now (physicochemical and biological), biological methods are preferable, mostly due to the restriction of use of hazardous and toxic solvents that sometimes lead to toxic byproducts (Zhang, Liu, Shen, & Gurunathan , 2016). Nevertheless, with careful selection of chemicals (reducing/stabilizing/capping agents), chemical reduction can be "greener". This careful selection involves eco-friendly chemicals that work for both charge repulsion and steric stabilization of NPs, to keep them in a standard shape and size and prevent agglomeration (*see* Figure 5.2). Many chemicals have been used in the past, resulting in the production of a variety of AgNPs sizes (*see* Table 5.2, Chapter 5).

In this study, Modified Turkevich Methods were used for AgNPs chemical synthesis. Turkevich Method initially involved the reduction of a metal solution by a citrate at boiling temperature, a procedure that is followed by color change of the solution depending on the morphology of the obtained particles (Pacioni, Borsarelli, Rey, & Veglia, 2015), (Piñero, Camero, & Blanco, 2017), (Mazzonello, Valdramidis, Farrugia, Grima, & Gatt, 2017). Previous studies had also tried to alter this method for AgNPs synthesis by the addition of Glycerol, which appeared to have a good stabilizing activity (Pacioni, Borsarelli, Rey, & Veglia, 2015), the addition of NaOH, which seemed to facilitate the reduction of $AgNO_3$ by changing the pH (when higher it deprotonates citrate, enabling its capping ability), and by changing the temperature (Caswell, Bender, & Murphy, 2003). At room temperature, more uniformly stabilized particles were found. The reaction rate when trisodium citrate was used as a capping agent, was also found to have an Arrhenius-like exponential relation to the temperature but with bigger nanoparticles' size synthesis at higher temperatures and bigger size distributions (Mazzonello, Valdramidis, Farrugia, Grima, & Gatt, 2017). The modifications of Turkevich Method in this study were: the use of only Glycerol (without water) as stabilizing and reduction agent, synthesized at room temperature with the addition of NaOH (MTM_R-1:10) and at 70°C (lower than boiling temperature) by changing the ratio of the capping agent with % nanoparticles concentration (MTM_70-1:10 and MTM_70-1:5) (*see* Chapter 7, Experimental procedure). In all cases, $AgNO_3$ was used as metal precursor and Trisodium Citrate as capping agent.

Synthesis of AgNPs by Reduction via plasma generation was also achieved in this study with the creation of an electrochemical cell through surface plasma-glycerol interaction under argon atmosphere at room temperature (*see* Chapter 7). $AgNO_3$ was used again as metal precursor and Trisodium Citrate as capping agent. Previous studies also achieved AgNPs production using different configurations (see Table 5.3, Chapter 5) with small nanoparticles' sizes (less than 10 nm in most cases) and mostly spherical. The main mechanism of plasma reduction is the solvated electrons but other reactive species may also play role in the whole procedure (ions, radicals, VUV photons) by producing H and OH atoms (Kondeti, Gangal, Yatom, & Bruggeman, 2017). This method is generally considered as green since no harmful byproducts are generated. Nevertheless, there are limitations to it concerning its expense and safety (Kondeti, Gangal, Yatom, & Bruggeman, 2017), (Misra, Schluter, & Cullen, 2016).

The obtained nanoparticles of this study were characterized via UV-Vis, ICP-Ms and TEM analysis. From UV-Vis analysis, the absorbance peaks appeared in all cases at the range of 350-600 nm confirming the AgNPs synthesis. According to the secondary band area, above 600 nm, where curve arising is a sign of nonspherical nanoparticles synthesis, MTM_R-1:10 and MTM_70-1:10 were expected to be spherical and MTM_70-1:5 and plasma samples were expected to be nonspherical. Furthermore, according to the absorbance strength, at samples where the same dilution was used, MTM_70-1:5 were expected to have almost double the concentration of MTM_70-1:10 AgNPs suspension. The smallest sizes were expected in the case of MTM_R-1:10 (blue shift) whereas the biggest ones were expected from MTM_70-1:5 sample (red shift). Finally, the stability of all samples was satisfying after being tested on 4 different dates in a one month time range, after protecting them with aluminum foil from light exposure (it was also tested with UV-Vis that strongly affects AgNPs stability). From ICP-Ms analysis, the concentrations found for MTM_R-1:10, MTM_70-1:10, MTM_70-1:5 and plasma samples were 6.2, 3.9, 8.2 and 3.9 ppm accordingly (after a 10-fold dilution of all samples except plasma), thus confirming the UV-Vis analysis results for MTM_70-1:5 and MTM_70-1:10 (double the concentration of the former). From TEM analysis, MTM_R-1:10 was found to consist of a mixture of shapes, but mostly spherical (in agreement with UV-vis), with a size distribution in the range of 18-57 nm. MTM_70-1:10 were found spherical (in agreement with UV-Vis) with a size range of 7-15 nm. MTM_70-1:5 were found to consist of a mixture of shapes, mostly pyramidal, with a large size distribution in the range of 6-84 nm. Finally, for plasma, no results could be obtained.

To investigate the obtained AgNPs antimicrobial properties in this study, the effect of a range of concentrations on *Salmonella enterica* was tested with exposure time of 0 (only the control sample with the inoculum), 2, 4 and 6 hours. The results (log(CFU/mL)-time) revealed that at 3.9 ppm, the plasma sample had the strongest antimicrobial action followed by MTM_70-1:10. The other 2 samples (MTM_R-1:10 and MTM_70-1:5) achieved a satisfying inhibition of *Salmonella enterica* after a 26 h exposure. At 6.2 ppm, the strongest action appeared from MTM_70-1:10 followed by MTM_R-1:10 sample (plasma was not tested at this concentration). The statistical analysis of the results, showed that the inhibition of *Salmonella enterica* was time, method and concentration-dependent (*see* Chapter 8). These concentrations that inhibited the microorganism growth in all samples (bigger inhibition by plasma and MTM_70-1:10) is in agreement with the aforementioned studies that found inhibition of *Salmonella enterica* by AgNPs in a concentration range of 3.12-16 ppm (e.g., (Omara, Zawrah, & Samy, 2017), (Mallevre, et al., 2016), *see* Table 4.4, Chapter 4, for more). Evidently, the spherical nanoparticles had a greater antimicrobial activity. One could expect that since edge-like and corner-like regions of nanoparticles have high-electron confinement and therefore are more chemical reactive, the nonspherical ones should have a greater effect on the microorganism (Sau, Rogach, Jäckel, Klar, & Feldmann, 2010), (Fedlheim & Foss, 2001), as Rai, Yadav, & Gade, 2009 also suggested. Plasma sample was also tested for its antimicrobial action on *Salmonella enterica* at 0.39 ppm concentration and a very high inhibition was observed even at this very low concentration. This leads to the hypothesis that there might be radical species in the sample which may also be of high toxicity when exposed at human cells.

However, AgNPs satisfying antimicrobial activity is not sufficient if their cytotoxicity is not tested. There is a rising concern regarding nanoparticles' toxicity worldwide, despite their use in many current applications. This concern is due to their small size as they can have access to highly protected organs such as the brain and the testes, after entering the human body, and their removal from tissues seems to be a very difficult task (Pietroiusti, Magrini, & Campagnolo, 2014) . Cell culture has helped in in-vitro analysis of AgNPs but a complete comparative analysis does not exist due to the many parameters that change in each case (culture conditions and methods of synthesis of AgNPs) (Vazquez-Muñoz, et al., 2017). It is proven though, that AgNPs reduce cell viability. Their mechanism of cytotoxicity is found to be cell apoptosis and necrosis (Ka-Ming Chan, Moriwaki, & De Rosa, 2014), mitochondrial dysfunction via interruption of their membrane permeability (Galandáková, et al., 2016), ROS generation and DNA damage (Zhang, Wang, Chen, & Chen, 2014) (*see* also Figure 6.1,

Chapter 6). The "corona" formation of AgNPs with biological molecules is also considered an important factor of their cytotoxicity (Pietroiusti, Magrini, & Campagnolo, 2014). Defense mechanisms of cells though tend to eliminate their impact (formation of silver sulfide (Ag_2S) and silver chloride ($AgCl_X$)) (Marchioni, Jouneau, Chevallet, Michaud-Soret, & Deniaud, 2018) . Of course, AgNPs cytotoxicity is concentration- and size-dependent with the smaller particles having been found more toxic in the past. The capping agent also plays an important role with citrate-coated AgNPs having been found less cytotoxic (Akter, et al., 2018). Many AgNPs (sizes 7-100 nm, concentrations 0.025-400 ppm) have been tested on various types of cell lines from previous studies (*see* Table 6.1, Chapter 6). Since it has been found in the past that Ag compounds may cause Argyria after high exposure levels, or cease the healing process of fibroblast and epithelial cells, and since AgNPs are used for epidermal applications in open wounds and burns (Galandáková, et al., 2016), (Marchioni, Jouneau, Chevallet, Michaud-Soret, & Deniaud, 2018), their toxicity on Normal Human Dermal Fibroblast cells is vital. AgNPs with size range of 1-200 nm have been tested in the past on Fibroblast cells. IC_{50} values for 6.03 nm AgNPs (mostly spherical), after a 24 and 48 h exposure, were found 30.64 and 14.98 ppm respectively, from a study by Paknejadi, Bayat, Salimi, & Razavi, 2018. From a study by Galandáková, et al., 2016, non-toxic concentrations for AgNPs with a mixture of sizes and a mean size of 10 nm, were found at a range of 0.25-25 ppm and 5 nm AgNPs were found more toxic than $AgNO_3$ whereas 20 and 50 nm were found to be less toxic than $AgNO_3$. Wildt, et al., 2016, also found that smaller nanoparticles were more toxic on mouse fibroblast cells due to silver-ions release. Avalos, Haza, Mateo, & Morales, 2014, revealed that 4.7 nm AgNPs (approximately spherical) at concentrations 6.72 and 13.45 ppm had high decrease in NHDF viability.

In this study, the effect of AgNPs on Normal Human Dermal Fibroblasts (NHDF) was tested after a 24, 48 and 72 h exposure, at a range of concentrations. The results were interpreted as viability (%) of control (Untreated) on day 0. Generally, both time and method of treatment had a significant effect on % viability ($p<0.0001$). Comparing to % viability of untreated, MTM_R-1:10 showed significant reduction of viability overall, at all concentrations, except at 0.49 ppm concentration that showed no toxicity effect on the 1st day (*see* Figure 8.23, Chapter 8, for significance). No more than 35% reduction of viability though, compared to the Untreated, was occurred at all concentrations, up to the 3rd day of exposure. Therefore, cells viability was not strongly concentration-dependent. MTM_70-1:10, also reduced cells viability at all concentrations used and in a time dependent manner, except for concentrations 0.49 and

0.98 ppm where no reduction of cells viability over time was observed. Cells viability in this case, seems to be strongly concentration-dependent and the reduction of viability reaches 62%, compared to the Untreated, at the last day of exposure and at the highest concentration (6.2 ppm) (*see* Figure 8.24, Chapter 8). 0.49 ppm concentration of MTM_70-1:10 showed toxic effects only on the 1st day but due to possible experimental errors related to the Untreated of the 2nd day and the great increase of viability on the 3rd day, this concentration should be repeated fro confirmation. MTM_70-1:5 at 0.49 ppm concentration, showed non toxic effect on Fibroblasts at all exposure times, whereas at 0.98 ppm was found toxic only on the 3rd day. Cells viability in this case is also concentration-dependent and the highest reduction achieved on the last day of exposure was up to 49% at the highest concentration (6.2 ppm). All concentrations used, also significantly reduced viability over time (*see* Figure 8.25, Chapter 8, for significance), except 0.49 ppm that no effect on % viability over time was observed. Plasma sample of AgNPs at 0.39 ppm concentration was found non-toxic only on the 3rd day, whereas on the other 2 days was found toxic with low significance ($p<0.05$) and a significant reduction of % viability over time can also be observed (*see* Figure 8.25, Chapter 8, for significance). When comparing all 3.9 ppm concentrations of all AgNPs samples, all of them presented toxicity effect during the whole time of exposure. When comparing all AgNPs samples only on the 3rd day, they also significantly reduced cells vibility at all concentrations, except MTM_70-1:10 at 0.49 ppm concnetration that in fact presented a significantly higher % viability than the Untreated ($p<0.001$). However, this concentration of MTM_70-1:10 sample should be repeated, due to possible experimental errors. As far as the control samples are concerned, DMSO appeared to have effectively killed half the populaton of cells throughout the study and AgNO3 showed significantly lower viability than the Untreated during the whole time exposure, and its reduction remained constant over time. Its significant difference with the AgNPs samples depends on both time and concentration at all cases (*see* Chapter 8.4). However, it could be noted, that on the 1st day of exposure, all AgNPs samples (except plasma), showed no significant difference with $AgNO_3$, as fas as cells viability is concerned, except at the lowest concentrations where AgNPs were less cytotoxic. After the 2nd day of exposure, AgNPs at the highest concentrations used (3.9 and 6.2 ppm), presented a more toxic behaviour than $AgNO_3$. Therefore, it could be assumed that the cytotoxicity action of AgNPs during the first 24 hours of exposure, is mostly connected to silver ions release, whereas in a longterm exposure (up to 72 h), 3.9 and 6.2 ppm AgNPs appear to be more toxic than $AgNO_3$.

IC_{50} values were found in the range of 4.40-13.54 ppm, after the 24-72 h exposure, for MTM_70-1:10 and MTM_70-1:5 AgNPs samples, with MTM_70-1:10 having the lowest value (*see* Table 8.5, Chapter 8). The IC_{50} value of MTM_R-1:10 could not be calculated since the range of concentrations tested on NHDF was not wide enough for a good dose-response model. It is estimated though to be in the range of 6.2-100 ppm. Despite the many efforts for a standardized method for nanoparticles toxicity assessment, there is not still a complete study on the matter, due to the change of many parameters. The basic thing changing is the in vivo to in vitro calculation of the results that change the toxicological data of nanoparticles. According to their dispersion, their behavior changes (agglomeration and aggregation and protein bio-corona at physiological fluids) (*see* Chapter 6) and the higher and upper limits of NPs exposure change. There is therefore, a need for estimation of realistic human exposure to NMs via the dermal, oral or respiratory route (Drasler, Sayre, Steinhäuser, Petri-Fink, & Rothen-Rutishauser, 2017). The lower limit, according to the UN Globally Harmonized System of Classification and Labelling of Chemicals, for oral route of exposure, can be taken at 100 ppm (Lee, et al., 2017). At the study by Farcal, et al., 2015, IC_{50} values below 100 ppm were also considered as the most toxic ones, especially IC_{50} values below 30 ppm. Therefore, nanoparticles produced in this study can be characterized as cytotoxic.

In conclusion, plasma AgNPs samples were found to have the highest antimicrobial efficacy at 3.9 and 0.39 ppm. Nevertheless, despite the very low concentration, this concentration was found cytotoxic at the first 2 days of exposure on NHDF cells. This result strengthens the previously made hypothesis that there might be radical species in the sample that harm *Salmonella enterica* but also human cells. Furthermore, their production was of very low yield and still nothing is known about their morphology and their cytotoxicity at higher concentrations. Therefore, the matter demands further studies. MTM_70-1:10 AgNPs sample, with spherical nanoparticles of sizes 7-15 nm, was also found very antimicrobial against *Salmonella enterica* but also presented the lowest IC_{50} value. MTM_70-1:5 (6-84 nm) was non-cytotoxic only at 0.49 ppm concentration. At 1.95 ppm concentration showed cytotoxic effects only on the last day of exposure. Comparing all AgNPs samples (except plasma) with $AgNO_3$, their cytotoxicity way of action on the 1st day of exposure seems to be similar, at the highest concentrations of AgNPs (3.9 and 6.2 ppm), whereas on the 3rd day, AgNPs at the same concentrations appear to be more cytotoxic than $AgNO_3$. This comes in contradistinction with a previously mentioned study by Galandáková, et al., 2016, since after 24 h, even the bigger AgNPs (MTM_70-1:5) at 6.2 ppm concentration were found more cytotoxic than $AgNO_3$.

Also, the same study mentioned non-toxic concentrations in the range of 0.25-25 ppm after a 24h exposure, which seems to be the case for only MTM_R-1:10 and MTM_70-1:5 samples of AgNPs (size range in accordance with the one mentioned in the study). IC_{50} values obtained in all nanoparticles cases of this study are in the same range with those mentioned from the study by Paknejadi, Bayat, Salimi, & Razavi, 2018 (< 30 ppm). Since IC_{50} values were below 100 ppm it is likely to be toxic when accessing the human body (e.g., via oral or dermal route of exposure). The smallest value in particular, derived from the smaller and spherical nanoparticles, something that also confirms previous studies that the smaller the nanoparticles, the more sensitive the human cells to nanoparticles' exposure (Souza, Franchi, Rosa, da Veiga, & Takahashi, 2016), (Zapór, 2016) and it comes with agreement with Avalos, Haza, Mateo, & Morales, 2014, that stated that concentration near 6.2 ppm of spherical nanoparticles showed high toxicity. Of cource, MTM_R-1:10 and MTM_70-1:5 had the widest range of sizes and therefore more replicates are required for these AgNPs samples to account for the variation in NPs sizes, as well as a wider range of concentrations to be tested on NHDF, for a better dose-response model in all cases.

It is also important to be noted, that AgNPs can interact with MTT and skew the results. Additionally, the MTT assay tests the ability of the cells to convert MTT to formazan by NADP(H) reductions through mitochondrial enzymes. Mitochondrial stress due to NP exposure can cause lower reading in the MTT assay even when live cells are present (Kaplan, Ciftci, & Kutlu, 2016). Another possible AgNPs interaction that may interfere with the results, is nanoparticles interaction with antibiotics (reported by many studies, e.g., (Katva, Das, Moti, Jyoti, & Kaushik, 2017), (Deng, et al., 2016), (Jamaran & Rahimian Zarif, 2016)), since the media used was complete. Therefore, more studies with different methods of reading of cell viability and the use of a not complete media will be needed.

10. Conclusions

In this study, silver nanoparticles were synthesized by the use of different bottom-up methods. These methods include various modified versions of the Turkevich method and reduction via plasma generation (3.9 ppm, no morphological characteristics were obtained). The modifications of the Turkevich method used were: the use of only Glycerol (without water) as stabilizing and reducing agent, at room temperature with NaOH (62 ppm, mixture of shapes, but mostly spherical, in a range of 18-57 nm) and at 70°C by changing the ratio of the capping agent and % nanoparticles concentration to 1:10 (39 ppm, spherical at a range of 7-15 nm) and 1:5 (82 ppm, mixture of shapes, mostly pyramidal at a range of 6-84 nm).

When these AgNPs dispersions were tested on *Salmonella enterica*, they were found to have a very satisfying antimicrobial action at both concentrations tested (3.9 and 6.2 ppm). The most antimicrobial of all was the AgNPs sample obtained by plasma reduction that inhibited Salmonella growth even at 0.39 ppm, followed by the AgNPs sample synthesized by Modified Turkevich Method at 70°C with molar ratio 1:10 of silver nitrate to trisodium citrate. Nevertheless, AgNPs sample obtained by plasma reduction, were found to be cytotoxic on the first 2 days of exposure, when AgNPs were tested on Normal Human Dermal Fibroblasts, even at this very low concentration, and AgNPs synthesized by Modified Turkevich Method at 70°C with molar ratio 1:10 showed the lowest IC_{50} value, at all days of exposure (4.40-8.96 ppm). When 0.49 ppm concentration was tested from the latter sample though, they showed very low cytotoxicity (only on the first day). AgNPs synthesized by Modified Turkevich Method at 70°C with molar ratio 1:5, showed low cytotoxicity action only at low concentrations also (0.49 ppm and 0.98 ppm), and its IC_{50} values were also very low (5.66-13.54 ppm). The IC_{50} values of AgNPs synthesized at room temperature with molar ratio 1:10 of silver nitrate to trisodium citrate, could not be calculated, but they are also estimated to be in the range of 6.2-100 ppm. Last but not least, AgNPs seem to be equally toxic and perhaps follow the same cytotoxicity action with $AgNO_3$ on the 1st day of exposure and at high concentrations (3.9 and 6.2 ppm), whereas after 24 h exposure, AgNPs of the same concentration appear to be more toxic than $AgNO_3$. The IC_{50} values, after 24, 48 and 72 h exposure, revealed that the smallest nanoparticles had the biggest cytotoxic effect.

From the above results, it seems that despite their antimicrobial efficacy, the silver nanoparticles synthesized were found to be cytotoxic. For that reason, their use in applications that allow their access to human body may lead to a high risk at human health. However, the

cytotoxicity results of this study were obtained by using only the MTT assay. A confirmation of these experimental data with a different method of reading of cell viability is needed. Also, the range of concentrations tested on NHDF cells was not sufficient to obtain the best fitted curve, and therefore the best model for cells viability's reduction according to concentration, in all cases. Furthermore, the suspension of AgNPs plays an important role in their cytotoxicity. AgNPs were initially suspended in water that has its own impact on cells and the culture media used was supplemented with FBS and antibiotics. Therefore, the behavior of AgNPs, their agglomeration, "corona" formation and their synergistic effect with antibiotics, change. The in vitro to in vivo studies also differ for the same reason. Being so, a thorough study of all the above factors that may alter the cytotoxic results obtained from this study, is needed before excluding their possible future use in applications.

Lower concentrations than 3.9 ppm of AgNPs could also be tested on *Salmonella enterica* in the future, to examine their antimicrobial action at concentrations that showed very low or no cytotoxicity effects (e.g., 0.49 and 0.98 ppm, for the rest of the samples except plasma). Furthermore, more studies to obtain the morphological characteristics of AgNPs synthesized by plasma reduction are needed, in order to obtain more information about their antimicrobial and cytotoxicity way of action. When changing the parameters of their production, perhaps it could lead to a very good antimicrobial agent that has low cytotoxicity effects.

11. References

Akter, M., Tajuddin Sikder, M., Mostafizur Rahman, M., Atique Ullah, A., Binte Hossain, K. F., Banik, S., . . . Kurasaki, M. (2018). A systematic review on silver nanoparticles-induced cytotoxicity:Physicochemical properties and perspectives. *Journal of Advanced Research*, 1-16.

Ammari, H., Deng, Y., & Millien, P. (2016). Surface Plasmon Resonance of Nanoparticles and Applications in Imaging. *Archive for Rational Mechanics and Analysis, 220*(1), 109-153.

Andrews, J. (2001). Determination of minimum inhibitory concentrations. *Journal of Antimicrobial Chemotherapy*, 5-16.

Avalos, A., Haza, A. I., Mateo, D., & Morales, P. (2014). Interactions of manufactured silver nanoparticles of different sizes with normal human dermal fibroblasts. *International Wound Journal*, 101-109.

Babaahmadi, V., Montazer, M., Toliyat, T., & Ghanbarafjeh, M. (2011). Photochemical reduction of silver nitrate to nano silver using Stannous Chloride, CTAB and Daylight irradiation. *Nanomaterials: Applications and Properties, 1*, 183-190.

Banach, M., & Pulit-Prociak, J. (2016). Proecological method for the preparation of metal nanoparticles. *Journal of Cleaner Production, 141*, pp. 1030-1039.

Berton, V., Montesi, F., Losasso, C., Rino Facco, D., Toffan, A., & Terregino, C. (2014). Study of the Interaction between Silver Nanoparticles and Salmonella as Revealed by Transmission Electron Microscopy. *Journal of Probiotics & Health, 3*, 123.

Beyenea, H., Werknehb, A., Bezabha, H., & Ambaye, T. (2017). Synthesis paradigm and applications of silver nanoparticles (AgNPs), a review. *Sustainable Materials and Technologies, 13*, 18-23.

Bondarenko, O., Ivask, A., Käkinen, A., Kurvet, I., & Kahru, A. (2013). Particle-Cell Contact Enhances Antibacterial Activity of Silver Nanoparticles. *PLOS ONE, 8*(5), e64060, 1-12.

Caswell, K., Bender, C., & Murphy, C. (2003). Seedless, Surfactantless Wet Chemical Synthesis of Silver Nanowires. *Nano Letters, 3*(5), 667-669.

Chand Dakal, T., Kumar, A., Majumdar, R. S., & Yadav, V. (2016). Mechanistic Basis of Antimicrobial Actions of Silver Nanoparticles. *Frontiers in Microbiology, 7*, 1831, 1-17.

Cheng, H.-W., Skeete, Z., Crew, E., Shan, S., Luo, J., & Zhong, C.-J. (2014). Synthesis of Gold Nanoparticles. In M. Valcárcel, & Á. López-Lorente, *Gold Nanoparticles in Analytical Chemistry*, Elsevier, 37-79.

Christian, P., Von der Kammer, F., Baalousha, M., & Hofmann, T. (2008). Nanoparticles: structure, properties, preparation and behaviour in environmental media. *Ecotoxicology, 17*, 326-343.

Connolly, M., Fernandez-Cruz, M.-L., Quesada-Garcia, A., Alte, L., Segner, H., & Navas, J. M. (2015). Comparative Cytotoxicity Study of Silver Nanoparticles (AgNPs) in a Variety of Rainbow Trout Cell Lines (RTL-W1, RTH-149, RTG-2) and Primary Hepatocytes. *International Journal of Environmental Research and Public Health*, 5386–5405.

Deepak, V., Kalishwaralal, K., Pandian, S., & Gurunathan, S. (2011). An Insight into the Bacterial Biogenesis of Silver Nanoparticles, Industrial Production and Scale-up. In *Metal Nanoparticles in Microbiology*. Springer-Verlag Berlin Heidelberg, 28-46.

Deng, H., McShan, D., Zhang, Y., Sinha, S. S., Arslan, Z., Ray, P. C., & Yu, H. (2016). Mechanistic Study of the Synergistic Antibacterial Activity of Combined Silver Nanoparticles and Common Antibiotics. *Environ Sci Technol., 50*, 8840–8848.

Desai, R., Mankad, V., Gupta, S., & Jha, P. (2012). Size Distribution of Silver Nanoparticles: UV-Visible Spectroscopic Assessment. *Nanoscience and Nanotechnology Letters, 4*, 30-34.

Drasler, B., Sayre, P., Steinhäuser, K. G., Petri-Fink, A., & Rothen-Rutishauser, B. (2017). In vitro approaches to assess the hazard of nanomaterials. *NanoImpact*, 99-116.

Ebrahiminezhad, A., Taghizadeh, S.-M., Taghizadeh, S., & Ghasemi, Y. (2017). Chemical and Biological Approaches for the Synthesis of Silver Nanoparticles; A mini Review. *Trends in Pharmaceutical Sciences (TiPS), 3*(2), 55-62.

Enemaduku Abalaka, M., Benjamin Akpor, O., & Osemwegie, O. (2017). Green synthesis and antibacterial activities of silver nanoparticles against Escherichia coli, Salmonella typhi, Pseudomonas aeruginosa and Staphylococcus aureus. *Advancements in Life Sciences (als), 4*, 60-65.

Erjaee, H., Rajaian, H., & Nazif, S. (2017). Synthesis and characterization of novel silver nanoparticles using Chamaemelum nobile extract for antibacterial application. *Advances in Natural Sciences: Nanoscience and Nanotechnology*, 8, 025004, 1-9.

Faedmaleki, F., Shirazi, F. H., Salarian, A.-A., Ahmadi Ashtiani, H., & Rastegar, H. (2014). Toxicity Effect of Silver Nanoparticles on Mice Liver Primary Cell Culture and HepG2 Cell line. *Iranian Journal of Pharmaceutical Research*, 235-242.

Farcal, L., Torres Andón, F., Di Cristo, L., Rotoli, B. M., Bussolati, O., Bergamaschi, E., . . . Fadeel, B. (2015). Comprehensive In Vitro Toxicity Testing of a Panel of Representative Oxide Nanomaterials: First Steps towards an Intelligent Testing Strategy. *PLoS One, 10*(5), e0127174, 1-34.

Fedlheim, D., & Foss, C. (2001). Overview. In D. L. Fedlheim, & C. A. Foss, *Metal Nanoparticles: Synthesis, Characterization, and Applications*. CRC press, 1-16.

Fernandes, I. R., Russo, F. B., Pignatari, G. C., Evangelinellis, M. M., Tavolari, S., Muotri, A. R., & Beltrão-Braga, P. C. (2016). Fibroblast sources: Where can we get them? *Cytotechnology, 68*, 223-228.

Franková, J., Pivodová, V., Vágnerová, H., Juráňová, J., & Ulrichová, J. (2016). Effects of silver nanoparticles on primary cell cultures of fibroblasts and keratinocytes in a wound-healing model. *Journal of Applied Biomaterials & Functional Materials, 14*, 137-142.

Galandáková, A., Franková, J., Ambrožová, N., Habartová, K., Pivodová, V., Zálešák, B., . . . Ulrichová, J. (2016). Effects of silver nanoparticles on human dermal fibroblasts and epidermal keratinocytes. *Human and Experimental Toxicology, 35*, 946-957.

García-Barrasa, J., López-de-Luzuriaga, J., & Monge, M. (2011). Silver nanoparticles: synthesis through chemical methods in solution and biomedical applications. *Central European Journal of Chemistry, 9*, 7-19.

Ghosh, B., & Ramamoorthy, D. (2010). Effects of silver nanoparticles on Escherichia Coli and it's applications. *International Journal of Chemical Sciences, 8*, S31-S40.

Greulich, C., Braun, D., Peetsch, A., Diendorf, J., Siebers, B., Epple, M., & Köller, M. (2012). The toxic effect of silver ions and silver nanoparticles towards bacteria and human cells occurs in the same concentration range. *RSC Advances*, 6981-6987.

Grzelczak, M., Vermant, J., Furst, E., & Liz-Marzán, L. (2010). Directed Self-Assembly of Nanoparticles. *ACS Nano, 4*, 3591-3605.

Guzman, M., Dille, J., & Godet, S. (2012). Synthesis and antibacterial activity of silver nanoparticles against gram-positive and gram-negative bacteria. *Nanomedicine: Nanotechnology, Biology and Medicine (Nanomedicine: NBM), 8*, 37-45.

Heinrichs, D. E., Yethon, J. A., & Whitfield, C. (1998). Molecular basis for structural diversity in the core regions of the lipopolysaccharides of Escherichia coli and Salmonella enterica. *Molecular Microbiology, 30*, 221–232.

Huang, X., Zhong, X., Lu, Y., Rider, A., Furman, S., & Ostrikov, K. (2013). Plasmonic Ag nanoparticles via environment-benign atmospheric microplasma electrochemistry. *Nanotechnology, 24 095604, 1-7*.

Hulla, J., Sahu, S., & Hayes, A. (2015). Nanotechnology: History and future. *Human and Experimental Toxicology, 34*, 1318–1321.

Inmaculada López-Lorente, A., & Valcárcel, M. (2014). Analytical Nanoscience and Nanotechnology. In *Gold Nanoparticles in Analytical Chemistry*. Valcárcel M. & Inmaculada López-Lorente A. (Eds.), Elsevier, Chapter 1, 3-35.

Jain, P. K., Seok Lee, K., El-Sayed, I. H., & El-Sayed, M. A. (2006). Calculated Absorption and Scattering Properties of Gold Nanoparticles of Different Size, Shape, and Composition: Applications in Biological Imaging and Biomedicine. *J. Phys. Chem.*, 7238-7248.

Jamaran, S., & Rahimian Zarif, B. (2016). Synergistic Effect of Silver Nanoparticles with Neomycin or Gentamicin Antibiotics on Mastitis-Causing Staphylococcus aureus. *Open Journal of Ecology*, 452-459.

J. Cohen, W. Powderly, & S. Opal (2017). Enterobacteriaceae. In *Infectious Diseases*. Jenkins, C., Rentenaar, R., Landraud, L., & Brisse, S. (Eds). Elsevier, 2, Chapter 180, 1565–1578.

Kamat, P. (2002). Photophysical, Photochemical and Photocatalytic Aspects of Metal Nanoparticles. *The Journal of Physical Chemistry B, 106*(32), 7729-7744.

Ka-Ming Chan, F., Moriwaki, K., & De Rosa, M. J. (2014). Detection of Necrosis by Release of Lactate Dehydrogenase (LDH) Activity. *Methods in molecular Biology*, 65-70.

Kaplan, A., Ciftci, G. A., & Kutlu, H. M. (2016). Cytotoxic, anti-proliferative and apoptotic effects of silver nitrate against H-ras transformed 5RP7. *Cytotechnology*, 1727–1735.

Kaplan, A., Ciftci, G. A., & Kutlu, H. M. (2016). Cytotoxic, anti-proliferative and apoptotic effects of silver nitrate against H-ras transformed 5RP7. *Cytotechnology*, 1727–1735.

Katva, S., Das, S., Moti, H. S., Jyoti, A., & Kaushik, S. (2017). Antibacterial Synergy of Silver Nanoparticles with Gentamicin and Chloramphenicol against Enterococcus faecalis. *Pharmacognosy Magazine*, S828–S833.

Khan, I., Saeed, K., & Khan, I. (2017). Nanoparticles: Properties, applications and toxicities. *Arabian Journal of Chemistry*, In Press.

Khandel, P., & Kumar Shahi, S. (2016). Microbes mediated synthesis of metal nanoparticles: current status and future prospects. *International Journal of Nanomaterials and Biostructures, 6*, 1-24.

Klein, C., Comero, S., Stahlmecke, B., Romazanov, J., Kuhlbusch, T., Van Doren, E., . . . Gawlik, B. (2011). *NM-Series of Representative Manufactured Nanomaterials NM-300 Silver Characterisation, Stability, Homogeneity*. JRC Scientific and Technical Reports, EUR 24693, Available online at http://www.jrc.ec.europa.eu/

Kondeti, V., Gangal, U., Yatom, S., & Bruggeman, P. (2017). Ag+ reduction and silver nanoparticle synthesis at the plasma–liquid interface by an RF driven atmospheric pressure plasma jet: Mechanisms and the effect of surfactant. *Journal of Vacuum Science & Technology A: Vacuum, Surfaces, and Films*, 35, 061302 .

Konwar, R., & Baquee, A. (2013). Nanoparticle: An overview of preparation, characterization and application. (M. P. House, Ed.) *International Research Journal of Pharmacy, 4*(4), 47-57.

Kouz, J., & Varma, R. (2013). Speedy fabrication of diameter-controlled Ag nanowires using glycerol under microwave irradiation conditions. *ChemComm (Chemical Communications), 49*, 692-694.

Lee N, Lim CH, Kim T, Son EK, Chung GS, Rho CJ et al. Which hazard category should specific nanomaterials or groups of nanomaterials be assigned to and how? Geneva: World Health Organization; 2017. Licence: CC BY-NC-SA 3.0 IGO.

Lem, K., Choudhury, A., Lakhani, A., Kuyate, P., Haw, J., Lee, D., . . . Brumlik, C. (2012). Use of Nanosilver in Consumer Products. *Recent Patents on Nanotechnology, 6*, 60-72.

Lynn, D. E. (2009). Cell Culture. In V. H. Resh, & R. T. Carde, *Encyclopedia of Insects*. U.S.A.: Elsevier, 144-145.

Madigan, M., Martinko, J., Bender, K., Buckley, D., & Stahl, D. (2015). Infectious deseases and their transmission. In *Brock Biology of Microorganisms* (14th ed.). Madigan, M., Martinko, J., Bender, K., Buckley, D., & Stahl, D. (Eds.), Pearson Education, Inc., Chapter 6, 28-32.

Mallevre, F., Templier , V., Mathey, R., Leroy, L., Roupioz, Y., Fernandes, T., . . . Livache, T. (2016). Real-time toxicity testing of silver nanoparticles to Salmonella Enteritidis using surface plasmon resonance imaging: A proof of concept. *NanoImpact, 1*, 55-59.

Marchioni, M., Jouneau, P.-H., Chevallet, M., Michaud-Soret, I., & Deniaud, A. (2018). Silver nanoparticle fate in mammals: Bridging in vitro and in vivo studies. *Coordination Chemistry Reviews, 364*, 118-136.

Mazzonello, A., Valdramidis, V. V., Farrugia, C., Grima, J. N., & Gatt, R. (2017). Synthesis and characterization of Silver Nanoparticles. *Journal Of Modern Engineering Research (IJMER)*, 41-47.

Misra, N., Schluter, O., & Cullen, P. (2016). Plasma in Food and Agriculture. In *Cold Plasma in Food and Agriculture: Fundamentals and Applications*. N. Misra, O. K. Schluter, & P. Cullen (Eds.), Elsevier, Chapter 1, 1-16

Mohammad Ali, B., Bauer, B., Tredget, E. E., & Ghahary, A. (2004). Dermal fibroblasts from different layers of human skin are heterogeneous in expression of collagenase and types I and III procollagen mRNA. *Wound repair and Regeneration, 12*, 175-182.

Mosselhy, D., El-Aziz, M., Hanna, M., Ahmed, M., Husien, M., & Feng, Q. (2015). Comparative synthesis and antimicrobial action of silver nanoparticles and silver nitrate. *Journal of Nanoparticle Research (JNR), 17*, 473, 1-10

Moulin, V., Mayrand, D., Laforce-Lavoie, A., Larochelle, S., & Genest, H. (2011). In Vitro Culture Methods of Skin Cells for Optimal Skin Reconstruction by Tissue Engineering. In: *Regenerative Medicine and Tissue Engineering - Cells and biomaterial,* D. Eberli (Ed.), InTech, Croatia, Chapter 8, 195-208.

Niemira, B. (2012). Cold Plasma Decontamination of Foods. *Annual Review of Food Science and Technology, 3,* 125-142.

Noguez, C. (2007). Surface Plasmons on Metal Nanoparticles: The Influence of Shape and Physical Environment. *The Journal of Physical Chemistry C, 111,* 3806-3819.

Omara, S. T., Zawrah, M. F., & Samy, A. A. (2017). Minimum bactericidal concentration of chemically synthesized silver nanoparticles against pathogenic Salmonella and Shigella strains isolated from layer poultry farms. *Journal of Applied Pharmaceutical Science,* 214-221.

Pacioni, N., Borsarelli, C., Rey, V., & Veglia, A. (2015). Synthetic Routes for the Preparation of Silver Nanoparticles. In E. Alarcon, M. Griffith, & K. Udekwu, *Silver Nanoparticle Applications*. Springer International Publishing, 13-46.

Paknejadi, M., Bayat, M., Salimi, M., & Razavi, V. (2018). Concentration- and Time-Dependent Cytotoxicity of Silver Nanoparticles on Normal Human Skin Fibroblast Cell Line. *Iran Red Crescent Med J., 20,* e79183, In press.

Panáček, A., Smékalová, M., Večeřová, R., Bogdanová, K., Röderová, M., Kolář, M., . . . Kvítek, L. (2016). Silver nanoparticles strongly enhance and restore bactericidal activity of inactive antibiotics against multiresistant Enterobacteriaceae. *Colloids and Surfaces B: Biointerfaces*, 392-399.

Pantidos, N., & Horsfall, L. E. (2014). Biological Synthesis of Metallic Nanoparticles by Bacteria, Fungi and Plants. *Journal of Nanomedicine & Nanotechnology, 5,* 233, 1-10.

Pietroiusti, A., Magrini, A., & Campagnolo, L. (2014). Mechanisms of nanomaterial toxicity. In J. Njuguna, K. Pielichowski, & H. Zhu, *Health and environmental safety of nanomaterials: Polymer nanocomposites and other materials containing nanoparticles*. Woodhead Publishing, 28-43.

Piñero, S., Camero, S., & Blanco, S. (2017). Silver nanoparticles: Influence of the temperature synthesis on the particles' morphology. *Journal of Physics: Conference Series, 786,* 012020, 1-5.

Poitras, E., Levine, M., Harrington, J., Essader, A., Fennell, T., Snyder, R., . . . Levine, K. (2014). Development of an analytical method for assessment of silver nanoparticle content in biological matrices by inductively-coupled plasma mass spectrometry. *Biological Trace Element Research*, 184-192.

Pourzahedi, L., Vance, M., & Eckelman, M. (2017). Life Cycle Assessment and Release Studies for 15 Nanosilver-Enabled Consumer Products: Investigating Hotspots and Patterns of Contribution. *Environmental Science & Technology*, 7148−7158.

Radzig, M., Nadtochenko, V., Koksharova, O., Kiwi, K., Lipasova, V., & Khmel, I. (2013). Antibacterial effects of silver nanoparticles on gram-negative bacteria: Influence on the

growth and biofilms formation, mechanisms of action. *Colloids and Surfaces B: Biointerfaces, 102,* 300-306.

Rai, M., Yadav, A., & Gade, A. (2009). Silver nanoparticles as a new generation of antimicrobials. *Biotechnology Advances, 27,* 76-83.

Richmonds, C., & Mohan Sankaran, R. (2008). Plasma-liquid electrochemistry: Rapid synthesis of colloidal metal nanoparticles by microplasma reduction of aqueous cations. *Applied Physics Letters, 93,* 131501, 1-3.

Sabri, M. A., Umer, A., Awan, G. H., Hassan, M. F., & Hasnain, A. (2016). Selection of Suitable Biological Method for the Synthesis of Silver Nanoparticles. *Nanomaterials and Nanotechnology, 6,* 29-49.

Saeb, A., Alshammari, A., Al-Brahim, H., & Al-Rubeaan, K. (2014). Production of Silver Nanoparticles with Strong and Stable Antimicrobial Activity against Highly Pathogenic and Multidrug Resistant Bacteria. *Scientific World Journa,* 704708, 1-9.

Saito, G., & Akiyama, T. (2015). Nanomaterial Synthesis Using Plasma Generation in Liquid. *Journal of Nanomaterials, 10,* 1-21.

Sato, S., Mori, K., Ariyada, O., Atsushi, H., & Yonezawa, T. (2011). Synthesis of nanoparticles of silver and platinum by microwave-induced plasma in liquid. *Surface & Coatings Technology, 206,* 955–958.

Sau, T., Rogach, A., Jäckel, F., Klar, T., & Feldmann, J. (2010). Properties and Applications of Colloidal NonsphericalNoble Metal Nanoparticles. *Advanced Materials, 22,* 1805-1825.

Seong, M., & Lee, D. (2017). Silver Nanoparticles Against Salmonella enterica Serotype Typhimurium: Role of Inner Membrane Dysfunction. *Current Microbiology, 74,* 661–670.

Singh, A. (2016). *Engineered nanoparticles: structure, properties and mechanisms of toxicity.* Elsevier, Chapter 1-3, 1-122.

Sondi, I., & Salopek-Sondi, B. (2004). Silver nanoparticles as antimicrobial agent: a case study on E. coli as a model for Gram-negative bacteria. *Journal of Colloid and Interface Science, 275,* 177-182.

Souza, T. A., Franchi, L. P., Rosa, L. R., da Veiga, M. A., & Takahashi, C. S. (2016). Cytotoxicity and genotoxicity of silver nanoparticles of different sizes in CHO-K1 and CHO-XRS5 cell lines. *Mutation Research - Genetic Toxicology and Environmental Mutagenesis,* 70-83.

Sriram, G., Bigliardi, P. L., & Bigliardi-Qi, M. (2015). Fibroblast heterogeneity and its implications for engineering organotypic skin models in vitro. *European Journal of Cell Biology,* 483–512.

Syafiuddin, A., Salmiati, Salim, M. R., Hong Kueh, A. B., Hadibarata, T., & Nur, H. (2017). A Review of Silver Nanoparticles: Research Trends, Global Consumption, Synthesis, Properties, and Future Challenges. *Journal of the Chinese Chemical Society*, 64, 732-756.

Sykes, J. E., & Rankin, S. C. (2014). Isolation and Identification of Aerobic and Anaerobic Bacteria. In J. E. Sykes, *Canine and Feline Infectious Diseases*. Elsevier, 17-28.

Tripathi, M., Kumar, A., & Kumar, S. (2017). Characterization of Silver Nanoparticles Synthesizing Bacteria and Its Possible Use in Treatment of Multi Drug Resistant Isolate. *Frontiers in Environmental Microbiology, 3*, 62-67.

Vance, M., Kuiken, T., Vejerano, E., McGinnis, S., Hochella Jr., M., Rejeski, D., & Hull, M. (2015). Nanotechnology in the real world: Redeveloping the nanomaterial consumer products inventory. *Beilstein Journal of Nanotechnology, 6*, 1769–1780.

Vazquez-Muñoz, R., Borrego, B., Juárez-Moreno, K., García-García, M., Mota Morales, J. D., Bogdanchikova, N., & Huerta-Saquero, A. (2017). Toxicity of silver nanoparticles in biological systems: Does the complexity of biological systems matter? *Toxicology Letters*, 11-20.

Wang, L., Hu, C., & Shao, L. (2017). The antimicrobial activity of nanoparticles: present situation and prospects for the future. *International Journal of Nanomedicine*, 1227–1249.

Waseem, M., Awan, T., Yasin, H., & Rehman, N. (2018). Studying the morphological features of plasma treated silver and PEGylated silver nanoparticles: antibacterial activity. *Materials Research Express, 5*, 035016, 1-19.

Wildt, B. E., Celedon, A., Maurer, E. I., Casey, B. J., Nagy, A. M., Hussain, S. M., & Goering, P. L. (2016). Intracellular accumulation and dissolution of silver nanoparticles in L-929 fibroblast cells using live cell time-lapse microscopy. *Nanotoxicology, 10*, 710-719.

Winfield, M. D., & Groisman, E. A. (2004). Phenotypic differences between Salmonella and Escherichia coli resulting from the disparate regulation of homologous genes. *Proceedings of the National Academy of Sciences of the United States of America, 101*, 17162-17167.

Wolny-Koładka, K. A., & Malina, D. (2017). Toxicity assessment of silver nanoparticles against Escherichia coli strainsisolated from horse dung. *Micro & Nano Letters*, 772-776.

Yousef, A., & Carlstrom, C. (2002). Basic Microbiological techniques. In *Food Microbiology: A Laboratory Manual.* Wiley-Interscience, 5-12.

Zaman, M., Ahmad, E., Qadee, A., Rabbani, G., & Khan, R. H. (2014). Nanoparticles in relation to peptide and protein aggregation. *International Journal of Nanomedicine*, 899–912.

Zapór, L. (2016). Effects of silver nanoparticles of different sizes on cytotoxicity and oxygen metabolism disorders in both reproductive and respiratory system cells. *Archives of Environmental Protection, 42*, 32–47.

Zarei, M., Jamnejad, A., & Khajehali, E. (2014). Antibacterial Effect of Silver Nanoparticles Against Four Foodborne Pathogens. *Jundishapur J Microb, 7*, e8720, 1-5.

Zhang, T., Wang, L., Chen, Q., & Chen, C. (2014). Cytotoxic Potential of Silver Nanoparticles. *Yonsei Medical Journal*, 283-291.

Zhang, X.-F., Liu, Z.-G., Shen, W., & Gurunathan , S. (2016). Silver Nanoparticles: Synthesis, Characterization, Properties, Applications, and Therapeutic Approaches. *International Journal of Molecular Sciences*, E1534, 1-34.

Zhang, X.-F., Shen, W., & Gurunathan, S. (2016). Silver Nanoparticle-Mediated Cellular Responses in Various Cell Lines: An in Vitro Model. *International Journal of Molecular Sciences, 17,* E1603.

Zhang, Y.-T., Guo, Y., & Ma, T.-C. (2011). Plasma Catalytic Synthesis of Silver Nanoparticles. *Chinese Physics Letters, 28*, 105201, 1-3.